FORAGING ECOLOGY AND STRESS IN SEA TURTLES

by

Chelsea E. Clyde-Brockway

A Dissertation

Submitted to the Faculty of Purdue University

In Partial Fulfillment of the Requirements for the degree of

Doctor of Philosophy

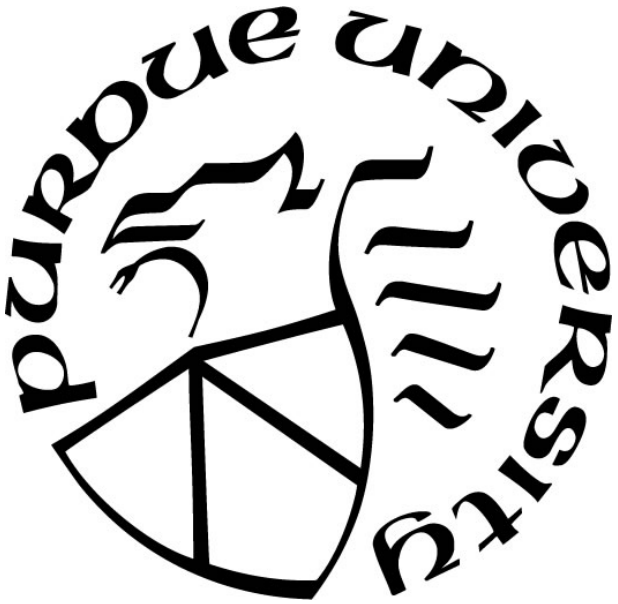

Department of Forestry and Natural Resources

West Lafayette, Indiana

August 2019

THE PURDUE UNIVERSITY GRADUATE SCHOOL
STATEMENT OF DISSERTATION APPROVAL

Dr. Elizabeth A. Flaherty, Co-Chair

Department of Forestry and Natural Resources

Dr. Frank V. Paladino, Co-Chair

Purdue Fort Wayne, Department of Biology

Dr. Reuben R. Goforth

Department of Forestry and Natural Resources

Dr. James R. Spotila

Drexel University, Department of Biodiversity, Earth and Environmental Science

Approved by:

Dr. Robert Wagner

Head of the Departmental Graduate Program

In memory of my father.

To my family
for their eternal love and support.

ACKNOWLEDGMENTS

Over the last four and a half years, I have amassed a notable group of guides, supporters, assistants, editors, mentors, advisors, and friends who have my eternal gratitude for helping me make this dream come true. My academic advisors, Drs. Liz Flaherty and Frank Paladino, have not only been invaluable educational mentors but have guided me through difficult times in my life. In moments when I needed extra support, they were unfailingly present, in both my personal and professional life. They encouraged me to pursue projects that interested and inspired me. Thank you from the bottom of my heart. Thank you to Dr. Jim Spotila, for serving on my dissertation committee, and for introducing me to the Herpetologists' League, where I learned precious lessons and met wonderful people. Thank you to Dr. Reuben Goforth, my fourth dissertation committee member, for his sage advice when graduate school seemed an insurmountable task. My committee was central in shaping the scientist and person that I am today. I am deeply grateful.

La familia que formé en El Jobo, fue fundamental en mi investigación y en mi sonrisa. This project would not have been posible without Maike. From organizing my field site, to introducing me to the community, to discussing life and science while watching the sun set, I truely enjoyed the time we spent together and look forward to every moment we will spend together. Special thanks to Kembly, Randall, Pirricho, Anibal, Jack, Mathilda, and Damien for taking me under their wings, assisting me with field work, housing me, feeding me, and becoming my second family. In addition to the core personnel of the Equipo Tora Carey (ETC), the volunteers they brought in were instrumental in my research moving forward. Specifically, I thank Melanie, Quintin, Paulina, Nicholi, Brian, Rocio, Emma, Elias, and Natalie for helping me with my research and for being my friends.

A big thanks to the researchers and veterinarians that collected samples for me, assisted me with analyses, and advised on my dissertation. Particularly, Drs. Bob George and Joe Smith for teaching me to collect blood from sea turtles; Drs. Matthew Godfrey and Emily Christensen and the team at the North Carolina Aquarium for guidance through permitting and collecting samples; Drs. Walter Mustin and Ana Malabia and the staff at the Cayman Islands Turtle Farm for samples; and Drs. Amber Jannasch and Christina

Ferreira for assistance through lab work and data analysis. I could not have done this without them.

I am blessed to have been a part of the Forestry and Natural Resources Department at Purdue where I have met so many wonderful people. Specifically, I thank Zoe, Randy, Brandon, Erin, Jacob, Cami, Dante, Ashley, Jameson, Landon, Holly, and Patrick for their help with my project, their help distracting me from my project, and general support when I needed it. Especially in -30ºF weather, which was almost more than my California spirit wanted to endure.

Saving the most important for last, I would like to thank my family and friends for their ongoing support. Be it reading drafts of my papers, hours of phone calls or care packages, my community provided me with the love and helped me find the confidence required to complete graduate school. Notably, I thank my mom Lisa, my grandma Jeannie, my brother Donovan, my sister Fiona, and friends Alyssa, Anna, and Jenell. I thank them for providing a steadfast base from which I had the courage to live in Costa Rica, move to Indiana, pursue my graduate degree, and survive some of the hardest years of my life. I thank my partner, Brandon, for motivating me in the last year of my dissertation and always making sure I was fed and happy. Lastly, I want to thank my dad, Pat, who is no longer with us, but always inspired me and encouraged me to follow my dreams. Look Dad, I did it!

TABLE OF CONTENTS

LIST OF TABLES

LIST OF FIGURES

LIST OF ABBREVIATIONS

CM – Green turtle (*Chelonia mydas*)

EI – Hawksbill turtle (*Eretmochelys imbricata*)

NC – North Carolina

CI – Cayman Islands Turtle Farm

DHT – Dihydrotestosterone

HPA – hypothalamus-Anterior Pituitary-Adrenal Axis

GS – Gulf Stream

CCL – Curved Carapace Length

SM – Sphingomyelin

PC – Phosphatidylcholine

FFA – Free Fatty Acid

CE – Cholesteryl Ester

PS – Phosphatidylserine

PI – Phosphatidylinositol

PG – Phosphatidylglycerol

PE – Phosphatidylethanolamine

Cer – Ceramide

Car – Acyl-Carnatine

TAG – Triglyceride

ENSO – El Niño Southern Oscillation

KUD – Kernel Utilization Density

WB – Whole Blood

EP – Epidermis

ABSTRACT

Author: Clyde-Brockway, Chelsea, E. PhD
Institution: Purdue University
Degree Received: August 2018
Title: Foraging Ecology and Stress in Sea Turtles.
Major Professor: Elizabeth A. Flaherty and Frank V. Paladino

As ectothermic marine megafauna, sea turtle physiology and ecology are tightly intertwined with temperature, seasonality, and oceanography. Identifying how turtles respond when exposed to cold water, how they adapt to cold environments when they need to explore cold environments in order to forage, and what foraging resources are exploited by sea turtles are all components central to their conservation. Cold-stunning is a well-documented phenomenon that occurs when water induced decreases in sea turtle body temperature cause turtles to become immobilized and wash ashore. While most cold-stunned turtles are rescued and rehabilitated, we do not know whether cold-stunning is an acute transient occurrence, or a symptom of a bigger environmental problem. Further, while in some environments avoiding cold water is preferential, in other habitats, sea turtles need to inhabit cold environments in order to forage. Along the Eastern Pacific Rim, discrete upwelling locations are characterized by high primary productivity and unusually cold water. In these environments, avoidance is not possible and sea turtles require physiological adaptions to mitigate body temperature decreases in cold water. Little is known about how turtles handle upwelling environments, despite the fact that sea turtles remain in these habitats regardless of water temperature fluctuations. Because upwelling habitats provide increased nutrient presence, and sea turtles are opportunistic foragers, quantification of diet composition will further our understanding of why sea turtles remain in cold water environments year-round. Diet composition in multiple populations of cohabitating sea turtles revealed partitioning that results in reduced inter-specific competition. Further, flexibility in diets provides a wide range of ecosystem services central to habitat resiliency. Therefore, conservation of endangered sea turtles requires complete ecosystem conservation, and complete understanding of the interconnectivity of sea turtles and their environments is crucial.

CHAPTER 1. TEMPERATURE DYNAMICS AND FORAGING ECOLOGY IN SEA TURTLES

1.1 Introduction

Sea turtles are migratory marine reptiles that inhabit temperate, sub-tropical and tropical ocean basins worldwide. As protection of nesting beaches increases in many parts of the world, conservation plans are now addressing conservation of in-water habitat use and threats to sea turtles in the open ocean. Population models suggest that without in-water protection, there is low likelihood for sea turtle recovery even with complete beach protection (Spotila et al., 2000).

Sea turtles are ectothermic and use external heat to regulate internal body temperature (Davenport, 1997). Beginning in nesting environments, temperature is an important determinant of sea turtle physiology and behavior. From determining sex (Morreale et al., 1982), to influencing behavior (Crear et al., 2016; Hochscheid et al., 2010), available habitats (Epperly et al., 1995, 2007, Van Houton et al., 2015), metabolism (Southwood et al., 2003) and health (Haines and Kleese, 1977), temperature plays a central role in sea turtle life history.

Hatchling turtles enter the water for the first time and are washed into oceanic foraging habitats for a period of time known as the "lost years" (Reich et al., 2007). At approximately 30 cm curved carapace length (carapace measured from the base of the neck to the posterior point of the carapace over the tail), juvenile sea turtles recruit to coastal foraging habitats furthering growth and development in more productive environments. Coastal foraging locations are often shared between neritic juveniles, sub-adults, and adults between nesting seasons. Once reproductively mature, sea turtles return to natal beaches to nest, before returning to previously established foraging habitats, a migration pattern that persists through the remainder of their lives. Therefore, understanding how turtles use foraging habitats is important to support future reproductive output and recovery of populations (Harrison et al., 2011). These factors are especially important when global water currents cause annual variations in water temperature and nutrient load through upwelling. Upwelling is an oceanographic phenomenon in which cold, nutrient rich water

is transported from the ocean floor along the continental shelf to the surface. As such, turtles rely on balancing avoidance of dangerously cold water with physiological adaptations that allow them to endure moderate hypothermic conditions in order to forage.

In the Atlantic Ocean, sea turtles migrate into nutrient rich waters when currents shift and water temperatures increase. They then migrate away from these habitats when cold water returns. Consequences of failure to avoid cold water results in cold-stunning. Cold-stunning occurs when turtles are unable to maintain functional body temperature due to decreasing water temperatures, resulting in loss of the ability to swim and regulate buoyancy. This puts them at risk for boat strikes, disease, and death. Hypothermia is a stressor for sea turtles, resulting in the initiation of the stress response. During the stress response, hormones are released into the blood stream that increase organism vigilance and survival. However, while necessary for acute survival, stress hormones are highly toxic to tissues and prolonged exposure can result in increased occurrences of damage and disease. Therefore, quantification of stress response in sea turtles indicates the degree of damage and danger facing sea turtles (Chapter 1).

Ideally, sea turtles avoid cold water to avoid stressful hypothermic stunning. However, cold water and foraging nutrients are interconnected through upwelling. North Pacific Costa Rica is a unique upwelling zone due to the interaction of the trade winds and the Costa Rica Dome water currents. Together, these phenomena create an environment supporting primary productivity and biodiversity, within the context of a cold habitat with a shallow thermocline. Accordingly, animals adapt their physiology to maintain metabolism and mitigate the influence of external temperature to exploit foraging resources in areas comparable to North Pacific Costa Rica. While homeothermic animals achieve this through body fat, counter current heat exchange, and increases in metabolic heat production, reptiles have limited physiological options to respond to cold temperatures.

In reptiles, body fat is primarily increased during foraging and used as fuel during times of nutrient scarcity (e.g., during reproduction). Although capable of regional endothermy through the organization of the circulatory system, minimal internal temperature is generated metabolically (Standora et al., 1982). However, variability in the lipid composition of cell and organelle membranes is one indication of cold-adaption in both endothermic and ectothermic animals. I explored this relationship and determined

baseline-lipid profiles in sea turtles to provide the framework to use lipid-profiling in the future as a measure of physiology and health. I also addressed the issue of unknown lipids in sea turtles by isolating lipids, and identified their chain lengths, saturation levels, and seasonal variability using multiple reaction monitoring (MRM) lipid profiling (Chapter 3).

When seasonal upwelling causes annual shifts in ocean temperature, it also causes seasonal shifts in food availability. Turtles foraging in Matapalito and Salinas Bays, Costa Rica, are foraging year-round despite the measured cessation of upwelling that occurs during the wet season (Stuhldreier et al., 2015). Therefore, if multiple populations of turtles are able to foraging continuously, understanding the diet of turtles and partitioning of resources is important for the ongoing conservation of endangered species. To address this question, I used stable isotope analysis to measure trophic niche, niche overlap, composition of diets and dietary shifts in spatially co-occurring populations of sea turtles (Chapter 4). This chapter adds to a growing understanding that diet in sea turtles is habitat specific and is influenced by interspecific competition.

1.2 Journal Selections and Justification

The following chapters are formatted differently as per the requirements by the selected journal. I organized Chapter 2, entitled "Comparative Tissue Corticosterone in Cold-Stunned Juvenile Green Turtles Suggest Transient Stress in Otherwise Healthy Turtles", to the requirements of General and Comparative Endocrinology because of the journal's focus on hormones in animals and their connection to animal behavior and habitat selection. For Chapter 3, entitled "Lipidomics Suggest Species Specificity and Cold Adaption in Pacific Green and Hawksbill Sea Turtles", I used the formatting for the Journal of Experimental Marine Biology because the focus of the journal is marine organisms in relation to their environment. Finally, Chapter 4, titled "Diet and Foraging Niche Partitioning in Green and Hawksbill Turtles" I present using the guidelines for the Journal of Marine Biology because of its focal point on understanding life in the ocean, interaction between marine organisms, and functioning of the marine biosphere.

1.3 Literature Cited

Crear, D.P., Lawson, D.D., Seminoff, J.A., Eguchi, T., LeRoux, R.A., Lowe, C.G., 2016. Seasonal shifts in the movement and distribution of green sea turtles *Chelonia mydas* in response to anthropogenically altered water temperatures. Mar. Ecol. Prog. Ser. 548, 219–232.

Davenport, J., 1997. Temperature and the life-history strategies of sea turtles. J. Therm. Biol. 22(6), 479–488.

Epperly, S.P., Braun, J., Veishlow, A., 1995. Sea turtles in North Carolina waters. Conserv. Biol. 9(2), 384–394.

Epperly, S.P., Braun-McNeill, J., Richards, P.M., 2007. Trends in catch rates of sea turtles in North Carolina, USA. Endanger. Species Res. 3, 283–293.

Haines, H., Kleese, W.C., 1977. Effect of water temperature on a herpesvirus infection of sea turtles. Infect. Immune. 15(3), 756–759.

Harrison, X.A., Blount, J.D., Inger, R., Norris, D.R., Bearhop, S., 2011. Carry-over effects as drivers of fitness differences in animals. J. Anim. Ecol. 80(1), 4–18.

Hochscheid, S., Bentivegna, F., Hamza, A., Hays, G.C., 2010. When surfacers do not dive: multiple significance of extended surface times in marine turtles. J. Exp. Biol. 213(8), 1328–1337.

Reich, K.J., Bjorndal, K.A., Bolten, A.B., 2007. The 'lost years' of green turtles: using stable isotopes to study cryptic lifestages. Biol. Lett. 3(6), 712–714.

Southwood, A.L., Darveau, C.A., Jones, D.R., 2003. Metabolic and cardiovascular adjustments of juvenile green turtles to seasonal changes in temperature and photoperiod. J. Exp. Biol. 206(24), 4521–4531.

Spotila, J.R., Reina, R.D., Steyermark, A.C., Plotkin, P.T. and Paladino, F.V., 2000. Pacific leatherback turtles face extinction. Nature 405(6786), 529–530.

Standora, E.A., Spotila, J.R., Foley, R.E., 1982. Regional endothermy in the sea turtle, *Chelonia mydas*. J. Therm. Biol. 7(3), 159–165.

Stuhldreier, I., Sánchez-Noguera, C., Rixen, T., Cortés, J., Morales, A., Wild, C., 2015. Effects of seasonal upwelling on inorganic and organic matter dynamics in the water column of eastern Pacific coral reefs. PLoS ONE 10(11), e0142681.

Van Houtan, K.S., Halley, J.M., Marks, W., 2015. Terrestrial basking sea turtles are responding to spatio-temporal sea surface temperature patterns. Biol. Lett. 11(1), p.20140744.

CHAPTER 2. COMPARATIVE TISSUE CORTICOSTERONE IN COLD-STUNNED JUVENILE GREEN TURTLES SUGGESTS TRANSIENT STRESS IN OTHERWISE HEALTHY TURTLES

Chelsea E. Clyde-Brockway, Elizabeth A. Flaherty, and Frank V. Paladino.

2.1 Abstract

Every year, thousands of green turtles (*Chelonia mydas*) are immobilized by rapid decreases in water temperature along the East Coast of the United States. Once stunned, these turtles become unable to swim then wash ashore. In order to preserve these endangered turtles, the North Carolina Aquarium works with the National Park Service to rescue cold-stunned turtles and transport them to the Aquarium for rehabilitation. To quantify the stress of cold-stunned juvenile green turtles, I measured corticosterone and cortisol (along with testosterone and dihydrotestosterone) in plasma and epidermal samples of cold-stunned juvenile green turtles upon arrival at the North Carolina Aquarium. Subsequently, I compared these results to hormone levels in captive juvenile green turtles reared and maintained by the Cayman Islands Turtle Farm, Grand Cayman. Turtles from North Carolina had significantly higher plasma concentrations of corticosterone in 2018 (101.76 ± 54.6 ng/mL) compared to 2017 (37.5 ± 37.0 ng/mL). Additionally, in 2018 turtles from North Carolina had significantly higher plasma corticosterone than turtles from the Cayman Islands (25.78 ± 22.89 ng/mL). However, in 2017, turtles from North Carolina had a similar stress response to captive animals, although all turtles were exhibiting activated stress responses. Plasma testosterone and dihydrotestosterone concentrations were similar between turtles from North Carolina in 2017 (testosterone: 27.71 ± 16.63 pg/mL; dihydrotestosterone: 13.96 ± 10.52 pg/mL) and in 2018 (testosterone: 36.5 ± 34.13 pg/mL; dihydrotestosterone: 16.72 ± 10.48 pg/mL). Further, plasma androgen hormone concentrations from turtles in North Carolina were significantly lower than turtles from the Cayman Islands Turtle Farm (testosterone: 840.6 ± 543.6 pg/mL; dihydrotestosterone: 497.88 ± 263.4 pg/mL). Lastly, I determined that epidermal hormone concentrations were consistent between years (North Carolina), and sites (North Carolina and Cayman Islands). My results demonstrate that non-dynamic tissues can be used to quantify long-term

organismal hormone levels in sea turtles. Further, the consistency in epidermal hormone concentrations suggests that neither captive turtles nor wild turtles were chronically stressed, suggesting rehabilitation of cold-stunned turtles will succeed and support recovery of endangered populations. Moreover, these data indicate that the stress response in sea turtles might be more complex than previously thought. I recorded significantly different testosterone concentrations between captive and wild turtles, this relationship could be due to age, sex, or an interaction between corticosterone and testosterone; however, no statistical relationship was present between the two. It is likely that global climate change will cause an increase in the number of cold-stunning events, although, my data suggest that rehabilitation of cold-stunned sea turtles is an effective strategy for their conservation.

2.2 Introduction

Sea turtles depend on water temperature to maintain muscle function and become incapable of swimming or regulating buoyancy in cold water (usually < 8°C; Hochscheid et al., 2002; Morreale et al., 1992; Witherington and Ehrhart, 1989). In attempt to survive, the hypothalamus-anterior pituitary-adrenal (HPA) axis induces the release of corticosterone into the blood stream, where it acts on several metabolic and behavioral pathways that assist in coping with, or escaping, stressful stimuli (Cockrem, 2013; Moore and Jessop, 2003; Pirhalla et al., 2015; Schwartz, 1978). Failure to escape decreasing water temperatures results in turtles that are unable to behaviorally thermoregulate, and they then rely on water current transport to warmer environments, or human intervention, to evade mortality (Keller et al., 2012).

Although initially beneficial, chronic activation of the stress response can damage tissues and negatively influence health (Kleist et al., 2018; Morici et al., 1997). Therefore, chronic stress, such as unrelenting repeated environmental stressors, can potentially influence population recovery and stability through diversion of resources away from immune function, reproduction, or growth (Bonier et al., 2009b; Breuner et al., 2008; Moberg, 2000; Möstle and Palme, 2002). Minimally invasive quantification of stress hormone concentration in non-dynamic tissues (such as skin) can be used as a measure of chronic stress, and therefore health, and is useful in the conservation of endangered animals

(Baxter-Gilbert et al., 2014; Berkvens et al., 2013; Warnock et al., 2010; Heimbürge et al., 2019). Although the stress response is complicated and the relationship between stress and fitness is dynamic, tissue concentrations of corticosterone can help researchers understand the ecology of wildlife (Bonier et al., 2009a; Breuner et al., 2008; Sapolsky et al., 2000), especially populations exposed to increasingly unstable environments as climate change progresses (Andres, 2016).

In the last few decades, the number of cold-stunned turtles stranded along the East Coast of the United States has increased with a record 1700 endangered juvenile green turtles (*Chelonia mydas*) becoming stranded in North Carolina in January 2016 (Anderson et al., 2011; IUCN, 2004; Morreale et al., 1992; North Carolina Veterinarian, Personal communication). These stranding events occur when turtles foraging in inshore sounds along North Carolina from April – November (up to 25.8°C water temperature) fail to migrate into offshore oceanic habitats in November when water temperature drops (low of 6.8°C; Epperly et al., 2007; Epperly et al., 1995; Willard et al., 2017). Increased occurrences of stranded turtles are likely linked to climate change-induced destabilization in the timing and location of the Gulf Stream's (GS) annual southern divergence from the coast, a phenomenon that is expected to worsen (Andres, 2016, Griffin et al., 2019). To mitigate this problem, the North Carolina Aquarium rescues stranded cold-stunned turtles during winter months (January – March). Rescued turtles are then transported to the Aquarium for rehabilitation and subsequent release in Florida (Aquarium veterinary staff, Personal communication). Most of these turtles are released within weeks of rescue, although the acute effects of cold-stunning and potential role of other environmental conditions in eliciting cold-stunning are unknown.

To investigate acute and chronic stress in cold-stunned turtles, I compared plasma concentrations of stress hormones to epidermal stress hormone concentrations in cold-stunned juvenile green turtles rescued by the North Carolina Aquarium during annual cold-stunning events. Subsequently, I compared stress hormones in cold-stunned turtles to turtles hatched and maintained in captivity. Like mammals, captivity does not necessarily cause chronic stress in reptiles if they are able to habituate to their environments (Jones and Bell, 2004; Burghardt, 2013). I therefore included captive animals in this study for comparison with wild turtle stress responses. Specifically, I measured corticosterone,

cortisol, dihydrotestosterone (DHT), and testosterone in plasma and epidermal tissue collected from juvenile green turtles upon arrival at the North Carolina Aquarium (NC) and captive green turtles housed at the Cayman Islands Turtle Farm (CI), Grand Cayman. I measured DHT and testosterone because stress can accompany a transient change in plasma androgens and plasma androgens interact with stress hormone secretion (Hunt et al., 2012; Lance et al., 2001). Applying endocrinological techniques to wild populations of sea turtles is difficult, and less invasive techniques to study turtles allow scientists to evaluate stress without incurring results skewed by capture stress. In addition, comparing cold-stunned turtles to captive turtles allowed us to determine how cold-stunning relates to general handling stress.

2.3 Methods

2.3.1 Sample Collection

I analyzed plasma samples collected during the 2017 and 2018 cold-stunning events (January – March) by the NC Aquarium veterinary team upon turtle arrival at the rehabilitation facility (post-cold-stunning and transport). I also analyzed plasma samples collected by CI veterinarians during the 2018 spring health assessment. At both sites, veterinarians collected blood samples (< 1mL/kg) using a 21 g needle from the cervical sinus and isolated plasma by centrifugation. They then stored plasma samples in 2 ml cryovials at -18°C for up to one year before transfer to Purdue University (Behrend et al., 1998; Owens and Ruiz, 1980). Additionally, veterinarians collected skin samples from the trailing edge of one of the hind flippers (CI only) or scraped from the carapace (both sites) using sterilized scalpels and forceps. Teams stored the epidermal samples in 2 ml cryovial at -18°C for up to a year until transfer to Purdue University. Lastly, veterinarians at the Aquarium measured curved carapace length (CCL, using a flexible measuring tape, ± 0.5 cm) and body mass (veterinary table scale ± 0.01 kg).

2.3.2 Plasma Sample Analysis

I quantified the level of hemolysis present in each plasma sample (0, +1, +2, +3, Adiga and Yogish, 2016; Goodhead and MacMillan, 2017; Killilea et al., 2017) and excluded samples with a hemolysis score >1.0 from analysis to avoid contaminated results

(Perrault J, unpublished results). At Purdue University, samples were stored at -20°C. I thawed each plasma sample and then transferred a 200 µl subsample to a new centrifuge vial. At the Bindley Metabolite Profiling Facility, I extracted corticosterone using a solid phase extraction method and Oasis PRIME HLB 1 cc columns (Waters Corporation, Milford, MA, USA). First, I created an internal standard composed of 5 ng d_8 corticosterone, 5 ng d_4 cortisol, 0.1 ng d_3 dihydrotestosterone (DHT), 0.1 ng $^{13}C_3$ testosterone (Toronto Research Chemicals, North York, ON, Canada) and methanol. I added 10 µl of this internal standard to each plasma sub-sample and vortexed the mixture until homogenized. I then loaded the sample into the Oasis PRIME HLB 1 cc column and centrifuged the column (1 min at 2000 rpm; Eppendorf Centrifuge 5810 R, Eppendorf North America, Hauppauge, NY, USA). Next, I washed the column with 5% methanol and centrifuged again (1 min at 200 rpm). I eluted the sample from the column with 100% acetonitrile and dried the sample for 4 hr (SpeedVac; Vacufuge 5301, Eppendorf North America, Hauppauge, NY, USA). At this point, the samples were stable in -80°C long-term storage, although I stored samples for < 1 mo. I resuspended and derivatized the samples using an Amplifex™ Diene Keto Reagent Kit (5037849/RUO-IDV-05-1872-A, SCIEX, Framingham, MA, USA) and vortexed the samples for 60 min at ambient temperature. I centrifuged the sample at 3000 rpm for 5 min and transferred the supernatant into plastic autosampler vials for analysis on a 6460C Triple Quadrupole LC/MS/MS (Agilent, Santa Clara, CA, USA).

2.3.3 Skin Sample Analysis

I thawed the epidermal samples (skin and/or scute), and soaked them in deionized water for 20 min to remove sand, and then dried them at 60°C for 48 hrs. Once dry, I weighed the samples using a microbalance (Sartoris CPA2P, Arvada, CO) and then homogenized them using a combination of cutting with fine scissors and grinding with a bead homogenizer (10 min at 6500 rpm; Precellys 24, Bertin Technologies, Rockville, MD, USA). Despite using a fast rotation metallic bead homogenizer and the supplied vials designed to powder samples, homogenizer vials occasionally cracked during the process. When this occurred, I added methanol and then pipetted the mixture to a new centrifuge vial. Once in a new vial, I added the same internal standard mixture outlined above and

allowed the solution to sit on a 3-D Rotator Waver for 24 hr (VWR W-150 Waver, VWR International, Radnor, PA, USA) to allow hormone extraction. After extraction, I centrifuged the sample (5 min at 8,000 rpm; centrifuge model VSX, Taylor Scientific, St Louis, MO, USA), collected the supernatant, and dried the sample using the same methods as the plasma samples.

2.3.3 Statistical Analysis

Because I analyzed samples with internal standards for each hormone of interest (corticosterone, cortisol, DHT, testosterone), I processed raw mass spectrometry data by comparing retention curve areas between the hormone in each sample and its comparable internal standard. I calculated the concentration of hormone per sample using the concentration of the standard. I then corrected the concentration by standardizing it against the volume (for plasma samples), or mass (for epidermal samples) and recorded corticosterone and cortisol in ng/mL and DHT and testosterone in pg/mL.

The data did not meet the assumptions for parametric tests, so I log-transformed concentrations of corticosterone, cortisol, DHT, and testosterone. In R statistical software (Version 3.4.4, Vienna, Australia) and SPSS (IBM, Armonk, New York), I used a one-way MANOVA to compare mass, corticosterone, cortisol, DHT and testosterone between turtles from NC in 2017 and 2018 for plasma and scute samples separately (CCL was analyzed separately because I did not have data for all turtles) followed by post-hoc one-way ANOVAs. Subsequently, I used a one-way ANOVA to compare CCL between years. I investigated size effects on hormone concentrations using linear regression models. I used multiple one-way MANOVAs (with post-hoc ANOVAs) to compare corticosterone, cortisol, DHT, and testosterone between scute and plasma collected from turtles between sites (NC 2017 and CI, NC 2018 and CI). To investigate interactions between stress hormones and sex hormones, I used a linear regression to compare plasma corticosterone and testosterone from all turtles pooled together. Finally, I used repeated measures MANOVAs to compare plasma and epidermal hormone concentrations for each individual. I accepted a statistical significance of $P < 0.05$.

2.4 Results

2.4.1 Captured Animals

I analyzed plasma and epidermal samples from 21 cold-stunned juvenile green turtles rescued by the NC Aquarium (2017 n = 12; 2018 n = 9) and 13 captive juvenile green turtles from the CI (all of unknown sex; Table 2.1). In 2018, the Aquarium team measured straight carapace length (SCL) instead of curved carapace length (CCL) and from these data I calculated CCL using the equation developed by Wynne (2016):

$$SCL = 0.9026\ CCL + 1.4705 \quad (1)$$

The data demonstrated that turtles captured in 2018 were significantly longer (CCL) and heavier than turtles captured in 2017, although I did not receive carapace length data on all turtles sampled (Table 2.1).

2.4.2 Hormone Concentrations

In NC, I determined that corticosterone, cortisol, dihydrotestosterone (DHT), testosterone and body mass were significantly different between years ($F_{5,15} = 7.103$, $p = 0.001$, Wilks' $\lambda = 0.297$). Specifically, plasma corticosterone was significantly higher in 2018 compared to 2017, while plasma cortisol, DHT and testosterone concentrations were not significantly different between years (Table 2.1, Fig. 2.1). Linear regression analyses, revealed no relationship between corticosterone and CCL or body mass (Fig. 2.2).

Plasma hormone concentrations were significantly different between cold-stunned juvenile turtles rescued in NC in 2017 and captive turtles ($F_{4,23} = 110.42$, $p < 0.001$, Wilks' $\lambda = 0.0433$, Fig. 2.1). However, plasma corticosterone concentrations were similar ($F_{1,23} = 0.355$, $p = 0.557$), while cortisol ($F_{1,23} = 29.649$, $p < 0.001$) was significantly higher in NC compared to CI, and DHT ($F_{1,23} = 145.12$, $p < 0.001$) and testosterone ($F_{1,23} = 134.87$, $p < 0.001$) were significantly lower (Fig. 2.1). Further, plasma hormone concentrations also varied between cold-stunned juveniles rescued in NC in 2018 and captive juveniles housed at CI ($F_{4,20} = 71.952$, $p < 0.001$, Wilks' $\lambda = 0.056$, Fig. 2.1). Post-hoc analysis indicated that plasma corticosterone ($F_{1,20} = 21.491$, $p < 0.001$) and cortisol ($F_{1,20} = 16.432$, $p < 0.001$) were significantly higher in NC in 2018, while DHT ($F_{1,20} = 112.83$, $p < 0.001$) and testosterone ($F_{1,20} = 69.242$, $p < 0.001$) were significantly lower in NC compared to CI

turtles (Fig. 2.1). There was no linear relationship between plasma corticosterone and testosterone (Adjusted $R^2 = 0.05$, $F_{1,32} = 2.702$, $p = 0.11$).

Scute corticosterone, cortisol, DHT, and testosterone concentrations were consistent across years (NC 2017 and 2018, $F_{4,16} = 1.94$, $p = 0.153$, Wilks' $\lambda = 0.673$, Fig. 2.3) and sites (NC and CI, $F_{4,29} = 0.733$, $p = 0.577$, Wilks' $\lambda = 0.908$, Fig. 2.3). When I compared plasma corticosterone, cortisol, DHT and testosterone to hormones in scute (NC and CI), and skin (CI only), plasma hormone concentrations were significantly higher in all cases (NC: $F_{4,16} = 489.803$, Wilks' $\lambda = 0.008$, $p < 0.001$; CI: $F_{8,44} = 20.932$, Wilks' $\lambda = 0.006$, $p < 0.001$; Table 2.2, 2.3).

2.5 Discussion

My results suggested that cold-stunning represents a significant acute stressor (plasma corticosterone concentration) in green turtles that is not a symptom of other environmentally induced chronic stress (epidermal corticosterone concentration). Additionally, cold-stunned turtles experienced similar or higher levels of acute stress than captive turtles undergoing handling stress. The low levels of epidermal stress hormones and similarity between NC and CI suggested that turtles from both sites were not chronically stressed. This conclusion is supported by the overall good health of juvenile turtles in this study.

2.5.1 Stress Hormones

In North Carolina, corticosterone was the only plasma hormone that varied significantly between years (Table 2.1, Fig. 2.1). In reptiles, corticosterone is the active stress hormone, while cortisol is a hormone within the greater glucocorticoid pathway and the active stress hormone in non-rodent mammals (Boucher et al., 2014). Higher circulating corticosterone in 2018 compared to 2017 was not due to differences in water temperature; in fact the range of temperatures between January and March were similar or slightly warmer in 2017 compared to 2018 (16°C to 20°C and 15°C to 19°C, respectively; https://seatemperature.info/). It could, however, be a result of variable air temperature and its effect on turtles once stranded on the beach. During 2018, North Carolina was exposed

to exceptionally cold weather (~ 6°C), increased rainfall (> 76 cm), and wind (> 160 km/h; https://www.weather.gov), which could increase the effects of cold-stunning and result in higher plasma corticosterone. Similarly, Galápagos marine iguanas (*Amblyrhynchus cristatus*) that reside on heavily visited tourist islands had lower baseline corticosterone and truncated stress response curves compared to those on uninhabited islands (Romero and Wikelski, 2002). Additionally, iguanas sampled during El Niño years had higher plasma corticosterone response curves compared to iguanas sampled in non-El Nino years, and higher corticosterone was negatively correlated to survival (Romero and Wikelski, 2001). Although El Niño Oscillations do not have dramatic effects along NC, the polar vortex in 2018 could induce a similar variability in stress hormones.

Turtles in 2018 were larger than turtles in 2017 (Table 2.1); however, linear regression analyses suggested that corticosterone concentration was not related to CCL or mass of animals (Fig. 2.2a, b). However, some of my CCL measurements (NC 2018) were calculated based on Wynne, (2016) and rely on the accuracy of that equation. Contrary to my findings, studies in green turtles and loggerhead turtles (*Caretta caretta*) reported lower baseline plasma corticosterone and smaller handling peaks in corticosterone in larger turtles (non-reproductive) compared to smaller juvenile turtles (Gregory et al., 1996; Jessop and Hamann, 2005). Variations across age could be a result of experience but is more likely a result of metabolism. Metabolic rate determines the speed at which hormones perfuse through the body, and larger turtles generally have higher metabolic rates due to thermal inertia referred to as gigantothermy (in leatherback turtles, *Dermochelys coriacea*; Paladino et al., 1990). Therefore, smaller cold-stunned turtles could be on a metabolic delay, which lowered the concentration of corticosterone measured. Without sequential blood samples to measure the rate of increase or decrease in plasma corticosterone, I was unable confirm this hypothesis.

Extended restraint stress (48 hr) in alligators (*Alligator mississippiensis)* induces a bimodal stress response where the initial rise in corticosterone (4 hrs, ~ 12 ng/mL) is followed by a decrease (24 hr mark) and subsequent exaggerated increase in corticosterone (48 hr, ~18 ng/mL, Elsey et al., 1991; Lance and Elsey, 1986, 1999). That study suggests that when a stressor is not eliminated, the alligators mount a larger stress response to increase chances of survival. Therefore, it is plausible that differential corticosterone

concentrations between years in cold-stunned turtles (this study) could represent two different time points within the stress response resulting from extended exposure to cold-stunning. Specifically, turtles rescued in 2018 might have been experiencing extended stress as a result of longer exposure to cold water/air or the duration of time passed between stranding and rescue. Similarly, if turtles are unwell, corticosterone concentrations might increase more rapidly and remain abnormally high for a lengthened period of time, similar to those found in green turtles with fibropapilloma infections (Aguirre et al., 1995). However, the Aquarium did not record visual symptoms of chronic infection. Nevertheless, further investigations into the strength and duration of sea turtle stress responses are warranted.

The lack of variability in epidermal samples across sites and significantly lower corticosterone in epidermis compared to plasma suggested that neither NC nor CI turtles are experiencing chronic (or captive) stress (Jones and Bell, 2004; Burghardt, 2013). The comparable patterns in plasma and epidermal hormones further suggest that scute tissue represent an accurate quantitative measure of animal hormones (Heimbürge et al., 2019; Fig. 2.1, 2.3). However, results could be skewed (under representation of actual values) if the size of epidermal sample (in this study 3 – 180 mg) was either not sufficient to accurately represent chronic stress hormone levels or the homogenizer used did not sufficiently break down the sample. Many of the skin samples remained in large chunks and were difficult to homogenize. Regardless, I demonstrate that it is possible to extract hormones from epidermal tissues in sea turtles, which provides valuable information on long-term physiological stress, similar to those studies done in mammals, birds, and other reptiles (Baxter-Gilbert et al., 2014; Berkvens, 2012; Fairhurst et al., 2015; Heimbürge et al., 2019).

Plasma samples from CI turtles had similar concentrations of corticosterone to NC turtles in 2017 and significantly lower plasma corticosterone and cortisol concentrations compared to cold-stunned turtles from NC in 2018 (Fig. 2.1). The concentration of stress hormones in turtles from CI suggest handling stress activation of the HPA axis and that the stress response was not truncated, further supporting the absence of chronic captive stress (Romero and Wikelski, 2002). In healthy sea turtles, handling stress reaches a maximum concentration at 8 hrs and begins to decrease by 24 hrs; however, there are no data for

response after 24 hrs (Aguirre et al., 1995; Gregory and Shmid, 2001; Jessop and Hamann, 2005). Without complete data on sea turtle HPA handling stress response through exhaustion of the response and subsequent return to baseline levels, I cannot determine whether results are extreme or not (Lance and Elsey, 1999). However, such analyses are difficult, and the endangered status of marine turtles precludes 24 – 48 hr restraint in most cases. Corticosterone results were higher than those measured 20 min post-disturbance in basking (~ 476 pg/mL), both solitary (~ 603 pg/mL) and arribada (~ 322 pg/mL) nesting, and male (~1,269 pg/mL) olive ridley turtles (*Lepidochelys olivacea;* Valverde et al., 1999). However, results from NC 2017 and CI were comparable to those from cold-stunned Kemp's ridley turtles upon arrival at the New England Aquarium (~ 40 ng/mL, Hunt et al., 2012) and at 60 min post-net capture in healthy Kemp's ridley turtles (82.87 ng/mL, Gregory and Shmid, 2001).

In this study, plasma corticosterone showed significant individual variation (Cockrem 2013, Fig. 2.4), while scute were comparable and represent a better measure of baseline hormone values. Given the limitations of this study, such as veterinarians collected samples and assessed health beyond baseline timing outside the 5-15 min required for baseline levels (Gregory and Shmid, 2001; Jessop and Hamann, 2005; Winters et al., 2016), I cannot confirm the specific cause of variability in corticosterone.

2.5.2 Sex Hormones

The NC turtles showed no difference in plasma or epidermal androgen (DHT and testosterone) hormones between years, and androgens were present in very low concentrations. In adult turtles and larger juveniles, testosterone and its metabolites can be used to estimate sex (Allen et al., 2015; Jensen et al., 2018). The low plasma androgen hormone concentrations may have been due to turtle size (CCL, Table 2.1), suggesting turtles were decades away from sexual maturity. In one study of juvenile and adult male green turtles, plasma testosterone concentrations (obtained using an ELISA) were 112.4 – 112,094.2 pg/mL, while juvenile and adult female green turtle plasma testosterone concentrations were 4.1– 281.2 pg/mL (Allen et al., 2015). However, a single female turtle, confirmed by laparoscopy, had a testosterone concentration of 1,333 pg/mL (Allen et al., 2015), suggesting that these concentration ranges are not definitive. In Kemp's ridleys,

males (classified by hormone concentrations) had testosterone concentrations from 20.6 – 427 pg/ml, while predicted females plasma testosterone concentration ranged from 2 – 10.5 pg/mL (Gregory and Shmid, 2001). In my study, NC plasma testosterone concentrations were 4 – 35 pg/mL (Table 2). This range could indicate that most turtles in my study were female, as classified by Allen et al. (2015) and Gregory and Shmid (2001). However, it is more likely that my results indicate that these turtles were too small and therefore too young (average CCL < 44 cm) to have concentrations of circulating androgens high enough to determine sex. The turtles in this present study had much smaller CCL than turtles in Allen et al. (2015), therefore, low testosterone concentrations were not suprising.

Turtles from CI had significantly higher DHT and testosterone plasma concentrations (i.e., 245 – 2035 pg/mL); however, there were no differences in epidermal androgen concentrations (Table 2.2, Fig. 2.2). Based on these previous studies, these turtles should be classified as immature males (Allen et al., 2015; Licht et al., 1985; Table 2.2). However, these results likely are not accurate indications of sex, as Allen et al. (2015) documented a female with a plasma testosterone concentration of 1,333 pg/mL. Further, this conclusion ignores the relationship between testosterone and corticosterone in other reptiles (Dayger and Lutterschmidt, 2016; Lance and Elsey, 1986; Lance et al., 2004).

I observed no significant relationship between corticosterone concentration and testosterone concentration. In Kemp's ridley turtles (Gregory and Shmid, 2001), frogs and toads (*Rhinella marina*; Narayan et al., 2012), snapping turtles (*Chelydra serpentine*; Mahmoud et al., 1989), male tuataras (S*phenodon* spp.; Cree et al., 1990), and desert tortoises (*Gopherus Polyphemus*; Lance et al., 2001) had testosterone concentrations that remained stable or increased with capture. However, in many studies, high levels of circulating corticosterone are inversly related to reproduction (and testosterone) in reptiles after as little as 2 hrs of restraint (Dayger and Lutterschmidt, 2016; Lance and Elsey, 1986; Lance et al., 2004). Further, in embryonic chickens, adrenal glands produce more testosterone than testes, although this pattern shifts once the chickens hatch (Tanabe et al., 1979). As such, it is possible that some of the androgen hormones in immature turtles are produced by the adrenal gland, not the testes, and therefore are upregulated during activation of the HPA axis. In sexually mature adult male turtles, testes are only active during seasonal enlargement that coincides with breeding (Licht et al., 1985; Valente et al.,

2011). Additionally, nesting influences corticosterone-testosterone relationships in female turtles (Jessop et al., 2000; Valverde et al., 1999; Winters et al., 2016). Therefore, although the testosterone concentrations I measured in this study could suggest that the stress response inflated testosterone concentrations, it is more likely that discrepancies in testosterone concentration were because CI turtles were closer to sexual maturity than NC turtles.

2.5.3 Fitness Implications

The Cort-Fitness Hypothesis delineates an inverse relationship between exposure to stressors and long-term fitness, suggesting that activation of the stress response allows animals to engage in life-saving behaviors at the expense of long-term survival and reproduction (Escribano-Avila et al., 2013; Wingfield and Sapolsky, 2003). This hypothesis is based on data indicating that alterations in physiology that accompany the stress response (i.e., increases in stress hormones, among others), can become directly and indirectly detrimental under chronic conditions (Breuner et al., 2013; Kleist et al., 2018; Morici et al., 1997).

In wildlife, studies suggest that the stress response-fitness relationship is more complicated than increased corticosterone resulting in decreased fitness (Bonier et al., 2009b). For example, the impact of baseline stress hormone concentrations on fitness varies between populations, within populations, and even within a single individual across life history stages (Bonier et al., 2009b; Schoech et al., 2011). In immune-compromised sea turtles, the stress response maintains peak levels for a longer period compared to healthy individuals despite comparable baseline corticosterone concentrations (Aguirre et al., 1995). Therefore, baseline corticosterone concentrations might suggest comparable fitness, although chronic viral infections should influence lifetime fitness. In addition, high levels of circulating stress hormones during reproductive seasons might increase reproductive success (Bonier et al., 2009a). The complicated relationship between stress and fitness is based on constant lifetime reproductive output while environmental stressors are dynamic (Henderson et al., 2017). Therefore, the sum total of all stressors over an animal's life relates to fitness, and quantification of a single event provides an inaccurate measure of overall condition.

While baseline stress hormone concentrations and quantification of acute stress on their own are not reliable predictors of lifetime fitness, chronic activation of the stress response results in chronic activation of a cascade of physiological responses aimed at mitigating stressors. These downstream responses can be quantified through measurements of glucose, free fatty acids, hematocrit, reproductive hormones, and immune function (for a complete review see Breuner et al., 2013). Throughout the lifespan of an individual, chronic stress can result in reduced capacity to respond to competition and predation, frequent incidence of disease and reduced ability to heal, reduced reproductive ability and body mass, high levels of oxidative stress, and shorter life-span. While these parameters provide additional metrics for understanding organismal fitness, the duration required to impose adverse physiological effects highlights the unreliability of predictions about fitness based on acute stressors are unreliable (Breuner et al., 2008).

In this study, juvenile turtles invoked the stress response to increase survival during cold-stunning events, with the long-term projection that turtle stress response would normalize once hypothermic stress passed and therefore not negatively affect reproductive output. Epidermal corticosterone concentrations from turtles in this study were within the range expected for healthy individuals (Aguirre et al., 1995; Jessop and Hamann, 2005); therefore, I suggest that rescued and rehabilitated turtles should not exhibit decreased health or reproductive output following acute cold-stunning. However, I avoid definitive life-long fitness conclusions despite research suggesting that turtles were not chronically stressed because I did not record baseline corticosterone plasma concentrations or downstream stress byproducts that are better indicators of fitness.

2.6 Conclusion

The general health of sea turtles in my study suggested that the cold-stunned turtles were undergoing acute stress that was not indicative of chronically stressful environments and that these animals were in good health (aside from the current cold-stunning). I also demonstrated that it is possible to extract steroid hormones from non-dynamic tissue such as scute and skin, providing a baseline for future research into the quantification of chronic hormone levels in endangered sea turtles. Additionally, the patterns in epidermal hormone concentration are mimicked in plasma hormone concentration. More studies are needed to

measure the complete duration of the sea turtle handling stress response and possible secondary peaks in corticosterone if the stressor is not removed. As with other endangered and threatened species, understanding the physiological responses of individuals to environmental stressors is critically important, especially as these environments are changing with increasing global temperatures. Furthermore, it is likely that cold-stunning events will increase in frequency in NC (and throughout the world) due to unpredictability and future destabilization of systems like the Gulf Stream (Andres, 2016; Epperly et al., 1995, 2007; Griffin et al., 2019). Therefore, rehabilitation of cold-stunned NC juvenile turtles and subsequent release of the turtles is very important for the continued success and conservation of this population.

2.7 Acknowledgements

I would like to thank Dr. E. Christiansen and Dr. M. Godfrey for their assistance with North Carolina permits and sample collection. I would like to thank Dr. W. Mustin, Dr. V. Baboolal and Dr. A. Malabia for collecting samples at the Cayman Islands Turtles farm and securing necessary export permits. This project was approved by the North Carolina Aquarium Institute for Animal Care and Use Committee (protocol #NCA16-005) and Purdue Animal Care and Use Committee (Protocol #1510001309). Samples from the Cayman Islands Turtle Farm were imported under USFWS CITES Permit 18US06369C/9. Samples from North Carolina were collected under permit number 18ST46. Additionally, I would like to thank Dr. D. Rostal, Dr. J. Spotila, and Dr. R. Goforth for reviewing the manuscript and providing council on results. This project was provided by The Leatherback Trust, Equipo Tora Carey, and by the USDA National Institute of Food and Agriculture, Hatch Project 1004115 (to EAF). Funding sources had no role in study design, analysis or interpretation of data, or writing of final report

2.8 Literature Cited

Adiga, U., Yogish, S., 2016. Hemolytic index–A tool to measure hemolysis in vitro. J. Biotechnol. Biochem. 2, 49–52.

Aguirre, A.A., Balazs, G.H., Spraker, T.R., Gross, T.S., 1995. Adrenal and hematological responses to stress in juvenile green turtles (*Chelonia mydas*) with and without fibropapillomas. Physiol. Zool. 68(5), 831–854.

Allen, C.D., Robbins, M.N., Eguchi, T., Owens, D.W., Meylan, A.B., Meylan, P.A., Kellar, N.M., Schwenter, J.A., Nollens, H.H., LeRoux, R.A., Dutton, P.H., 2015. First assessment of the sex ratio for an East Pacific green sea turtle foraging aggregation: validation and application of a testosterone ELISA. PLoS ONE 10(10), e0138861.

Anderson, E.T., Harms, C.A., Stringer, E.M., Cluse, W.M., 2011. Evaluation of hematology and serum biochemistry of cold-stunned green turtles (*Chelonia mydas*) in North Carolina, USA. J. Zoo Wildl. Med. 42(2), 247–255.

Andres, M., 2016. On the recent destabilization of the gulf stream path downstream of cape hatteras. Geophys. Res. Lett. 43, 9836–9842.

Baxter-gilbert, J.H., Riley, J.L., Mastromonaco, G.F., Litzgus, J.D., 2014. A novel technique to measure chronic levels of corticosterone in turtles living around a major roadway. Conserv. Physiol. 2, 1–9.

Behrend, E.N., Kemppainen, R.J., Young, D.W., 1998. Effect of storage conditions on cortisol, total thyroxine, and free thyroxine concentrations in serum and plasma of dogs. J. Am. Vet. Med. Assoc. 212, 1564–1568.

Berkvens, C.N., Hyatt, C., Gilman, C., Pearl, D.L., Barker, I.K., Mastromonaco, G.F., 2013. Validation of a shed skin corticosterone enzyme immunoassay in the African House Snake (*Lamprophis fuliginosus*) and its evaluation in the Eastern Massasauga Rattlesnake (*Sistrurus catenatus catenatus*). Gen. Comp. Endocrinol. 194, 1–9.

Bonier, F., Moore, I.T., Martin, P.R., Robertson, R.J., 2009a. The relationship between fitness and baseline glucocorticoids in a passerine bird. Gen. Comp. Endocrinol. 163, 208–213.

Bonier, F., Martin, P.R., Moore, I.T., Wingfield, J.C., 2009b. Do baseline glucocorticoids predict fitness? Trends Ecol. Evol. 24(11), 634–642.

Boucher, E., Provost, P.R., Tremblay, Y., 2014. Ontogeny of adrenal-like glucocorticoid synthesis pathway and of 20α-hydroxysteroid dehydrogenase in the mouse lung. BMC Res. Notes 7(1):119, 1–10.

Breuner, C.W., Patterson, S.H., Hahn, T.P., 2008. In search of relationships between the acute adrenocortical response and fitness. Gen. Comp. Endocrinol. 157, 288–295.

Breuner, C.W., Delehanty, B., Boonstra, R., 2013. Evaluating stress in natural populations of vertebrates: total CORT is not good enough. Funct. Ecol. 27(1), 24–36.

Burghardt, G.M., 2013. Environmental enrichment and cognitive complexity in reptiles and amphibians: concepts, review, and implications for captive populations. Appl. Anim. Behav. Sci. 147(3-4), 286–298.

Chaloupka, M., 2002. Stochastic simulation modelling of southern Great Barrier Reef green turtle population dynamics. Ecol. Model. 148(1), 79–109.

Chaloupka, M., Limpus, C. and Miller, J., 2004. Green turtle somatic growth dynamics in a spatially disjunct Great Barrier Reef metapopulation. Coral Reefs 23(3), 325–335.

Cockrem, J.F., 2013. Individual variation in glucocorticoid stress responses in animals. Gen. Comp. Endocrinol. 181, 45–58.

Cree, A., Guillette Jr, L.J., Cockrem, J.F., Joss, J.M., 1990. Effects of capture and temperature stresses on plasma steroid concentrations in male tuatara (*Sphenodon punctatus*). J. Exp. Zool. 253(1), 38–46.

Dayger, C.A., Lutterschmidt, D.I., 2016. Seasonal and sex differences in responsiveness to adrenocorticotropic hormone contribute to stress response plasticity in red-sided garter snakes (*Thamnophis sirtalis parietalis*). J. Exp. Biol. 219(7), 1022–1030.

Elsey, R.M., Lance, V.A., Joanen, T., McNease, L., 1991. Acute stress suppresses plasma estradiol levels in female alligators (*Alligator mississippiensis*) Comp. Biochem. Physiol. 100A, 649–651.

Escribano-Avila, G., Pettorelli, N., Virgós, E., Lara-Romero, C., Lozano, J., Barja, I., Cuadra, F.S., Puerta, M., 2013. Testing Cort-Fitness and Cort-Adaptation hypotheses in a habitat suitability gradient for roe deer. Acta Oecol. 53, 38–48.

Epperly, S.P., Braun, J., Veishlow, A., 1995. Sea turtles in North Carolina waters. Conserv. Biol. 9(2), 384–394.

Epperly, S.P., Braun-McNeill, J., Richards, P.M., 2007. Trends in catch rates of sea turtles in North Carolina, USA. Endanger. Species Res. 3, 283–293.

Fairhurst, G.D., Bond, A.L., Hobson, K.A., Ronconi, R.A., 2015. Feather-based measures of stable isotopes and corticosterone reveal a relationship between trophic position and physiology in a pelagic seabird over a 153-year period. Ibis 157(2), 273–283.

Goodhead, L.K., MacMillan, F.M., 2017. Measuring osmosis and hemolysis of red blood cells. Adv. Physiol. Educ. 41(2), 298–305.

Gregory, L.F., Gross, T.S., Bolten, A.B., Bjorndal, K.A., Guillette Louis, J., 1996. Plasma Corticosterone Concentrations Associated with Acute Captivity Stress in Wild Loggerhead Sea Turtles (*Caretta caretta*). Gen. Comp. Endocrinol. 104, 312–320.

Gregory, L.F., Schmid, J.R., 2001. Stress responses and sexing of wild Kemp's ridley sea turtles (*Lepidochelys kempii*) in the northeastern Gulf of Mexico. Gen. Comp. Endocrinol. 124(1), 66–74.

Griffin, L.P., Griffin, C.R., Finn, J.T., Prescott, R.L., Faherty, M., Still, B.M., Danylchuk, A.J., 2019. Warming seas increase cold-stunning events for Kemp's ridley sea turtles in the northwest Atlantic. PloS ONE 14(1), e0211503.

Heimbürge, S., Kanitz, E., Otten, W., 2019. The use of hair cortisol for the assessment of stress in animals. Gen. Comp. Endocrinol. 207, 10–17.

Henderson, L.J., Evans, N.P., Heidinger, B.J., Herborn, K.A., Arnold, K.E., 2017. Do glucocorticoids predict fitness? Linking environmental conditions, corticosterone and reproductive success in the blue tit, *Cyanistes caeruleus*. Royal Soc. Open Sci. 4(10), p.170875.

Hochscheid, S., Bentivegna, F., Speakman, J.R., 2002. Regional blood flow in sea turtles: implications for heat exchange in an aquatic ectotherm. Physiol. Biochem. Zool. 75(1), 66–76.

Hunt, K.E., Innis, C., Rolland, R.M., 2012. Corticosterone and thyroxine in cold-stunned kemp's ridley sea turtles (*Lepidochelys kempii*). J. Zoo Wildl. Med. 43(3), 479–493.

IUCN (International Union for Conservation of Nature and Natural Resources)., 2004. IUCN redlist of threatened species. The Conservation Union, Cambridge. www.iucnredlist.org

Jensen, M.P., Allen, C.D., Eguchi, T., Bell, I.P., LaCasella, E.L., Hilton, W.A., Hof, C.A., Dutton, P.H., 2018. Environmental warming and feminization of one of the largest sea turtle populations in the world. Curr. Biol. 28(1), 154–159.

Jessop, T.S., Hamann, M., Read, M.A., Limpus, C.J., 2000. Evidence of a hormonal tactic maximizing green turtle reproduction in response to a passive ecological stressor. Gen. Comp. Endocrinol. 118, 407–417.

Jessop, T. S., Hamann, M., 2004. Hormonal and metabolic responses to nesting activities in the green turtle, *Chelonia mydas*. J. Exp. Mar. Biol. Ecol. 308, 253–267.

Jessop, T.S., Hamann, M., 2005. Interplay between age class, sex and stress response in green turtles (*Chelonia mydas*). Aust. J. Zool. 53(2), 131–136.

Jones, S.M., Bell, K., 2004. Plasma corticosterone concentrations in males of the skink *Egernia whitii* during acute and chronic confinement, and over a diel period. Comp. Biochem. Physiol., Part A Mol. Integr. Physiol. 137(1), 105–113.

Keller, K.A., Innis, C.J., Tlusty, M.F., Kennedy, A.E., Bean, S.B., Cavin, J.M., Merigo, C., 2012. Metabolic and respiratory derangements associated with death in cold-stunned Kemp's ridley turtles (*Lepidochelys kempii*): 32 cases (2005–2009). J. Am. Vet. Med. Assoc. 240(3), 317–323.

Killilea, D.W., Rohner, F., Ghosh, S., Otoo, G.E., Smith, L., Siekmann, J.H., King, J.C., 2017. Identification of a hemolysis threshold that increases plasma and serum zinc concentration. J. Nutr. 147(6), 1218–1225.

Kleist, N.J., Guralnick, R.P., Cruz, A., Lowry, C.A., Francis, C.D., 2018. Chronic anthropogenic noise disrupts glucocorticoid signaling and has multiple effects on fitness in an avian community. Proc. Natl. Acad. Sci. 115(4), E648–E657.

Lance, V.A., Elsey, R.M., 1986. Stress-induced suppression of testosterone secretion in male alligators. J. Exp. Zool. 239, 241–246.

Lance, V.A., Elsey, R.M., 1999. Plasma catecholamines and plasma corticosterone following restraint stress in juvenile alligators. J. Exp. Zool. 283(6), 559–565.

Lance, V.A., Grrumbles, J.S., Rostal, D.C., 2001. Sex differences in plasma corticosterone in desert tortoises, *Gopherus agassizii*, during the reproductive cycle. J, Exp. Zool. 289, 285–289.

Lance, V.A., Elsey, R.M., Butterstein, G., Trosclair III, P.L., 2004. Rapid suppression of testosterone secretion after capture in male American alligators (*Alligator mississippiensis*). Gen. Comp. Endocrinol. 135(2), 217–222.

Licht, P., Wood, J.F., Wood, F.E., 1985. Annual and diurnal cycles in plasma testosterone and thyroxine in the male green sea turtle *Chelonia mydas*. Gen. Comp. Endocrinol. 57(3), 335–344.

Mahmoud, I.Y., Guillette Jr, L.J., McAsey, M.E., Cady, C., 1989. Stress-induced changes in serum testosterone, estradiol-17β and progesterone in the turtle, Chelydra serpentina. Comp. Biochem. Physiol. Part A Physiol. 93(2), 423–427.

Moberg, G.P., 2000. Biological responses to stress: implications for animal welfare. In: Moberg, G.P., Mench, J.A. (Eds), The Biology of Animal Stress. CABI Publishing, Wallingford, New York, pp. 1–21.

Möstl, E., Palme, R., 2002. Hormones as indicators of stress. Domest. Anim. Endocrinol. 23, 67–74.

Moore, I.T., Jessop, T.S., 2003. Stress, reproduction, and adrenocortical modulation in amphibians and reptiles. Horm. Behav. 43, 39–47.

Morici, L.A., Elsey, R.M., Lance, V.A., 1997. Effects of long-term corticosterone implants on growth and immune function in juvenile alligators, *Alligator mississippiensis*. J. Exp. Zool. 279(2), 156–162.

Morreale, S.J., Meylan, A.B., Sadove, S.S., Standora, E.A., 1992. Annual occurrence and winter mortality of marine turtles in New York waters. J. Herpetol. 26(3), 301–308.

Narayan, E.J., Molinia, F.C., Cockrem, J.F., Hero, J.M., 2012. Changes in urinary testosterone and corticosterone metabolites during short-term confinement with repeated handling in wild male cane toads (*Rhinella marina*). Aust. J. Zool. 59(4), 264–269.

Owens, D.W., Ruiz, G.J., 1980. New Methods of Obtaining Blood and Cerebrospinal Fluid from Marine Turtles. Herpetologica 36, 17–20.

Paladino, F.V., O'Connor, M.P., Spotila, J.R., 1990. Metabolism of leatherback turtles, gigantothermy, and thermoregulation of dinosaurs. Nature 344(6269), 858–860.

Pirhalla, D.E., Sheridan, S.C., Ransibrahmanakul, V., Lee, C.C., 2015. Assessing cold-snap and mortality events in south Florida coastal ecosystems: Development of a biological cold stress index using satellite SST and weather pattern forcing. Estuaries Coast 38(6), 2310–2322.

Romero, L.M., Wikelski, M., 2001. Corticosterone levels predict survival probabilities of Galapagos marine iguanas during El Nino events. Proc. Natl. Acad. Sci. 98(13), 7366– 7370.

Romero, L.M., Wikelski, M., 2002. Exposure to tourism reduces stress-induced corticosterone levels in Galapagos marine iguanas. Biol. Conserv. 108, 371–374.

Sapolsky, R.M., Romero, L.M., Munck, A.U., 2000. How do glucocorticoids influence stress responses? Integrating permissive, suppressive, stimulatory, and preparative actions. Endocr. Rev. 21, 55–89.

Schoech, S.J., Rensel, M.A., Heiss, R.S., 2011. Short-and long-term effects of developmental corticosterone exposure on avian physiology, behavioral phenotype, cognition, and fitness: a review. Curr. Zool. 57(4), 514–530.

Schwartz, F.J., 1978. Behavioral and tolerance responses to cold water temperatures by three species of sea turtles (*Reptilia, Cheloniidae*) in North Carolina. Fla. Mar. Res. Publ. 33, 16–18.

Tanabe, Y., Nakamura, T., Fujioka, K., Doi, O., 1979. Production and secretion of sex steroid hormones by the testes, the ovary, and the adrenal glands of embryonic and young chickens (*Gallus domesticus*). Gen. Comp. Endocrinol. 39(1), 26–33.

Valente, A.L.S., Velarde, R., Parga, M.L., Marco, I., Lavin, S., Alegre, F., Cuenca, R., 2011. Reproductive status of captive loggerhead sea turtles based on serum levels of gonadal steroid hormones, corticosterone and thyroxin. Vet. J. 187(2), 255–259.

Valverde, R.A., Owens, D.W., MacKenzie, D.S., Amoss, M.S., 1999. Basal and stress-induced corticosterone levels in olive ridley sea turtles (*Lepidochelys olivacea*) in relation to their mass nesting behavior. J. Exp. Zool. 284(6), 652–662.

Warnock, F., McElwee, K., Seo, R.J., McIsaac, S., Seim, D., Ramirez-Aponte, T., Macritchie, K.A.N, Young, A.H., 2010. Measuring cortisol and DHEA in fingernails: a pilot study. Neuropsychiatr. Dis. Treat. 6, 1–7.

Williard, A.S., Hall, A.G., Fujisaki, I., McNeill, J.B., 2017. Oceanic overwintering in juvenile green turtles *Chelonia mydas* from a temperate latitude foraging ground. Mar. Ecol. Prog. Ser. 564, 235–240.

Wingfield, J.C., Sapolsky, R.M., 2003. Reproduction and resistance to stress: when and how. J. Neuroendocrinol. 15, 711–724

Winters, J.M., Carruth, W.C., Spotila, J.R., Rostal, D.C., Avery, H.W., 2016. Endocrine indicators of a stress response in nesting diamondback terrapins to shoreline barriers in Barnegat Bay, NJ. Gen. Comp. Endocrinol. 235, 136–141.

Witherington, B.E., Ehrhardt, L., 1989. Hypothermic stunning and mortality of marine turtles in the Indian River Lagoon System, Florida. Copeia 1989 (3), 696–703.

Wynne, S.P., 2016. Biometric relationships, size class structures, and growth rates of foraging Hawksbill (*Eretmochelys imbricata*) and Green (*Chelonia mydas*) sea turtles in Anguilla, with observations on occurrence and prevalence of fibropapilloma. Anguilla Fish. Mar. Resour. Res. Bull. 04, 1–9.

Table 2.1 Morphology in Cold-Stunned Green Turtles

Morphological measurements and hormone concentrations (corticosterone, cortisol, dihydrotestosterone (DHT), and testosterone) from juvenile green turtles rescued by the North Carolina Aquarium during the 2017 and 2018 cold-stunning events. PL = plasma, EP = epidermis, plasma and epidermal corticosterone and cortisol are measured in ng/mL and ng/mg respectively, plasma and epidermal DHT and testosterone are measured in pg/mL and pg/mg respectively. Data presented as mean ± standard deviation for turtles sampled each year (January – March) of 2017 and 2018. Statistical results from multiple one-way ANOVAs using log transformed hormone concentrations. Epidermal hormone concentrations were not significant and have been excluded from this table.

Parameter	2017 (mean±SD)	2017 Range	2018 (mean±SD)	2018 Range	n	Statistical Results	
						$F_{1,19}$	p
CCL (cm)	32.5 ± 2.9	29 - 36	38 ± 3.7	33.7 – 43.8	15	9.722*	0.008*
Mass (kg)	3 ± 0.8	2.1 – 4.3	5.3 ± 1.5	3.4 - 8	21	20.377	< 0.001
PL Corticosterone (ng/mL)	37.5 ± 37	5.8 – 126.45	101.76 ± 54.6	53.4 – 193.3	21	12.352	0.002
PL Cortisol (ng/mL)	4.95 ± 3.1	0.7 – 10.3	4.81 ± 4.3	1 - 10	21	0.244	0.627
PL DHT (pg/mL)	13.96 ± 10.52	3.5 - 41	16.72 ± 10.48	4 – 35.5	21	0.543	0.470
PL Testosterone (pg/mL)	27.71 ± 16.63	4.5 – 51.5	36.5 ± 34.13	3 – 92.5	21	0.046	0.833

*CCL had degrees of freedom of 1,13.

Table 2.2 Comparison of Tissue Hormone Concentrations in Cold-Stunned Green Turtles

Post-Hoc ANOVA test results from repeated measurers MANOVA comparing hormone concentration between plasma and scute samples from cold-stunned juvenile green turtles taken upon arrival to the North Carolina Aquarium (NC) during the 2017 and 2018 cold stunning events (January – March). PL = plasma, EP = epidermis, SC = scute. Corticosterone and cortisol were measured in ng/mL and ng/mg respectively; dihydrotesterone (DHT) and testosterone were measured in pg/mL and pg/mg respectively.

Site	Hormone	Concentration (mean ± SD)	Concentration Range	n	Post-Hoc ANOVA	
					$F_{1,19}$	p
NC	PL Corticosterone	64.04 ± 54.98	5.8 – 193.3	21	522.254	< 0.001
	SC Corticosterone	0.41 ± 0.85	0.01 – 3.3			
	PL Cortisol	4.89 ± 3.58	0.7 – 10.3	21	253.259	< 0.001
	SC Cortisol	0.04 ± 0.11	0 – 0.4			
	PL DHT	15.14 ± 10.33	3.5 - 41	21	233.79	< 0.001
	SC DHT	0.29 ± 0.43	0 – 1.5			
	PL Testosterone	31.48 ± 25.26	3 – 92.5	21	116.207	< 0.001
	SC Testosterone	0.6 ± 1.02	0 – 4.8			

Table 2.3 Comparison of Tissue Hormone Concentrations in Captive Green Turtles

Post-Hoc ANOVA test results from repeated measurers MANOVA comparing hormone concentration between plasma, epidermal, and scute samples from juvenile green turtles from the Cayman Islands Turtle Farm (CI) in 2018. PL = plasma, EP = epidermis, SC = scute. Corticosterone and cortisol were measured in ng/mL and ng/mg; dihydrotestosterone (DHT) and testosterone were measured in pg/mL and pg/mg.

Site	Hormone	Concentration	Concentration Range	n	Post-Hoc ANOVA	
					$F_{2,24}$	p
CI	PL Corticosterone	25.78 ± 22.89	2.5 – 76.7			
	EP Corticosterone	0.49 ± 0.8	0.03 – 2.5	13	259.054	< 0.001
	SC Corticosterone	0.01 ± 0.01	0.002 – 0.03			
	PL Cortisol	0.84 ± 0.4	0.3 – 1.5			
	EP Cortisol	0.01 ± 0.01	0 – 0.03	13	94.333	< 0.001
	SC Cortisol	0 ± 0	0 – 0.002			
	PL DHT	497.88 ± 263.4	61 - 980			
	EP DHT	1.49 ± 1.39	0.19 – 4.99	13	182.763	< 0.001
	SC DHT	0.98 ± 2.13	0.13 – 7.95			
	PL Testosterone	840.6 ± 543.6	245 - 2034			
	EP Testosterone	2.04 ± 0.78	0.36 – 3.4	13	518.306	< 0.001
	SC Testosterone	1.32 ± 0.85	0.14 – 2.72			

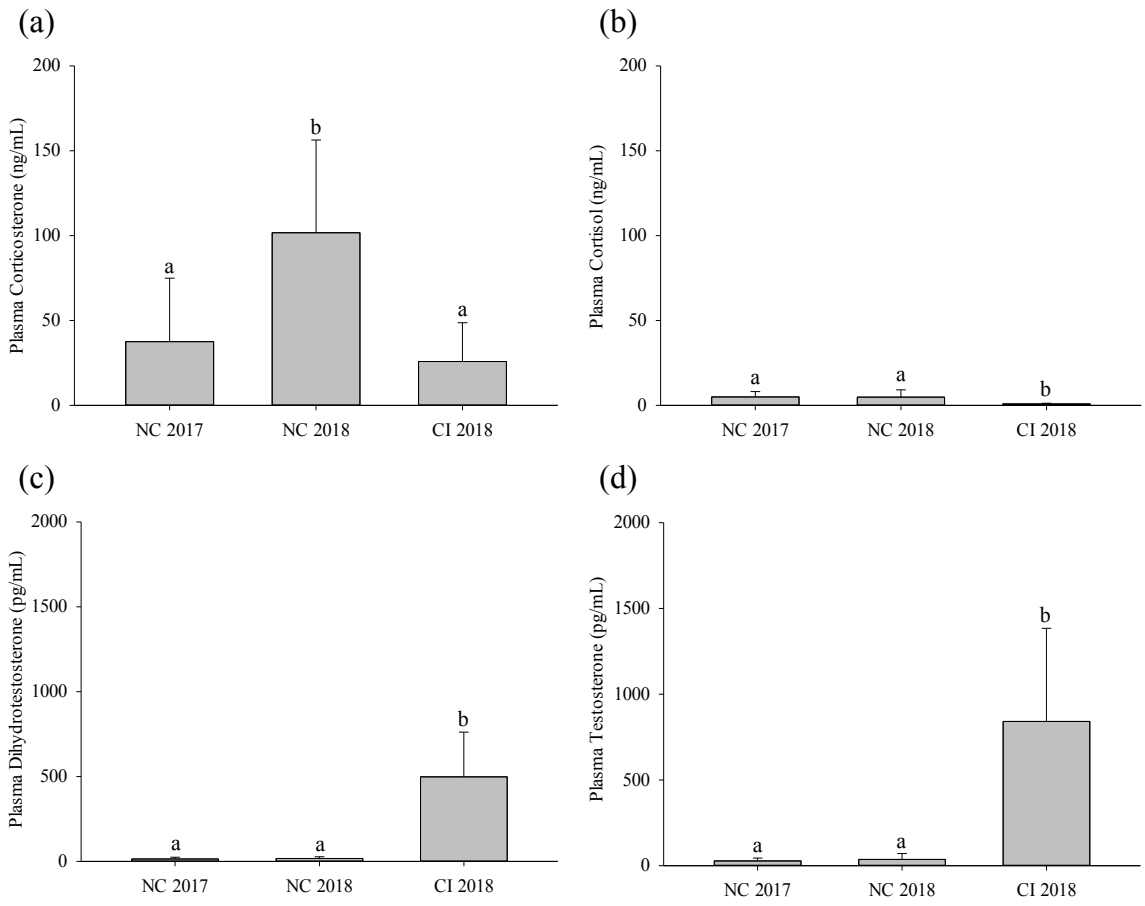

Figure 2.1 Plasma Hormone Concentrations in Green Turtles
Plasma concentrations of corticosterone (a), cortisol (b), dihydrotestosterone (c) and testosterone (d) in juvenile green sea turtle from cold-stunned turtles sampled on intake to the North Carolina Aquarium (NC) during the winter cold stunning events (January – March) of 2017 (N = 12) and 2018 (N = 9), and from the Cayman Islands Turtle Farm (CI, N = 13) during the 2018 health assessment. Letters above bars represent post-hoc ANOVA statistical tests with significant threshold of $p < 0.05$.

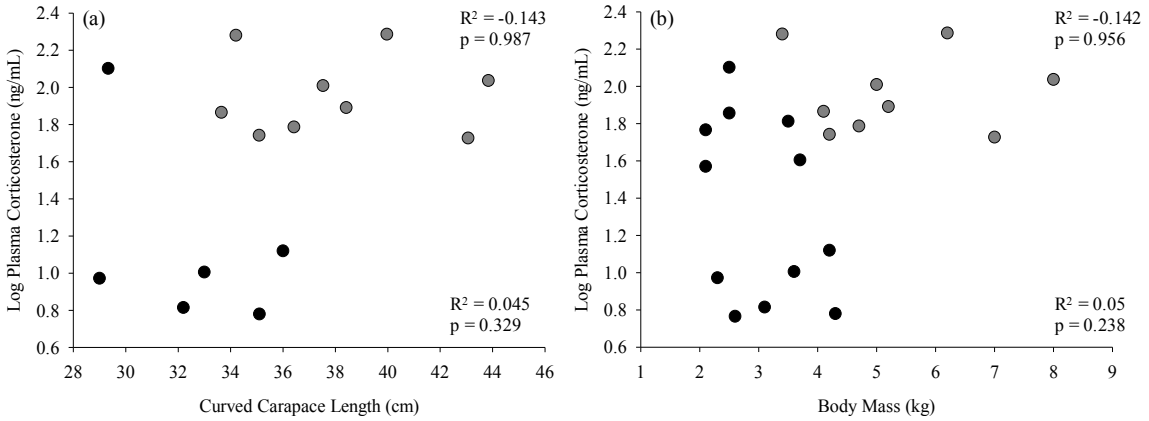

Figure 2.2 Linear Relationships between Corticosterone and Body Size
Linear relationship between curved carapace length (CCL, a) and body mass (b) against log transformed plasma corticosterone concentration in cold-stunned juvenile green turtles rescued by the North Carolina Aquarium during the 2017 (black) and 2018 (gray) cold-stunning events (January – March). The data include 12 turtles in 2018, and 9 turtles in 2017.

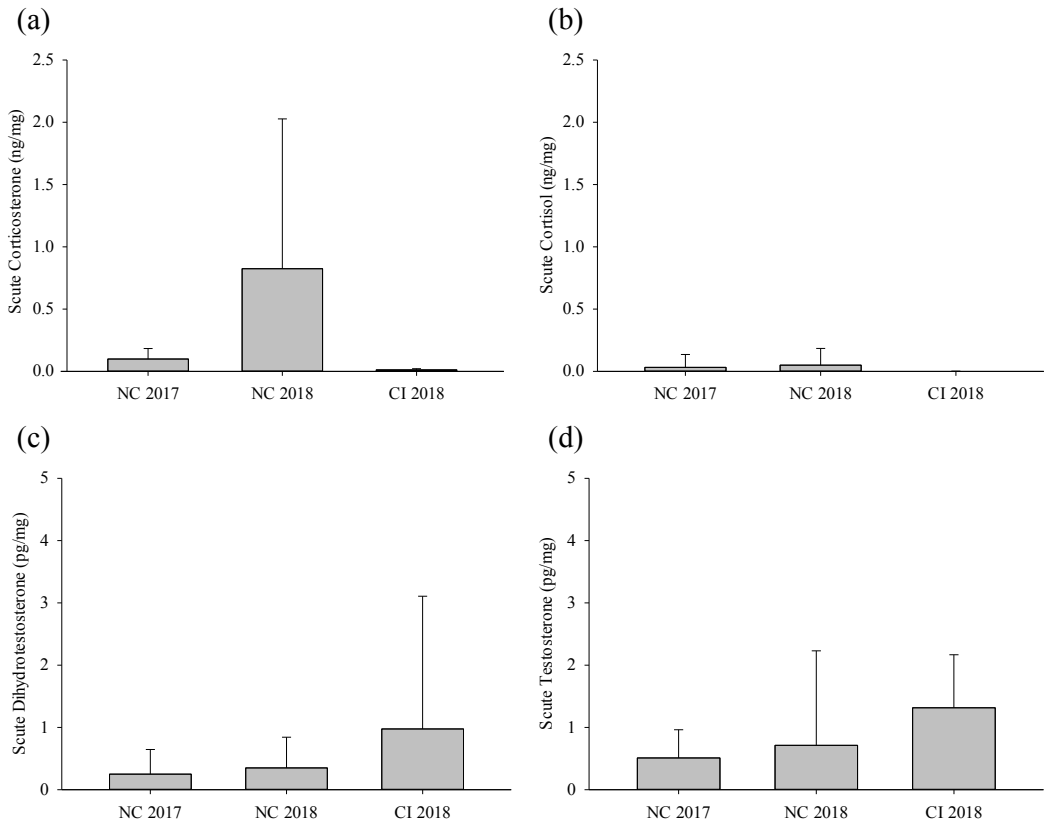

Figure 2.3 Scute Concentrations of Hormones in Green Turtles
Scute concentrations of corticosterone (a), cortisol (b), dihydrotestosterone (c) and testosterone (d) in juvenile green sea turtle from cold-stunned turtles sampled on intake to the North Carolina Aquarium (NC) during the winter cold stunning events (January – March) of 2017 (N = 12) and 2018 (N = 9), and from the Cayman Islands Turtle Farm (CI, N = 13) during the 2018 health assessment. There was no statistical difference between years or sites (one-way MANOVA) with a significant threshold of $p < 0.05$.

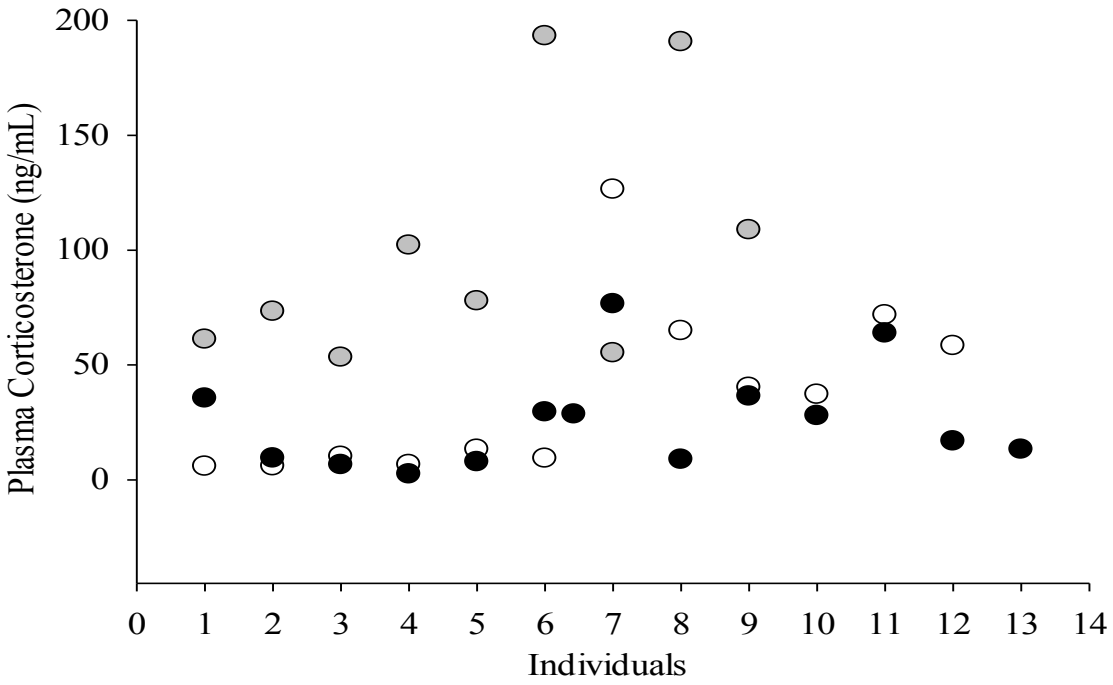

Figure 2.4 Individual Variability in Plasma Corticosterone
Individual variation in plasma corticosterone for all turtles in this study. Samples from cold-stunned juvenile green turtles from North Carolina (NC) were collected once turtles were returned to the Aquarium, post-rescue, during the 2017 (N = 12; white circles) and 2018 (N = 9; gray circles) cold-stunning events (January – March). Samples from the Cayman Islands Turtle Farm (CI) were collected from captive juvenile green turtles during annual health assessments in 2018 (N = 13; black circles).

CHAPTER 3. LIPIDOMICS SUGGESTS SPECIES SPECIFICITY AND COLD ADAPTION IN PACIFIC GREEN AND HAWKSBILL TURTLES

Chelsea E. Clyde-Brockway, Christina R. Ferreira, Elizabeth A. Flaherty and Frank V. Paladino.

3.1 Abstract

Sea turtles rely on external heat to maintain body temperature and physiological adaptions that allow them to exploit cold water foraging resources. Because sea turtles are endangered, application of powerful analytical tools such as lipidomics assists in quantification of latent aspects of ecology and health. Here, I applied MRM-profiling to explore diverse lipid classes and develop baseline lipid profiles in foraging juvenile green (*Chelonia mydas*) and hawksbill (*Eretmochelys imbricata*) turtles and assessed species and seasonal variability. I analyzed plasma lipids from live caught turtles foraging in North Pacific Costa Rica during 2017. I collected a single plasma sample from 17 black morphotype green turtles, 11 yellow morphotype green turtles, and 16 hawksbill turtles. I identified 688 baseline lipids and metabolites belonging to 10 lipid classes (sphingomyelin, phosphatidylcholine, free fatty acids, cholesteryl esters, phosphatidylserine, phosphatidylinositol, phosphatidylglycerol, phosphatidylethanolamine, ceramides, and triglycerides), and 1 metabolite group (acyl-carnitines), and measured significant species and season differences in relative ion intensities. Lipids varied in chain length and saturation level, and some lipids (n = 100) were weakly correlated to body size. In total, I isolated 126 lipids with heterogeneous relative ion intensities between species, suggesting foraging niche specificity in physiology; however, principle component analyses clustered turtles into species groups (combining both morphotypes), indicating that phylogeny also determines lipid profiles. Further, I isolated 43 lipids that varied with season, indicating compositional shifts in lipid profiles favoring unsaturated lipids in the colder seasons. Seasonal variability in lipid profiles suggests cold-adaptation that retain membrane permeability as temperature drops, which allows turtles to maintain metabolism across variable water temperatures. I did not record many foraging lipids (n = 7) that varied across

seasons. However, from these lipids hawksbill turtle demonstrated seasonal adaption not present in green turtles. Therefore, I concluded that green turtles in this study continued to forage year-round while hawksbill turtles varied foraging and metabolism between seasons. Here, I provide the framework to apply lipidomics in the assessment of health, physiology, and behavior in endangered sea turtles.

3.2 Introduction

Global oceanic temperatures fluctuate on diurnal, seasonal, and multiannual cycles, which poses physiological challenges to sea turtle survival (Davenport, 1997; Mrosovsky, 1980; Stuhldreier et al., 2015). While sea turtles depend on external sources of heat to maintain body temperature, they also rely on regional upwelling events that bring to the surface cold water and sedimentary nutrients needed for primary productivity (Broenkow, 1965; Lavín et al., 2006; Stuhldreier et al., 2015). Therefore, sea turtles must balance avoiding hypothermic shock with physiological adaptions to withstand cold water in order to forage (Schwartz, 1978; Spotila and Standora, 1985). Failure to behaviorally and metabolically adapt results in reduced reproductive output and mortality (Harrison et al., 2011; Solow et al., 2002). In Hawaii, green turtles bask on the beach during the day, presumably to cope with cold water temperatures (Van Houtan et al., 2015; Whittow and Balazs, 1982). Further, sea turtles alter dive behavior in response to cold water and float at the surface which increases absorbtion of solar radiation (Hochscheid et al. 2010). Additionally, sea turtles avoid cold water by migrating into foraging habitats when water temperatures increase before vacating these environments as water temperatures decrease (Coles and Musick, 2000; Crear et al., 2016).

Sea turtles rely on physiological adaptations to withstand cold water temperatures while foraging. In leatherback sea turtles (*Dermochelys coriacea*), the thermal inertia generated by large body size is sufficient to buffer loss of body heat while foraging (Paladino et al., 1990). However, the smaller hard-shelled turtles, although still capable of regional endothermy, do not possess comparable thermal inertia (Hochscheid et al., 2002; Standora et al., 1982). Consequently, they must rely on alternative adaptations to maintain metabolism in cold water. While marine mammals vary body fat composition by season or location to aid in thermoregulation (Liwanag et al., 2012), reptiles in general use body fat

stores as nutritional reservoirs for hibernation (Edge et al., 2009), to avoid starvation (Price et al. 2013, Price, 2017), and for reproduction (Lance and Rostal, 2002). In sea turtles, body fat reserves increase in foraging habitats and decrease during nesting seasons, suggesting that the primary purpose of body fat is reproduction (Kwan, 1994). However, both mammals and herpetofauna can achieve temperature adaptation through seasonally differential composition of membrane lipids (Hazel and Williams, 1990; Mineo et al., 2019; Price et al., 2017), yet, the lipidomics of temperature adaption is not documented in sea turtles.

Because sea turtles are endangered, research emphasizes understanding life history patterns to better guide conservation strategies. To date, lipid studies in sea turtles have focused on foraging ecology (Price et al., 2013) and reproductive biology (Hamann et al., 2002; Kawazu et al., 2015; Kwan, 1994). However, lipid dynamics can also provide information on non-temperature related aspects of physiology, such as chemosensory communication in lizards (Alberts et al., 1992; Ibáñez et al., 2018; Khannoon et al., 2011), lung structure and function (Daniels et al., 1996; Gutierrez et al., 2015; Johnston et al., 2001), and as indication of disease status (Zhao et al., 2015) and aging (Almaida-Pagan et al., 2019). Comprehensive lipid-profiling is a powerful tool that highlights latent aspects of animal ecology and health. However, targeted assessment required to quantify lipid concentrations depends on knowledge of specific lipid chain lengths and saturation levels. To resolve this, I isolated lipids and acyl-carnitines (a metabolite) from sea turtle plasma. Here, I present all lipids present in foraging non-reproductive green (*Chelonia mydas,* Linnaeus, 1758) and hawksbill (*Eretmochelys imbricata,* Linnaeus, 1766) sea turtles from Costa Rica, including specific chain lengths and saturation levels. I also compared lipid and metabolite profiles between foraging green and hawksbill sea turtles during normal El Niño conditions (Wang et al., 2017) by MRM-profiling (de Lima et al. 2018). Specifically, I isolated lipids from 10 lipid classes (Sphingomyelin, Phosphatidylcholine, Free Fatty Acids, Cholesteryl Esters, Phosphatidylserine, Phosphatidylinositol, Phosphatidylglycerol, Phosphatidylethanolamine, Ceramides, and Triglycerides), one metabolite group (Acyl-Carnitines) and investigated species differences and seasonality of lipids and metabolites in turtles foraging in Costa Rica. I identified reference lipids and metabolites and provided

a framework in which to investigate health and productivity in endangered sea turtles using an easy and cost-effective method.

3.3 Methods

3.3.1 Study Area

I conducted this study during 2017 in Matapalito Bay (10.9°N; -85.79°W) and Salinas Bay (11.1°N; -85.7°W) in North Pacific Costa Rica (Fig. 3.1). This area represents one of three major upwelling areas along the Central American coast (Lavín et al., 2006). Costa Rican upwelling is especially strong because of the interaction between trade winds and Costa Rica Dome water patterns (Broenkow, 1965; Lavín et al., 2006; Stuhldreier et al., 2015). Therefore, sea turtles inhabiting these waters are exposed to unusually cold-water temperatures (< 20°C at 10 m) during upwelling that takes place in the dry season (November – March), and warmer temperatures (~28°C at 10 m) during the wet season when upwelling is reduced (April – October). This transition time between seasons is not definite and varies between years. Additionally, the Eastern Pacific is exposed to multiannual (~4 yr) water cycles known as the El Niño Southern Oscillation (ENSO). During El Niño years, water temperatures are warmer than usual (decreased primary productivity), while La Niña years are characterized by colder than normal temperature and increased upwelling (Wang et al., 2017). In this study, I collected samples during normal El Niño conditions (https://ggweather.com/enso/oni.htm).

3.3.2 Study Animals

In North Pacific Costa Rica, yellow and black morphotype green turtles (CM) and hawksbill turtles (EI) inhabit coastal sites concurrently (Bowen et al., 1992). I live captured black, yellow, and hawksbill turtles using turtle tangle nets (Heidemeyer et al., 2014). I deployed nets in each bay once a month; however, I canceled the monthly sampling during dangerous weather. Further, I opportunistically hand-caught turtles encountered when snorkeling. I brought turtles into the boat for processing, where I measured curved carapace length (CCL; ± 0.5 cm), and mass (Detecto 11S200HKG “S” hook hanging scale, Webb City, MO; ± 0.5 kg). To avoid pseudo-replication, I marked turtles with a unique passive

integrated transponder (PIT) tag injected into the right shoulder (AVID2028 FriendChip, Norco, California, USA), and metal flipper tags (Style 681IC, National Band and Tag Company, Newport, KY, USA) in both hind flippers (Heidemeyer et al., 2018).

3.3.3 Plasma Collection and Preparation

I collected a single blood sample (< 1 ml/kg) per individual using a 21 g non-heparinized needle from the cervical sinus (Owens and Ruiz, 1980), transferred the sample to a lithium-heparin tube, and stored it on ice until I returned to the lab. At the lab in Costa Rica, I centrifuged blood samples for 5 min at 3000 rpm (Clay Adams Analytical Centrifuge, New York, NY), isolated the plasma in a non-heparinized tube, and stored the plasma at -18°C for up to 1 year until I transported samples back to Purdue University. At Purdue University, I stored all samples at -20°C until analysis (within 9 months). I quantified the level of hemolysis present in each plasma samples (0, + 1, + 2, + 3, Adiga and Yogish, 2016; Goodhead and MacMillan, 2017) and excluded samples with a hemolysis score > 1.0 from analysis to avoid contaminated results (Perrault J, unpublished data).

3.3.4 Lipid Analysis

I extracted lipids and fat-soluble metabolites from plasma samples following the chloroform-methanol Bligh and Dyer (1959) lipid extraction procedure and stored extracted lipids at -80°C until analysis. For identification of lipid profiles, I used a recently published strategy, MRM-profiling mass spectrometry (de Lima et al., 2018), which uses a triple-quadrupole Agilent 6410 QQQ (Agilent Technologies, Santa Clara, CA, USA) and a two-step process to identify relevant lipids (de Lima et al. 2018). This allowed me to identify and process only lipids and metabolites with ion intensities greater than that of the blank, suggesting significance to sea turtle physiology (for complete methods see appendix). MRM lipid-profiling provides information on diverse lipid classes (Sphingomyelin, Phosphatidylcholine, Free Fatty Acids, Cholesteryl Esters, Phosphatidylserine, Phosphatidylinositol, Phosphatidylglycerol, Phosphatidylethanolamine, Ceramides, and Triglycerides), one metabolite group (Acyl-Carnitines), and aids in screening for shifts in lipid physiology that indicate environmental

pressures, metabolic impairments and resource allocation (de Lima et al., 2018; Cordeiro et al., 2017; Wenk, 2005; Zhao et al., 2015). I processed the raw MRM mass spectrometry data using an in-house script and MRM transitions and exported the resulting ion intensity values to Microsoft Excel (v2016, Microsoft Corporation, Redmond, WA). I normalized the absolute ion intensity of lipids and metabolites against the total ion current of the class for each turtle. The resulting relative ion intensity of lipids and metabolites represented the proportion of total class ion current for each turtle. To investigate the diversity of lipids present in the sea turtles, I divided each lipid class by carbon chain length (short, medium, long). I categorized short, medium, and long lipids by organizing lipids by carbon chain length, then calculating the difference between the longest and shortest chain in each class followed by division of this difference by three and presented the results as percent (%) of lipid class profile. To quantify the saturation of lipids present in sea turtles, I divided each lipid class by saturation (0 = unsaturated, 1-2 = mono and di-unsaturated lipids, 3+ = polyunsaturated lipids) and presented percent of lipid profile within each saturation level. For significant lipids (those that varied by species or season), I again presented percent of significant lipid profiles at each saturation level.

3.3.5 Statistical Analysis

I conducted univariate and multivariate analyses on relative ion abundances using MetaboAnalyst 4.0 (http://www.metaboanalyst.ca, Rv3.4.3; Chong and Xia, 2018; Chong et al., 2018). For each analysis, I normalized the data within MetaboAnalyst using the auto-scaling method (mean-centered and divided by the standard deviation of each variable). To overview the data, I used principal component analyses (PCA) and a partial least-squares discriminant analysis (PLS-DA) to evaluate clustering of turtles based on lipid profiles. Within MetaboAnalyst, I then used the permutation test function with 100 iterations and the cross-validation (CV) results to determine if the PLS-DA model fit (Westerhuis et al., 2008). If my PLS-DA permutations test was not significant or CV lacked predictive ability, I used my PCA model. To identify differential lipids, I calculated the variable importance in the projection (VIP) based on PLS-DA models for each lipid separately. In addition, I used univariate analyses (two-group data: t-test and fold change analysis; multi-group: one-way ANOVA with Fisher's Least Significant Difference post hoc analysis), to further

discriminate the significance of each lipid. I classified differential lipids as those with VIP values > 1, significant univariate test results ($p < 0.05$), and, where applicable, fold change threshold of 2. To investigate the effects of turtle size (CCL and body mass), I conducted Pearson R correlations. I classified lipids into 5 categories based on correlation coefficient (r): strong negative correlation (-1.0 – -6.6), weak negative correlation (-6.5 – -4.0), no correlation (-3.9 – 3.9), weak positive correlation (4.0 – 6.6), and strong positive correlation (6.6 – 1.0).

I analyzed each class separately; for each class, I compared black turtles between bays and seasons (dry = November – March; wet = April – October). If I did not identify differential lipids between these groups, I combined them and compared relative ion intensity for each lipid class between black and yellow morphotype green turtles and all green turtles across seasons. Lastly, assuming statistical similarity within all green turtles, I compared green turtles to hawksbill turtles and all individuals across seasons. When groups were not statistically similar, I used a one-way ANOVAs to compare species and seasons simultaneously by dividing the data into 4 or 6 groups, depending on the analysis (by population and season). I analyzed lipid data by relative ion intensity of lipids, where higher relative ion intensity suggests higher levels of lipid in plasma. Furthermore, I compared turtle size across species, seasons, and locations using Kruskal-Wallis tests in R statistical software (Version 3.4.4, Vienna, Australia). In all analyses, I accepted a statistical significance threshold of $p < 0.05$.

3.4 Results

I analyzed plasma from sea turtles ranging from 39 – 92 cm CCL and 6 – 88 kg body mass (Table 3.1). Due to scale malfunction, I recorded body mass of 39 turtles (out of 44 total turtles; Table 3.1). Throughout 2017, I captured 22 turtles during the wet season and 22 turtles during the dry season (Table 3.1). Turtle length and body mass did not vary with season or location in black morphotype green sea turtles, or by season in yellow morphotype and hawksbill turtles.

3.4.1 Relevant Lipids and Metabolites

I identified 688 relevant lipids and acyl-carnitines (relative ion intensities higher than the blank) in sea turtles from 11 classes (Table 3.2, Table A.5.1, A.5.2). Short chain lipids comprised a higher percentage of total lipid profile in free fatty acid (FFA), triglyceride (TAG), phosphatidylcholine (PC), and phosphatidylserine (PS) lipid classes, while long chain lipids comprised most of the lipid profiles in phosphatidylethanolamine (PE), and phosphatidylinositol (PI) lipid classes. In the cholesteryl ester (CE) lipid class, medium chain length encompassed the highest percentage of lipids, and in the phosphatidylglycerol (PG) lipid class, short and long chain lipids were more prevalent than medium chain lipids (Fig. A.5.1). Saturation graphs revealed that a higher percentage of PC, PE, and PI lipid classes were polyunsaturated (Fig. A.5.2). Most CE and TAG lipids were mono/diunsaturated. Further, the proportion of all saturated and unsaturated lipids were similar in PG and PS lipids. Finally, the highest percentage of FFA were saturated (Fig. A.5.2). I did not include sphingomyelin (SM), Acyl-carnitine (Car), or ceramide (Cer) classes due to structure (Table A.5.1, A.5.2).

Most (588) relevant lipids had no relationship with turtle size, suggesting that age did not influence relative ion intensity (Table 3.2). Of the 100 lipids that had significant correlation coefficients (r), I identified 64 that were negatively correlated and 27 that were positively correlated to CCL. Further, I discovered nine lipids that were negatively correlated and 14 that were positively correlated to body mass; 14 lipids were correlated to both CCL and body mass. A negative correlation indicated that as turtle size increased (older turtles), relative ion intensity decreased (less lipid), while a positive correlation indicated the opposite relationship. I did not identify any correlation between Car (a metabolite) and CCL or body mass (Table 3.2). Results from my PCA (FFA, PG, PS) and PLS-DA (CE, Cer, PC, PE, PI, SM, TAG) revealed partial overlap between green and hawksbill turtles and between seasons, with greater overlap between seasons than species (Fig. 3.3, Fig. A.5.3). However, in the FFA lipid class, I observed almost complete overlap between species and seasons.

3.4.2 Differential Lipids and Metabolites

I defined differential lipids and metabolites as those that had significantly different relative ion intensities between species or season (Table 3.2; Table A.5.1, A.5.2). My univariate analyses and VIP scores identified 129 differential lipids and metabolites: 127 differential lipids and metabolites between species, and 44 differential lipids and metabolites between season (some lipids varied by species and season; Table 3.2). I discovered that species variability was lipid specific, but of the lipids that displayed clear division between species, EI had higher relative ion intensities in more lipids (CE = 16; Cer = 2; FFA = 1; PC = 9; PE = 2; PG = 10; PI = 4; PS = 1; SM = 8; TAG = 34), while CM samples had higher relative ion intensities in fewer lipids (CE = 3; Cer = 0; FFA = 0; PC = 5; PE = 1; PG = 1; PI = 1; PS = 0; SM = 3; TAG = 10). Within TAG profiles, longer lipids had higher relative ion intensities in hawksbill turtles (Table 3.3). Additionally, I discovered that relative ion intensities of differential lipids and metabolites were higher in the dry season within the Car (1), CE (2), Cer (1), FFA (2), and PI (1) lipid classes, none of which displayed higher relative ion intensities in the wet season. Further, in the PC, PG, SM, and TAG lipid classes, I documented variable effect with season, although most lipids had higher relative ion intensity in the dry season (PC = 10; PG = 3; SM = 9; TAG = 4) compared to the wet season (PC = 3; PG = 4; SM = 3; TAG = 1). In hawksbill turtles, 12 of the 13 PC lipids that varied by season displayed higher relative ion intensities in the wet season compared to the dry season (Table 3.3). In green turtles, most PC lipids had higher relative ion intensities in the dry season, and the 3 lipids that displayed higher relative ion intensities in the wet season had less saturation (Table 3.3). The PE and PS lipid classes displayed no seasonal effects (Table 3.2). Finally, I identified limited variability in lipids and metabolites between black and yellow morphotype green turtles (Car = 2, PC = 13, SM = 6).

In all lipid classes aside from TAG, the proportional chain lengths shifted towards short lipids (Fig. 3.2) and proportional saturation of lipids shifted towards increased saturation (Fig. 3.4). In the TAG lipid class, I observed a shift towards mono/diunsaturated lipids. However, within the profile of differential lipids, I did not observe large proportional differences between seasons (N = 5), because all lipids present varied by species (Fig. 3.4; Table 3.3). Further, small seasonal differences observed were larger in hawksbill turtles

(larger relative ion intensity in the wet season) than in green turtles (comparable relative ion intensity between seasons). Lastly, I identified large standard deviations within my data, suggesting prevalent individual variation. I omitted FFAs and PS from Fig. 3.4 because the lipids that varied by season (two and one, respectively) were within the same saturation category (diunsaturated and polyunsaturated, respectively). I omitted SM, Car, and Cer from figures due to structure.

3.5 Discussion

Establishing a metabolomic approach is a key step to assess adaptations to environmental perturbations and therefore facilitate understanding of sea turtle physiology in dynamic environments. This has important ecological implications, particularly within the context of global climate change. Lipid profiling requires a single plasma sample, thereby eliminating repeated sampling and reducing potential adverse effects associated with handling endangered species. I determined that lipid profiles reflected species differences and seasonality in foraging juvenile sea turtles. By applying MRM lipid-profiling, a powerful technique with high sensitivity and specificity, I detected significant differences between lipid classes that suggest sea turtles not only modify physiology to variations in nutrient availability, but also to ambient water temperatures. Although there was heterogeneity between morphotypes of green turtles captured within the same environment in terms of trophic niche (Chapter 4), plasma metabolomic signatures grouped them together as a single species. Further, despite trophic level overlap between yellow and hawksbill turtles (Chapter 4), PCA clusters based on lipid profiles identified them as separate species. Differential lipid composition in animals is an important indicator of adaption to their environment (Hazel and Williams, 1990; Price et al., 2017) and foraging status (Kwan, 1994; Price et al., 2013).

I isolated all lipids and acyl-carnitines (a metabolite) present in sea turtles, which addresses the initial issue of unknown lipid species, and their chain lengths and saturation levels within sea turtles. Quantification of lipid and metabolite concentrations in plasma require the use of standards that are only effective if specific targeted lipids are known. Therefore, using the data I present here (Table A.5.1, A.5.2), researchers can further investigate concentrations and patterns of expression within sea turtles. Due to the

similarity between FFA in green and hawksbill turtles (this study) and those in loggerhead turtles (*Caretta caretta*), I predict that my data are applicable to other sea turtle species foraging in other environments throughout world (Guitart et al., 1999).

The most remarkable difference I observed in relative ion intensities of lipids was between species. In tuatara (*Sphenodon punctatus*: Blair et al., 2000; Cartland-Shaw et al., 1998), lizards (*Amphibolurus nuchalis*: Geiser and Learmonth, 1994), alligators (*Alligator mississippiensis*: Lance et al., 2001; Staton et al., 1990), frogs (*Leptodactylus fallax*: Jayson et al., 2018), and fish (Watanabe, 1982), lipid compositions of diets influence plasma lipid profiles. In birds (*Anatidae*), phylogeny could be more important than dietary differences in yolk lipids (Speake et al., 2002); however, diet lipid profiles in lizards are similar to those in yolk (Speake et al., 2004). Therefore, I suggest that the species variability in plasma lipids in sea turtles (this study) were partially due to variability in diet. However, because my PCA/PLS-DA results grouped turtles by species, I suggest that like birds, there was also a phylogenetic basis in lipid profiles. When foraging within the same habitat, green and hawksbill turtles have minimal overlap in diets (Bjorndal and Bolten, 2010; Hill, 1998; Stringell et al., 2016); however, diet explains minimal variability in lipid relative ion intensity found between morphotypes in green turtles (Sampson et al., 2018).

In foraging studies, TAG, FFA, and Car are the classes used to predict foraging and metabolism (Price et al., 2013). I recorded lower relative ion intensities in TAG, FFA, and Car metabolites during the wet season, suggesting slight decreases in foraging when upwelling decreases (McCue, 2008; Price et al., 2013; Williams et al., 1999). However, when I separated turtles by species, I discovered that this trend was not true for the TAG (N = 5) in hawksbill turtles, where relative ion intensity was higher in the wet season compared to the dry season. This suggests that hawksbill turtles were foraging to a higher degree in the non-upwelling (wet) season compared to the upwelling (dry) season. In green turtles, TAGs relative ion intensity was comparable across seasons suggesting consistent foraging behavior throughout the year. Starvation in reptiles is accompanied by a shift from saturated to unsaturated FFAs (Price et al., 2013; McCue, 2008) that was present in the 2 FFA observations in this study. However, these conclusions are based on minimal observations (FFA = 2; TAG = 5). Moreover, although weakly correlated to CCL and body

mass, correlation analyses suggest consistency of TAG and FFA profiles through age classes, with smaller turtles potentially growing at a slightly faster rate than larger turtles.

My study identified seasonality in lipid classes, specifically in those related to membrane fluidity (Cer, PC, PE, PG, PI, PS, and SM; Van Meer et al., 2008). I discovered that of all differential lipids, most increased from the wet season to the dry season when water temperatures decreased, accompanied by an increase in saturation level. Specifically, in complete profiles, most PC, PE, and PI lipids were unsaturated and short, and within differential lipid profiles, this relationship became more pronounced. However, PE lipids did not vary by season. While CE lipids displayed similar saturation patterns, chain lengths were a longer proportion of the complete profile compared to other membrane lipids. Further, while complete PG and PS lipid profiles revealed even distribution in saturation, differential lipid profiles shifted towards increased proportion in unsaturated lipids. In the PC lipid class, higher relative ion intensity in hawksbill turtles during the wet season suggests an increase in metabolism during the wet season compared to dry season. These results corroborate results in TAGs further suggesting that hawksbill turtles have lower metabolism and foraging rates in the dry season (potentially resting during this time). Further, green turtle PC lipids revealed compositional changes with season supporting metabolism (and foraging) year-round. My results suggest that sea turtles display homeoviscous adaptation similar to other amphibians and reptiles (Mineo et al., 2019; Price et al., 2017). Specifically, decreases in membrane rigidity were associated with increases in saturation level of lipids and decreases in lipid chain lengths (Price et al. 2017; Rawicz et al., 2000), which maintains trans-lipid transport and metabolism in cold environments. Ecologically, my results support studies that suggest that although sea turtles avoid areas with cold-water (Coles and Musick, 2000; Crear et al., 2016), they are capable of prioritizing behaviors to maximize nutrient acquisition (Zepeda-Borja et al., 2017) and minimize migration time (Hays et al., 2001) when necessary. Although my results reveal that seasonal behaviors might be species specific.

In wildlife studies, lipidomics is also used to estimate age, lung function, and long-term thermal adaption. Although mitochondrial phospholipids vary with age and growth in fishes, my correlation results suggest no such relationship in sea turtles (Almaida-Pagan et al., 2019; Lucas-Sánchez et al., 2013). However, in these studies, researchers isolated

mitochondrial membranes, as opposed to quantifying lipid composition of plasma, which could explain why I failed to detect age related shifts in lipid profiles. In addition to their role in membranes, CE lipids are also present in lung surfactant in lizards and their concentration is temperature dependent (Daniels et al., 1990). In newts, lipid profiles indicated long-term thermal adaptation between populations captured in warm habitats to those captured in cold environments (Mineo et al., 2019). My results, therefore, might be skewed towards shorter chain and unsaturated lipids due to long-term cold adaptation based on chain lengths and saturation levels. In order to verify this hypothesis, further studies comparing my results to those from sea turtles from warmer temperatures are warranted.

Lung PCs indicate dive capacity in mammals, therefore the same could be true of sea turtles, allowing researchers to infer depth use between populations or species without depth-recorders that require recapturing the individual or expensive satellite transmitters (Gutierrez et al., 2015). Additionally, in human studies, lipidomics assist in biomarker discovery for disease (Cordeiro et al., 2017; Deng et al., 2018), which could be expanded to sea turtles. Therefore, I suggest further comparative studies between sea turtles of different reproductive statuses (Hamann et al., 2002; Price, 2017), comparative studies between tissues types (Osthoff et al., 2014), different thermal habitats (Mineo et al., 2019), and between wild and captive animals (Cartland-Shaw et al., 1998; Lance et al., 2001).

It is important to note that reproduction in reptiles can have dramatic effects on lipid profiles (Price, 2017). Some of the individual variability seen in my profiles could be caused by turtles approaching reproductive maturity, although lipid profiles do not indicate initiation of nesting seasons (Hamann et al., 2002; Kawazu et al., 2015). To investigate this pattern, I suggest further studies comparing lipid profiles in reproductive adults and those in larger juveniles/sub-adults to my findings.

3.6 Conclusion

To address the lack of identified specific species of lipids in sea turtles, I quantified chain lengths and saturation level of a diverse group of lipid classes (10 classes) and a single metabolite group to support future research into sea turtle lipidomics (Table A.5.1, A.5.2). Through comparison of lipid profiles across seasons, I determined a continuous foraging regime within habitats of Costa Rica despite variability in upwelling. However,

lipid profiles indicated potential species-specific variability in feeding and metabolism across season. Comparisons between turtle morphotypes and species of green and hawksbill turtles suggested population variability in diet. However, I identified a strong phylogenetic basis for differential lipid profiles. Within phospholipid classes, compositional alterations in lipid profiles that suggest sea turtles are undergoing homoviscous adaptation to maintain cellular processes in colder climates. Due to the high proportional contribution of unsaturated lipids to total profiles, I suggest that turtles in Costa Rica are displaying signs of long-term cold adaption, a concept that warrants more investigation. I conclude that Matapalito and Salinas are important habitats to protect because the quality of foraging sites is directly related to reproductive output, recovery and long-term sustainability of endangered populations (Harrison et al., 2011).

MRM-profiling is a powerful tool allowing researchers to evaluate wildlife foraging across habitats and over time, which has implications for both the future reproductive output of the population and ecosystem management. Understanding the consistency of ecosystem services provided by wildlife is integral for understanding the environment and prioritizing conservation measures. Plasma lipid profiles can be used to infer trade-off behaviors in sea turtles. For example, in the present study, turtles were varying nutrient acquisition and cold-water avoidance throughout the year (species specific). This study provides the baseline from which MRM-profiling can be extended to sea turtles through a simple, inexpensive, and minimally invasive technique that fosters future investigations of sea turtle health, physiology, and ecology.

3.7 Acknowledgments

I would like to thank The Leatherback Trust, Equipo Tora Carey, and all their volunteers for assistance with the fieldwork for this study; especially M. Heidemeyer, K. Mora, R. Mora, M. Mora, A. Lara, and M. Giry for assistance in Costa Rica. Funding for this project was provided by the Department of Forestry and Natural Resources at Purdue University, The Leatherback Trust, and by the USDA National Institute of Food and Agriculture, Hatch Project 1004115 (to EAF). I thank the Guanacaste Conservation Areas (ACG) of the Ministry of Environment of Costa Rica for granting the permits to conduct this work and for supporting sea turtle research in Costa Rica (ACG-PI-PC-019, R-ACG-

057-2016), and USFWS for import permits and continued support of endangered species research (CITES permit 17US06369C/9). Additionally, I thank Dr. R. Goforth and Dr. J. Spotila for reviewing the manuscript. This research was authorized under the Purdue Animal Care and use Committee (protocol #1510001309).

3.8 Literature Cited

Adiga, U., Yogish, S., 2016. Hemolytic index–A tool to measure hemolysis in vitro. J. Biotechnol. Biochem. 2, 49–52.

Alberts, A.C., Sharp, T.R., Werner, D.I., Weldon, P.J., 1992. Seasonal variation of lipids in femoral gland secretions of male green iguanas (*Iguana iguana*). J. Chem. Ecol. 18, 703–712.

Almaida-Pagan, P.F., Ortega-Sabater, C., Lucas-Sanchez, A., Gonzalez-Silvera, D., Martinez-Nicolas, A., de Lama, M.A.R., Mendiola, P., de Costa, J., 2019. Age-related changes in mitochondrial membrane composition of *Nothobranchius furzeri.*: comparison with a longer-living *Nothobranchius* species. Biogerontology 20(1), 83–92.

Bjorndal, K.A., Bolten, A.B., 2003. From ghosts to key species: restoring sea turtle populations to fulfill their ecological roles. Mar. Turtle. Newsl. 100(100), 16–21.

Bjorndal, K.A., Bolten, A.B., 2010. Hawksbill sea turtles in seagrass pastures: success in a peripheral habitat. Mar. Biol. 157(1), 135–145.

Bowen, B.W., Nelson, W.S., Avise, J.C., 1993. A molecular phylogeny for marine turtles: trait mapping, rate assessment, and conservation relevance. Proc. Natl. Acad. Sci. 90(12), 5574–5577.

Blair, T.A., Cree, A., Skeaff, C.M., 2000. Plasma fatty acids, triacylglycerol and cholesterol of the tuatara (*Sphenodon punctatus punctatus*) from islands differing in the presence of rats and the abundance of seabirds. J. Zool. 252(4), 463–472.

Bligh, E.G., Dyer, W.J., 1959. A rapid method of total lipid extraction and purification. Can. J. Biochem. Physiol. 37(8), 911–917.

Broenkow, W.W., 1965. The distribution of nutrients in the Costa Rica Dome in the eastern tropical Pacific Ocean. Limnol. Oceanogr. 10(1), 40–52.

Cartland-Shaw, L.K., Cree, A., Skeaff, C.M., Grimmond, N.M., 1998. Differences in dietary and plasma fatty acids between wild and captive populations of a rare reptile, the tuatara (*Sphenodon punctatus*). J. Comp. Physiol. B 168(8), 569–580.

Chong, J., Xia, J., 2018. MetaboAnalystR: an R package for flexible and reproducible analysis of metabolomics data. Bioinformatics 27 4313–4314.

Chong, J., Soufan, O., Li, C., Caraus, I., Li, S., Bourque, G., Wishart, D.S., Xia, J., 2018. MetaboAnalyst 4.0: towards more transparent and integrative metabolomics analysis. Nucl. Acids Res. 46, W486–494.

Coles, W., Musick, J.A., 2000. Satellite sea surface temperature analysis and correlation with sea turtle distribution off North Carolina. Copeia 2000 (2), 551–554.

Cordeiro, F.B., Ferreira, C.R., Sobreira, T.J.P., Yannell, K.E., Jarmusch, A.K., Cedenho, A.P., Lo Turco, E.G. and Cooks, R.G., 2017. Multiple reaction monitoring (MRM)-profiling for biomarker discovery applied to human polycystic ovarian syndrome. Rapid Commun. Mass Spectrom. 31(17), 1462–1470.

Crear, D.P., Lawson, D.D., Seminoff, J.A., Eguchi, T., LeRoux, R.A., Lowe, C.G., 2016. Seasonal shifts in the movement and distribution of green sea turtles *Chelonia mydas* in response to anthropogenically altered water temperatures. Mar. Ecol. Prog. Ser. 548, 219–232.

Daniels, C.B., Barr, H.A., Power, J.H. and Nicholas, T.E., 1990. Body temperature alters the lipid composition of pulmonary surfactant in the lizard *Ctenophorus nuchalis*. Exp. Lung Res. 16(5), 435–449.

Daniels, C.B., Orgeig, S., Smits, A.W., Miller, J.D., 1996. The influence of temperature, phylogeny, and lung structure on the lipid composition of reptilian pulmonary surfactant. Exp. Lung Res. 22(3), 267–281.

Davenport, J., 1997. Temperature and the life-history strategies of sea turtles. J. Therm. Biol. 22(6), 479–488.

de Lima, C.B., Ferreira, C.R., Milazzotto, M.P., Sobreira, T.J.P., Vireque, A.A. and Cooks, R.G., 2018. Comprehensive lipid profiling of early stage oocytes and embryos by MRM profiling. J. Mass Spectrom. 53(12), 1247–1252.

Deng, K., Han, P., Song, W., Wang, Z., Zhang, F., Xie, H., Zhao, W., Xu, H., Cai, Y., Rong, Z., Yu, X., 2018. Plasma metabolomic profiling distinguishes right-sided from left-sided colon cancer. Clin. Chim. Acta 487, 357–362.

Edge, C.B., Steinberg, B.D., Brooks, R.J., Litzgus, J.D., 2009. Temperature and site selection by Blanding's Turtles (*Emydoidea blandingii*) during hibernation near the species' northern range limit. Can. J. Zool. 87(9), 825–834.

Geiser, F., Learmonth, R.P., 1994. Dietary fats, selected body temperature and tissue fatty acid composition of agamid lizards (*Amphibolurus nuchalis*). J. Comp. Physiol. B 164, 55–61.

Goodhead, L.K., MacMillan, F.M., 2017. Measuring osmosis and hemolysus of red blood cells. Adv. Physiol. Educ. 41(2), 298–305.

Guitart, R., Silvestre, A.M., Guerrero, X., Mateo, R., 1999. Comparative study on the fatty acid composition of two marine vertebrates: striped dolphins and loggerhead turtles. Comp. Biochem. Physiol. Part B Biochem. Mol. Biol. 124(4), 439–443.

Gutierrez, D.B., Fahlman, A., Gardner, M., Kleinhenz, D., Piscitelli, M., Raverty, S., Haulena, M., Zimba, P.V., 2015. Phosphatidylcholine composition of pulmonary surfactant from terrestrial and marine diving mammals. Respir. Physiol. Neurobiol. 211, 29–36.

Hamann, M., Limpus, C., Whittier, J., 2002. Patterns of lipid storage and mobilisation in the female green sea turtle (*Chelonia mydas*). J. Comp. Physiol. B, 172 (6), 485–493.

Harrison, X.A., Blount, J.D., Inger, R., Norris, D.R., Bearhop, S., 2011. Carry-over effects as drivers of fitness differences in animals. J. Anim. Ecol. 80(1), 4–18.

Hays, G.C., Dray, M., Quaife, T., Smyth, T.J., Mironnet, N.C., Luschi, P., Papi, F., Barnsley, M.J., 2001. Movements of migrating green turtles in relation to AVHRR derived sea surface temperature. Int. J. Remote Sens. 22(8), 1403–1411.

Hazel, J.R., Williams, E.E., 1990. The role of alterations in membrane lipid composition in enabling physiological adaptation of organisms to their physical environment. Prog. Lipid. Res. 29, 167–227.

Heidemeyer, M., Arauz-Vargas, R., López-Agüero, E., 2014. New foraging grounds for hawksbill (*Eretmochelys imbricata*) and green turtles (*Chelonia mydas*) along the northern Pacific coast of Costa Rica, Central America. Rev. Biol. Trop. 62(4), 109–118.

Heidemeyer, M., Delgado-Trejo, C., Hart, C.E., Clyde-Brockway, C.E., Fonseca, L.G., Mora, R., Mora, M., Lara, A., Obando, R., 2018. Long-term in-water recaptures of adult black turtles (*Chelonia mydas*) provide implications for flipper tagging methods in the eastern pacific. Herpetol. Rev. 49(4), 653–657.

Hill, M.S., 1998. Spongivory on Caribbean reefs releases corals from competition with sponges. Oecologia 117(1-2), 143–150.

Hochscheid, S., Bentivegna, F., Speakman, J.R., 2002. Regional blood flow in sea turtles: implications for heat exchange in an aquatic ectotherm. Physiol. Biochem. Zool. 75, 66–76.

Hochscheid, S., Bentivegna, F., Hamza, A., Hays, G.C., 2010. When surfacers do not dive: multiple significance of extended surface times in marine turtles. J. Exp. Biol. 213(8), 1328–1337.

Ibáñez, A., Klein., C., Quezada, G., Krüger, M., Brodesser, S., Steinfartz, S., 2018. Characterization of lipid structures in femoral secretions of Galápagos marine iguanas by shotgun lipidomics. Chemoecology 28(1), 21–28.

Jayson, S., Ferguson, A., Goetz, M., Routh, A., Tapley, B., Harding, L., Michaels, C.J., Dawson, J., 2018. Comparison of the nutritional content of the captive and wild diets of the critically endangered mountain chicken frog (*Leptodactylus fallax*) to improve its captive husbandry. Zoo Biol. 37(5), 332–346.

Johnston, S.D., Daniels, C.B., Booth, D.T., 2001. Development of the pulmonary surfactant system in the green sea turtle, *Chelonia mydas*. Respir. Physiol. 126(1), 75–84.

Kawazu, I., Kino, M., Yanagisawa, M., Maeda, K., Nakada, K., Yamaguchi, Y., Sawamukai, Y., 2015. Signals of vitellogenesis and estrus in female hawksbill turtles. Zool. Sci. 32(1), 114–119.

Khannoon, E.R., El-Gendy, A. and Hardege, J.D., 2011. Scent marking pheromones in lizards: cholesterol and long chain alcohols elicit avoidance and aggression in male *Acanthodactylus boskianus* (*Squamata: Lacertidae*). Chemoecology 21(3), 143–149.

Kwan, D., 1994. Fat reserves and reproduction in the green turtle, *Chelonia mydas*. Wildl. Res. 21(3), 257–265.

Lance, V.A., Morici, L.A., Elsey, R.M., Lund, E.D., Place, A.R., 2001. Hyperlipidemia and reproductive failure in captive-reared alligators: vitamin E, vitamin A, plasma lipids, fatty acids, and steroid hormones. Comp. Biochem. Physiol. Part B Biochem. Mol. Biol. 128(2), 285–294.

Lance, V.A., Rostal, D.C., 2002. The annual reproductive cycle of the male and female desert tortoise: Physiology and endocrinology. Chelonian Conserv. Biol. 4(2), 302–312.

Lavín, M.F., Fiedler, P.C., Amador, J.A., Ballance, L.T., Färber-Lorda, J., Mestas-Nuñez, A.M., 2006. A review of eastern tropical Pacific oceanography: Summary. Prog. Oceanogr. 69(2-4), 391–398.

Liwanag, H.E., Berta, A., Costa, D.P., Budge, S.M., Williams, T.M., 2012. Morphological and thermal properties of mammalian insulation: the evolutionary transition to blubber in pinnipeds. Biol. J. Linn. Soc. 107(4), 774–787.

Lucas-Sánchez, A., Almaida-Pagán, P.F., Tocher, D.R., Mendiola, P., de Costa, J., 2013. Age-related changes in mitochondrial membrane composition of Nothobranchius rachovii. J. Gerontol. Ser. A Biomed. Sci. Med. Sci. 69(2), 142–151

McCue, M.D., 2008. Fatty acid analyses may provide insight into the progression of starvation among squamate reptiles. Comp. Biochem. Physiol. Part A Mol. Integr. Physiol. 151(2), 239–246.

Mrosovsky, N., 1980. Thermal biology of sea turtles. Am. Zool. 20(3), 531–547.

Mineo, P.M., Waldrup, C., Berner, N.J., Schaeffer, P.J., 2019. Differential plasticity of membrane fatty acids in northern and southern populations of the eastern newt (*Notophthalmus viridescens*). J. Comp. Physiol. B 1–12.

Osthoff, G., Hugo, A., Govender, D., Huchzermeyer, F., Bouwman, H., 2014. Comparison of the lipid composition of three adipose tissue types of male and female wild Nile crocodiles (*Crocodylus niloticus*). J. Herpetol. 48(4), 525–531.

Owens, D.W., Ruiz, G.J., 1980. New Methods of Obtaining Blood and Cerebrospinal Fluid from Marine Turtles. Herpetologica 36, 17–20.

Paladino, F.V., O'Connor, M.P., Spotila, J.R., 1990. Metabolism of leatherback turtles, gigantothermy, and thermoregulation of dinosaurs. Nature 344(6269), 858–860.

Price, E.R., Jones, T.T., Wallace, B.P., Guglielmo, C.G., 2013. Serum triglycerides and ß-hydroxybutyrate predict feeding status in green turtles (*Chelonia mydas*): evaluating a single blood sample method for assessing feeding/fasting in reptiles. J. Exp. Mar. Biol. Ecol. 439, 176–180.

Price, E.R., 2017. The physiology of lipid storage and use in reptiles. Biol. Rev. 92, 1406–1426.

Price, E.R., Sirsat, T.S., Sirsat, S.K., Kang, G., Keereetaweep, J., Aziz, M., Chapman, K.D., Dzialowski, E.M., 2017. Thermal acclimation in American alligators: effects of temperature regime on growth rate, mitochondrial function, and membrane composition. J. Therm. Biol. 68, 45–54.

Rawicz, W., Olbrich, K.C., McIntosh, T., Needham, D., Evans, E., 2000. Effect of chain length and unsaturation on elasticity of lipid bilayers. Biophys. J. 79(1), 28–339.

Sampson, L., Giraldo, A., Payán, L.F., Amorocho, D.F., Ramos, M.A., Seminoff, J.A., 2018. Trophic ecology of green turtle *Chelonia mydas* juveniles in the Colombian Pacific. J. Mar. Biol. Assoc. UK 98(7), 1817–1829.

Schwartz, F., 1978. Behavioral and tolerance responses to cold water temperatures by three species of sea turtles (*Reptilia, Cheloniidae*) in North Carolina. Florida, Mar. Res. Publ. 33, 16–18.

Solow, A.R., Bjorndal, K.A., Bolten, A.B., 2002. Annual variation in nesting numbers of marine turtles: the effect of sea surface temperature on re-migration intervals. Ecol. Lett. 5(6), 742–746.

Speake, B.K., Surai, P.F., Bortolotti, G.R., 2002. Fatty acid profiles of yolk lipids of five species of wild ducks (*Anatidae*) differing in dietary preference. J. Zool. 257(4), 533–538.

Speake, B.K., Herbert, J.F., Thompson, M.B., 2004. Comparison of the fatty-acid compositions of prey items and yolks of Australian insectivorous scincid lizards. J. Comp. Physiol. B 174(5), 393–397.

Spotila, J.R., Standora, E.A., 1985. Environmental constraints on the thermal energetics of sea turtles. Copeia 1985, 694–702.

Standora, E.A., Spotila, J.R., Foley, R.E., 1982. Regional endothermy in the sea turtle, *Chelonia mydas*. J. Therm. Biol. 7, 159–165.

Staton, M.A., Edwards, H.M.J., Brisbin, I.L.J., Joanen, T., McNease, L., 1990. Essential fatty acid nutrition of the American alligator (*Alligator mississippiensis*). J. Nutr. 120, 674–685.

Stringell, T.B., Clerveaux, W.V., Godley, B.J., Kent, F.E., Lewis, E.D., Marsh, J.E., Phillips, Q., Richardson, P.B., Sanghera, A., Broderick, A.C., 2016. Taxonomic distinctness in the diet of two sympatric marine turtle species. Mar. Ecol. 37(5), 1036–1049.

Stuhldreier, I., Sánchez-Noguera, C., Rixen, T., Cortés, J., Morales, A., Wild, C., 2015. Effects of seasonal upwelling on inorganic and organic matter dynamics in the water column of eastern Pacific coral reefs. PloS ONE 10(11), e0142681.

Van Houtan, K.S., Halley, J.M., Marks, W., 2015. Terrestrial basking sea turtles are responding to spatio-temporal sea surface temperature patterns. Biol. Lett. 11(1), p.20140744.

Van Meer, G., Voelker, D.R., Feigenson, G.W., 2008. Membrane lipids: where they are and how they behave. Nat. Rev. Mol. Cell Biol. 9(2), 112–124.

Wang, C., Deser, C., Yu, J.Y., DiNezio, P., Clement, A., 2017. El Niño and southern oscillation (ENSO): a review. In Coral reefs of the eastern tropical Pacific (pp. 85-106). Springer, Dordrecht.

Watanabe, T., 1982. Lipid nutrition in fish. Comp. Biochem. Physiol. 73B, 3–15

Westerhuis, J.A., Hoefsloot, H.C., Smit, S., Vis, D.J., Smilde, A.K., van Velzen, E.J., van Duijnhoven, J.P., van Dorsten, F.A., 2008. Assessment of PLSDA cross validation. Metabolomics 4(1), 81–89.

Wenk, M.R., 2005. The emerging field of lipidomics. Nat. Rev. Drug Discov. 4(7), 594–610.

Wertz, P.W., 2015. Epidermal lipids and the intercellular pathway. Percutaneous Penetration Enhancers Chemical Methods in Penetration Enhancement (pp. 13-18). Springer, Berlin, Heidelberg.

Whittow, G.C., Balazs, G.H., 1982. Basking behavior of the Hawaiian green turtle (*Chelonia mydas*). Pac. Sci. 36(2), 129–140.

Williams, T.D., Guglielmo, C.G., Egeler, O., Martyniuk, C.J., 1999. Plasma lipid metabolites provide information on mass change over several days in captive Western Sandpipers. The Auk 116(4), 994–1000.

Zepeda-Borja, K.M., Ortega-Ortiz, C.D., Orozco, E.T., Ortiz, A.O., 2017. Spatial and temporal distribution of sea turtles related to sea surface temperature and chlorophyll-a in Mexican Central Pacific waters. Rev. Biol. Mar. Oceanogr. 52(2), 375–385.

Zhao, Y.Y., Cheng, X.L., Lin, R.C., Wei, F., 2015. Lipidomics applications for disease biomarker discovery in mammal models. Biomark. Med. 9(2), 153-168.

Table 3.1 Morphological Measurements in Pacific Sea Turtles

Morphological measurements of sea turtles sampled including curved carapace length (CCL) in cm, and body mass in kg, with values representing mean ± standard deviation and ranges present. Wet season (April – October) represent the number of turtles captured during the wet season, while dry season (November – March) represent the number of turtles captured during the dry season. B-CM = black morphotype green turtles, Y-CM = yellow morphotype green turtles, and EI = hawksbill turtles.

	CCL (cm)	CCL range	Mass (kg)*	Mass range*	n	Wet Season	Dry Season
B-CM	77.5 ± 7	66 – 92	49.5 ± 14.5	32 – 88	17	6	10
Y-CM	66.5 ± 10	50 – 80.5	30.5 ± 17.5	13 – 66	11	3	8
EI	51 ± 11.5	38.5 – 83	13 ± 11.5	6 – 50	16	13	4

*Mass measurements presented for EI n = 16, Y-CM n = 7, and B-CM n = 16.

Table 3.2 Lipid Profiles in Pacific Sea Turtles

Sea turtle plasma lipid and metabolite classes and their correlation to curved carapace length (CCL, cm) and body mass (kg). Relevant lipids are those lipids and metabolites with relative ion intensities greater than the blank. Differential lipids are those lipids and metabolites identified by comparative analyses between species and season. Columns labeled "by species" and "by season" indicate the number of lipids that had significantly different relative ion intensities, (-) indicates no data or no correlation. All turtles were captured in Costa Rica in 2017.

Class	Relevant Lipids	Differential Lipids	By Species	By Season	Correlation Coefficient CCL				Correlation Coefficient Body Mass			
					Strong -	Weak -	Weak +	Strong +	Strong -	Weak -	Weak +	Strong +
SM	27	17	17	12	-	3	-	2	-	-	1	-
PC	113	21	21	13	-	7	6	-	-	1	3	-
FFA	26	2	1	2	-	1	1	-	-	-	-	-
CE	55	19	19	2	-	5	2	-	-	-	3	-
Car	48	2	1	1	-	-	-	-	-	-	-	-
PS	24	1	1	-	-	-	-	-	-	1	1	-
PI	50	5	5	1	-	7	1	-	-	4	-	-
PG	33	13	13	7	-	7	1	-	-	-	-	-
PE	55	3	3	-	-	2	1	-	-	-	-	-
Cer	27	2	2	1	-	1	-	-	-	1	1	-
TAG	171	44	44	5	1	30	13	-	-	2	5	-

Table 3.3 Seasonal Differential Lipids in Pacific Sea Turtles

Average relative ion intensity of differential lipids that varied by season (wet and dry) in green turtles (CM) and hawksbill turtles (EI) live captured in Costa Rica in 2017.

Lipids	CM Wet	CM Dry	EI Wet	EI Dry
16:2 Cholesteryl ester, zymosteryl palmitoleate	0.003 ± 0.001	0.004 ± 0.001	0.004 ± 0.001	0.0045 ± 0.001
18:3 Cholesteryl ester, 16:2 Stigmasteryl ester, 16:3 Sitosteryl ester	0.017 ± 0.008	0.022 ± 0.018	0.023 ± 0.015	0.037 ± 0.014
CerP(d18:1/16:0)	0.030 ± 0.003	0.031 ± 0.002	0.032 ± 0.002	0.0345 ± 0.005
C18:3; C18:3	0.016 ± 0.002	0.018 ± 0.004	0.018 ± 0.003	0.018 ± 0.002
PC (30:1)	0.034 ± 0.010	0.023 ± 0.008	0.031 ± 0.006	0.021 ± 0.008
PCo(34:1)	0.023 ± 0.006	0.017 ± 0.006	0.028 ± 0.024	0.055 ± 0.036
PC (34:4)	0.002 ± 0.000	0.002 ± 0.001	0.002 ± 0.000	0.002 ± 0.000
PC (34:3)	0.002 ± 0.001	0.004 ± 0.004	0.003 ± 0.002	0.006 ± 0.002
PC (34:2)	0.012 ± 0.003	0.015 ± 0.007	0.020 ± 0.008	0.028 ± 0.005
PC (36:5)	0.017 ± 0.013	0.034 ± 0.015	0.012 ± 0.003	0.016 ± 0.005
PC (36:1)	0.046 ± 0.011	0.043 ± 0.012	0.036 ± 0.005	0.027 ± 0.003
PC (38:7)	0.002 ± 0.001	0.002 ± 0.001	0.003 ± 0.001	0.004 ± 0.002
PCo(38:0)	0.002 ± 0.001	0.002 ± 0.001	0.003 ± 0.001	0.005 ± 0.002
PC (38:6)	0.023 ± 0.012	0.024 ± 0.008	0.039 ± 0.015	0.057 ± 0.012
PC (38:5)	0.045 ± 0.024	0.065 ± 0.023	0.044 ± 0.018	0.034 ± 0.008
PC (40:5)	0.013 ± 0.006	0.017 ± 0.006	0.016 ± 0.009	0.009 ± 0.003
PC (40:0)	0.002 ± 0.000	0.002 ± 0.001	0.002 ± 0.001	0.001 ± 0.000
PG (12:0)	0.026 ± 0.003	0.026 ± 0.002	0.028 ± 0.001	0.027 ± 0.001
PGp (18:0)	0.026 ± 0.003	0.025 ± 0.002	0.028 ± 0.001	0.028 ± 0.002
PG (18:4)	0.025 ± 0.002	0.025 ± 0.002	0.027 ± 0.001	0.027 ± 0.002
PG (22:2)	0.026 ± 0.003	0.025 ± 0.002	0.027 ± 0.001	0.027 ± 0.001
PG (30:1)	0.034 ± 0.012	0.033 ± 0.005	0.026 ± 0.001	0.027 ± 0.002

Table 3.3 continued

PG (34:1)	0.041 ± 0.020	0.047 ± 0.015	0.032 ± 0.006	0.033 ± 0.003
PG (36:2)	0.038 ± 0.024	0.053 ± 0.017	0.030 ± 0.005	0.028 ± 0.002
PI (38:5)	0.062 ± 0.029	0.087 ± 0.028	0.040 ± 0.011	0.045 ± 0.011
SM (d18:0/12:0)	0.009 ± 0.001	0.010 ± 0.002	0.003 ± 0.001	0.003 ± 0.000
SM (d18:2/14:0)	0.005 ± 0.001	0.008 ± 0.003	0.005 ± 0.001	0.007 ± 0.002
SM (d16:1/18:1)	0.004 ± 0.001	0.008 ± 0.004	0.004 ± 0.001	0.005 ± 0.001
SM (d18:1/16:0)	0.134 ± 0.025	0.110 ± 0.026	0.158 ± 0.017	0.125 ± 0.032
SM (d18:0/16:0)	0.016 ± 0.003	0.013 ± 0.003	0.019 ± 0.003	0.017 ± 0.002
SM (d18:2/18:1)	0.001 ± 0.000	0.002 ± 0.001	0.001 ± 0.000	0.002 ± 0.000
SM (d18:2/20:1)	0.002 ± 0.000	0.002 ± 0.001	0.002 ± 0.001	0.003 ± 0.001
SM (d16:1/22:1)	0.004 ± 0.001	0.005 ± 0.003	0.003 ± 0.002	0.007 ± 0.002
SM (d18:1/20:0)	0.014 ± 0.004	0.016 ± 0.006	0. 019 ± 0.007	0.028 ± 0.005
SM (d18:2/22:1)	0.029 ± 0.011	0.042 ± 0.013	0.036 ± 0.010	0.048 ± 0.008
SM (d18:1/24:1)15Z))	0.102 ± 0.019	0.097 ± 0.017	0.142 ± 0.021	0.122 ± 0.007
SM (d18:0/24:0)	0.004 ± 0.001	0.005 ± 0.001	0.005 ± 0.001	0.005 ± 0.001
TAG(48:1)_FA 16:1	0.005 ± 0.001	0.006 ± 0.001	0.008 ± 0.000	0.010 ± 0.002
TAG(48:1)_FA18:0	0.025 ± 0.013	0.036 ± 0.016	0.005 ± 0.002	0.005 ± 0.001
TAG(48:2)_FA 16:0	0.006 ± 0.001	0.006 ± 0.001	0.012 ± 0.003	0.010 ± 0.003
TAG(50:2)_FA 16:1	0.004 ± 0.001	0.004 ± 0.001	0.005 ± 0.000	0.007 ± 0.001
TAG(54:4)_FA 16:0	0.004 ± 0.001	0.004 ± 0.001	0.005 ± 0.001	0.006 ± 0.002

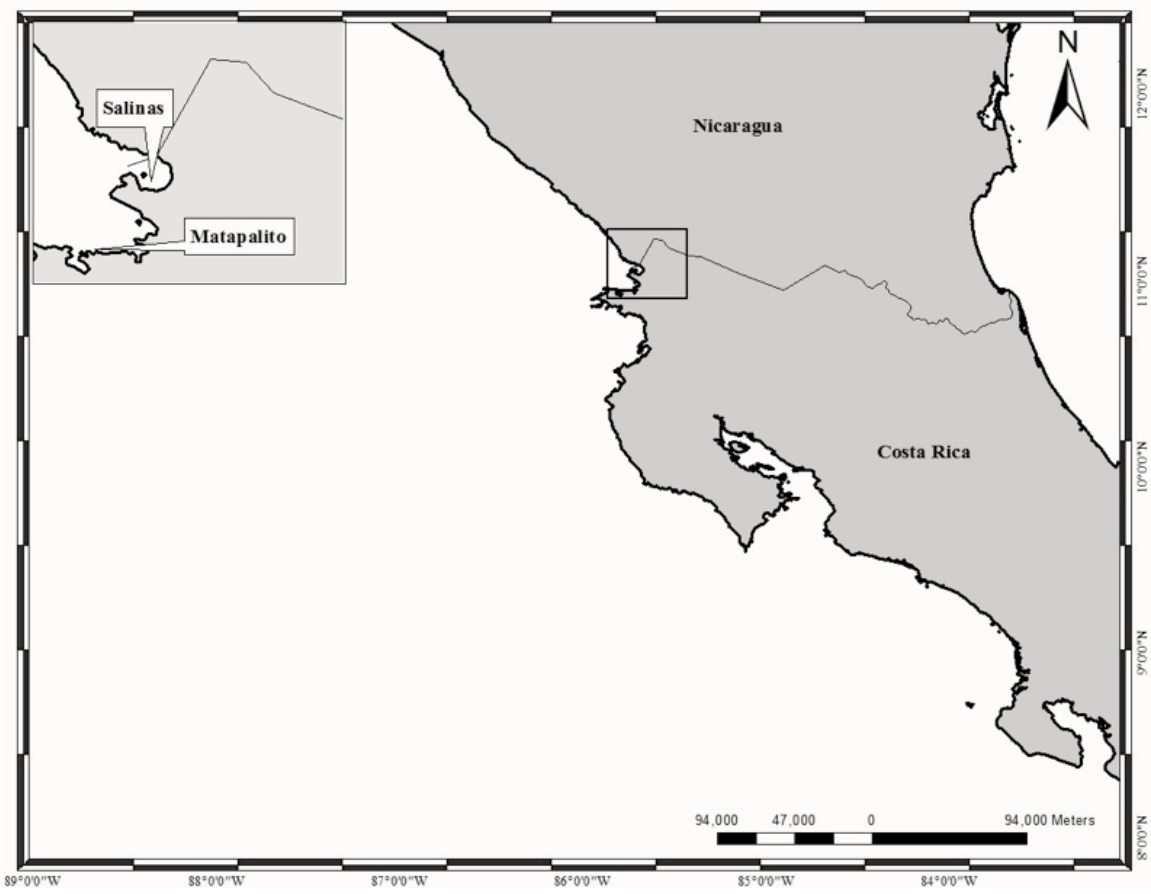

Figure 3.1 Study Sites, Costa Rica
Map of sampling sites in North Pacific Costa Rica. I sampled black morphotype green turtles from Salinas Bay and Matapalito Bay. I sampled yellow morphotype green turtles and hawksbill turtles from Matapalito Bay because no turtles were sited in in Salinas Bay. Sampling occurred once per month at each location during 2017, weather permitting.

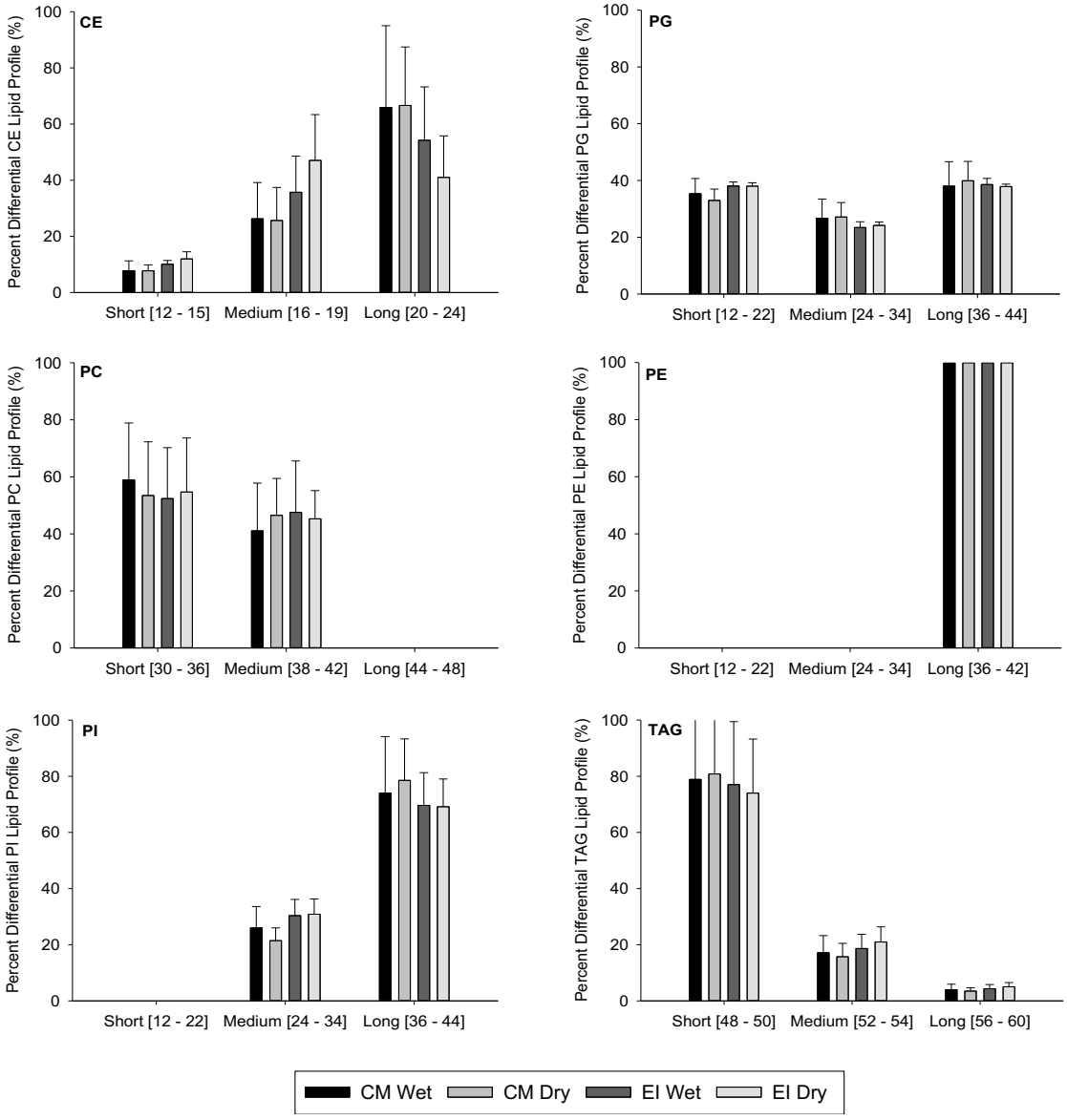

Figure 3.2 Differential Chain Lengths
Percent differential lipids within each lipid class profile from sea turtles divided by chain length and by species (green turtle = CM, hawksbill = EI). The x-axis represents chain length and was divided based on each profile separately. Bars and error bars represent mean ± standard deviation

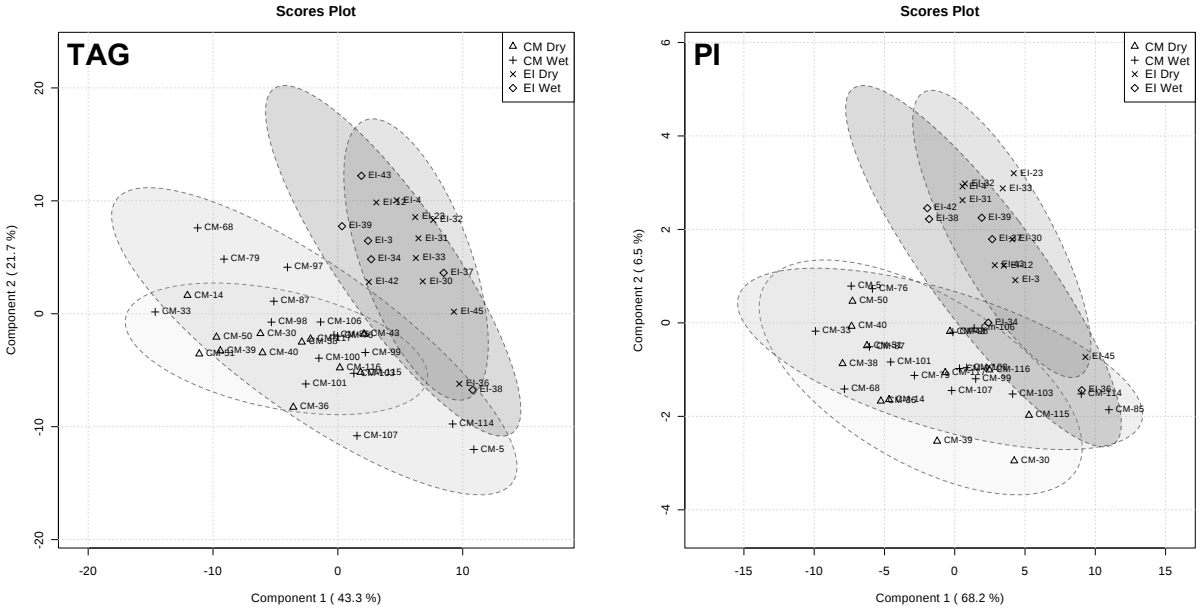

Figure 3.3 Exemplary PLS-DA
Exemplary principle partial least-squares discriminant analysis (PLS-DA) generated using component 1 (x-axis) and component 2 (y-axis) demonstrating species and seasonal clusters as a result of lipids in green turtles (CM) and hawksbill turtles (EI) between seasons (wet and dry). I captured all turtles in North Pacific Costa Rica in 2017. For complete data see Fig. A1.

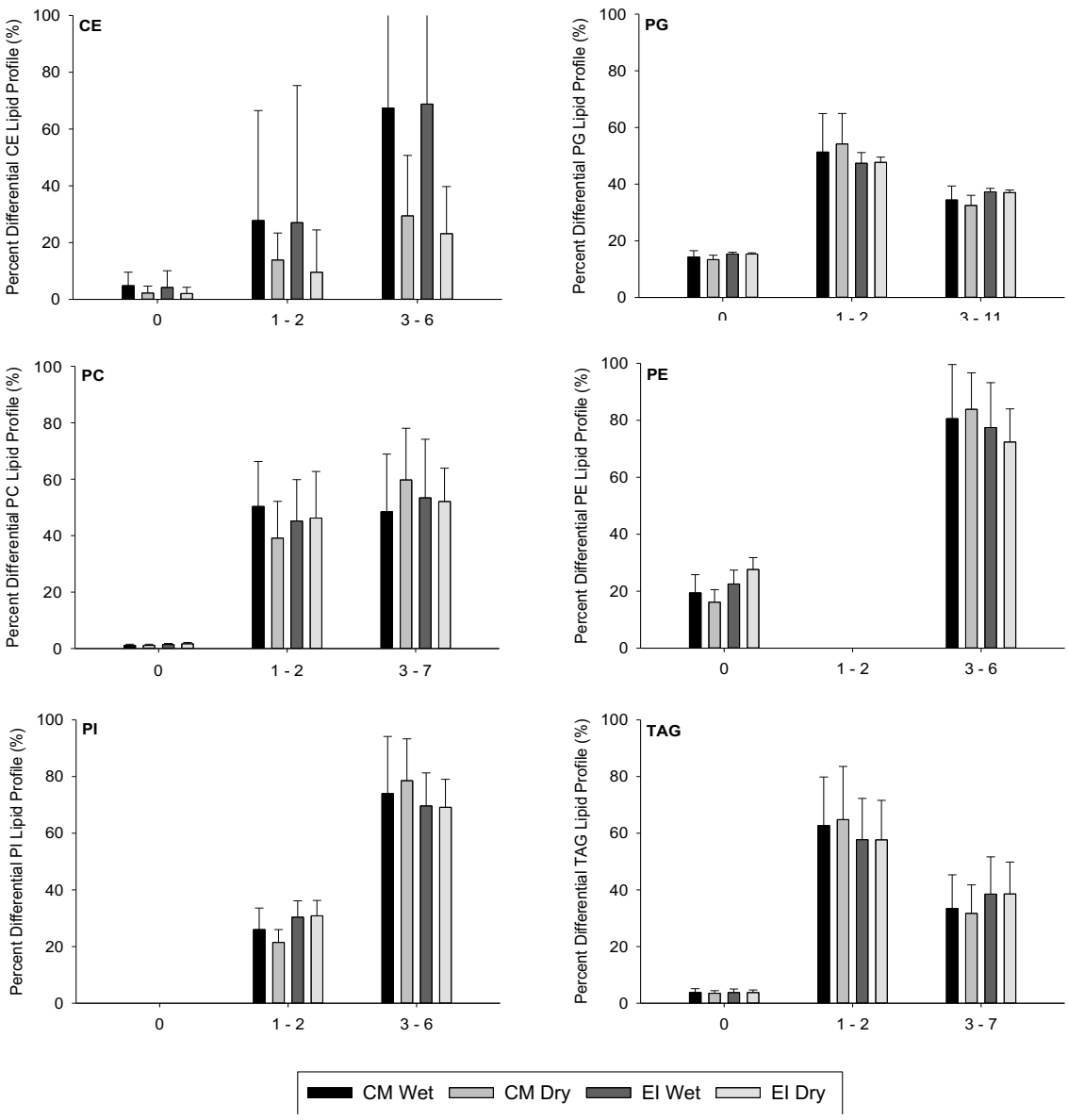

Figure 3.4 Differential Saturation
Percent differential lipids by class and divided by season (wet and dry) and species (green turtle = CM, hawksbill = EI). Bars and error bars represent mean ± standard deviation. The x-axis represents saturation level where 0 = unsaturation, 1 – 2 = mono and di unsaturated, and 3+ = polyunsaturated lipids.

CHAPTER 4. DIET AND FORAGING NICHE PARTITIONING IN GREEN AND HAWKSBILL TURTLES

Chelsea E. Clyde-Brockway, Maike Heidemeyer, Frank V. Paladino, and Elizabeth A. Flaherty.

4.1 Abstract

Investigating the niche overlap of similar species can reveal competition, niche partitioning, and a variety of ecosystem services among sympatric species. Therefore, understanding the mechanisms that allow similar species to coexist is important for both species and ecosystem conservation. I investigated diet, niche width and niche overlap in green turtles (black and yellow morphotype *Chelonia mydas*; 50 – 95 cm curved carapace length) and hawksbill turtles (*Eretmochelys imbricata*; 41 – 83 cm curved carapace length) in a recently described foraging habitat in North Pacific Costa Rica using stable isotope analysis. Whole blood $\delta^{13}C$ values were positively related to curved carapace length in black turtles, while epidermal $\delta^{15}N$ values were negatively related to curved carapace length in hawksbill turtles. However, in all cases, both $\delta^{13}C$ and $\delta^{15}N$ were depleted in whole blood compared to epidermis across all populations. In black turtles, sponges and tunicates constituted most of the diet (> 90% of total diet), while yellow turtles preferred red algae (~ 55%) but consumed green algae (~ 15%) and sponges and tunicates (~ 25%) as well, and hawksbill turtles foraged on a combination of red algae (~ 45%), green algae (~ 15%) and tunicates and sponges (~ 35%). Using whole blood, niche space revealed distinct enrichment in $\delta^{15}N$ isotopic space in black turtles and significant overlap between yellow turtles and hawksbill turtles. This study demonstrated that trophic niche and diet composition show patterns of resource partitioning supporting coexistence among spatially overlapping species. These results add to a growing understanding that diet in sea turtles is habitat specific and is influenced by species composition.

4.2 Introduction

Eastern Pacific upwelling zones harbor diverse foraging opportunities exploited by endangered green (*Chelonia mydas*) and critically endangered hawksbill (*Eretmochelys imbricata*) turtles (IUCN, 2004, 2008). Understanding the mechanisms that allow sympatric species to coexist are important for both species and ecosystem conservation (Thayer et al., 1982; Hill, 1998). As small juveniles (< 30 cm curved carapace length), both green and hawksbill turtles are oceanic with omnivorous diets (Bolten, 2003; Reich et al., 2007; Fukuoka et al., 2019) before recruiting to coastal foraging habitats where diets shift towards herbivory in green turtles and specialization on sponges in hawksbill turtles (Howell et al., 2016; Burgett et al., 2018; Ferriera et al., 2018). However, the degree of this shift is temporally and spatially variable (Bell, 2013; Carman et al., 2014; Santos et al., 2015; Tomaszewicz et al., 2018) and individualistic (Vander Zanden et al., 2013; Thomson et al., 2018). For example, investigations in a variety of habitats used by adult green turtles revealed that diet composition can range from a species-wide specialization on sea grass, algae or invertebrates, to opportunistic combinations of all three, sometimes including terrestrial plant matter, especially in the Eastern Pacific (Seminoff et al. 2002; Amorocho and Reina, 2007; Parker et al., 2011). Further, hawksbill turtles in specific habitats subsist on algae, or a combination of algae, sponges, and tunicates, although diets are generally more specialized than those in green turtles (Carr and Stancyk, 1975; Bell, 2013; Carrión-Cortez et al., 2013).

In spatially co-occurring, related species, within-site niche partitioning between species produces taxonomically distinct diets that may result from competition (Bjorndal and Bolten, 2010; Stringell et al., 2016; Ferrreira et al., 2018). Additionally, green and hawksbill turtles sharing foraging grounds support habitat health and biodiversity through partitioned ecosystem services (Hill, 1998; Bjorndal and Bolten, 2003; Goatley et al., 2012). For example, grazing by green turtles promotes nutrient cycling, stimulates growth in sea grass, and increases reef durability (Thayer et al., 1982; Moran and Bjorndal, 2005; Wabnitz et al., 2010). Further, hawksbill turtle foraging in reef systems advances coral growth and biodiversity (Meylan, 1988; Hill, 1998; León and Bjorndal, 2002). Therefore, simultaneous conservation of green and hawksbill turtles fosters and advances ecosystem management.

Green and hawksbill turtles forage concurrently in specific habitats in Costa Rica that are exposed to intense upwelling throughout the year (Heidemeyer et al., 2014; Stuhldreier et al., 2015). Green turtles in Pacific Costa Rica exist in two distinct morphotypes (Bowen et al., 1993; Pritchard, 1999); East-Pacific green turtles (or black morphotype green turtles) are confined to the Eastern Pacific Ocean, while the more common yellow morphotype green turtle forages in the Eastern Pacific but nests elsewhere (Bowen et al., 1992, 1993). Although identical to global hawksbill morphology, East-Pacific hawksbills are restricted to the Eastern Pacific Ocean (Gaos et al., 2017, 2019; Bell and Jensen, 2018). Despite persistent migratory behavior, sea turtles demonstrate fidelity to foraging habitats established during early neritic recruitment stages (Shimada et al., 2016; Bradshaw et al., 2017; Conrad et al., 2018; Hancock et al., 2018). Moreover, quality and sustainability of foraging habitats is directly related to future reproductive output (Harrison et al., 2011). Therefore, defining diet and foraging niche is critical when providing quality management and conservation strategies for the recovery of endangered sea turtles in the Eastern Pacific.

To understand foraging ecology in green and hawksbill turtles, it is important to investigate not only current diet, but also potential foraging strategies employed in past years. Stable isotopes are increasingly used in ecology to study diet and dietary shifts because the analysis measures assimilation of foods into body tissues. Because cellular turnover in tissues occurs at varied rates, use of different tissue types reflects diet across differing time scales from weeks to decades or even the animal's entire lifespan (Gannes et al., 1998; Post, 2002). Stable carbon ($\delta^{13}C$) and nitrogen ($\delta^{15}N$) isotope analysis provides low-resolution dietary information through estimates of proportional contribution of prey items to sea turtle tissue (Parnell et al., 2012). Stable isotope analysis can be used to infer trophic position, niche width, and niche overlap between spatially coexisting consumers (Bearhop et al., 2004; Flaherty and Ben-David, 2010; Cummings et al., 2012). Stable isotope studies are prevalent in green turtles and are gaining popularity in hawksbill sea turtles (Pearson et al., 2017). However, few studies have investigated segregation of diet, niche, and niche overlap in sympatric sea turtle species to directly explore trophic niche partitioning despite the endangered status of sea turtles and their roles in ecosystem functionality.

I used stable carbon and nitrogen signatures to explore diet and trophic niche diversity in black morphotype green turtles, yellow morphotype green turtles, and hawksbill turtles in a recently discovered foraging location in North Pacific Costa Rica (Heidemeyer et al., 2014). My objectives were to determine diet of green and hawksbill turtles using $\delta^{13}C$ and $\delta^{15}N$ isotope signatures of turtle tissues between neighboring gulfs and across seasons. I also compared whole blood stable isotope signatures to epidermal stable isotope signatures as a measure of temporal diet switching (shift in diet in the last 5 - 10 years) because of the differing turnover rate in the two tissues. Finally, I modeled niche space overlap within turtle groups to estimate habitat use and interspecific competition. By combining these results, I evaluated use of discrete diets by populations of turtles in Costa Rica, investigated shifts in diets from previous foraging habitats, and infer potential ecosystem services provided by sea turtles.

4.3 Methods

4.3.1 Sample Collection

I collected whole blood (WB; collected and stored without additives, black = 40, yellow = 13, hawksbill = 15; Lemons et al. 2012), and epidermal (EP) samples (black = 44, yellow = 13, hawksbill = 10) from live green and hawksbill turtles captured in Matapalito Bay (10.9°N; -85.79°W) and Salinas Bay (11.1°N; -85.7°W) Costa Rica (Fig. 4.1) from January to November 2017 (Heidemeyer et al., 2014). I collected WB samples (< 1 ml/kg) from the cervical sinus (Owens and Ruiz, 1980) using a 21 g needle, placed samples in a cryovial, and stored these on ice until I returned to shore. I removed EP (1 cm^2) samples using sterilized scalpel and forceps from the trailing edge of one of the hind flippers and placed in a 2 ml cryovial on ice until I returned to shore. On shore, I transferred EP samples to a high concentration saline solution (Arrington and Winemiller, 2002) and stored both WB and EP sampels at -18 °C in Costa Rica for up to one year before transport to Purdue University.

At the time of sample collection, I measured curved carapace length (CCL), tail length, and plastron-anus distance (P-A) to the nearest 0.5 cm using a flexible measuring tape. I measured tail length and P-A to estimated sex (Ross, 1984). I identified each turtle

using a passive integrated transponder (PIT) tag (AVID2028 FriendChip, Norco, California, USA) injected into the right shoulder beneath the skin, and two metal flipper tags (Style 681IC, National Band and Tag Company, Newport, KY, USA) attached to the hind flippers (Heidemeyer et al. 2018) to avoid repeated sampling. I gathered potential diet items throughout the year during turtle sampling days. These included small mobile invertebrates (*Ophiothrix spiculata, Telephrys cristulipes, Tripneustes depressus, Centrostephanus coronatus, Harpacticoida* spp.), red (*Rhodophyta*), brown (*Phaeophyceae*) and green (*Chlorophyta*) algae, sponges and tunicates (*Halichondria* spp. *Haliclona* spp., *Urochordata*), and sea grass (*Halophila ovalis*) from sites where I encountered turtles. I stored diet samples in salt, similar to skin samples.

4.3.2 Sample Preparation

I analyzed turtle tissue samples and whole prey items for stable isotope analysis. At the Purdue University Wildlife Physiology Lab, I thawed WB samples, placed them in individual aluminum weigh boats, and dried samples for 48 hr at 60°C. I thawed EP and diet samples and then cleaned them by soaking three separate times for 20 min in reverse osmosis deionized water to remove salt. Subsequently, I dried EP and diet samples in an oven at 60°C for 48 hrs. I homogenized dried samples into a fine powder using a mixer mill (Retsch MM 200, Glen Mills Inc., Clinton, NJ) for larger samples such as WB and large invertebrates, or using small scissors for smaller samples such as EP samples and small algal samples. I weighed a subsample of each homogenized sample into a miniature tin weigh boat (3.5 x 5 mm, Costech Analytical Technologies, Valencia, CA) and sent duplicate samples to the University of Wyoming Stable Isotope Facility (UWOSIF) for analysis of $\delta^{13}C$ and $\delta^{15}N$. In some cases, multiple individuals of small diet samples were combined to produce required dry weight for measurement. At UWOSIF, the lab analyzed samples using a Thermo Finnigan Delta Plus XP mass spectrometer (Thermo Fisher Scientific Inc., Waltham, MA) attached to a Costech 4010 (Costech Analytical Technologies, Valencia, CA) and Carlo Erba 1110 Elemental Analyzer (CE Elantech, Inc., Lakewood, NJ) using PeeDee belemnite (PDB) for the carbon standard and atmospheric air as the nitrogen standard. I report stable isotope ratios from this analysis relative to the isotope standard and expressed in delta (δ) notation in parts per thousand (‰):

$$\delta = ((R_{sample}/R_{standard}) - 1)(1000), \quad (1)$$

where R_{sample} is the ratio of the heavy to light isotope in the sample and $R_{standard}$ is the ratio of the heavy to light isotope in the standard ($^{13}C/^{12}C$ and $^{15}N/^{14}N$). Because I analyzed samples in duplicate, I averaged duplicates and only included individuals if between-sample variances were within that of machine error (between 0.1 – 0.25 ‰ depending on the individual run; Table 4.1). Despite large C:N ratios (Table 4.2), I did not apply a post hoc lipid correction because diet items (algae, invertebrates, sea grass) do not have a high lipid composition (Dodge et al., 2001; Kiljunen et al., 2006; Post et al., 2007; Burkholder et al., 2011).

4.3.3 Statistical Analysis

I conducted my statistical analyses using R statistical software (Version 3.4.4, Vienna, Australia) and SPSS (IBM, Armonk, New York). I used linear regression analyses to compare $\delta^{15}N$ and $\delta^{13}C$ signatures by CCL in all green turtles and then grouped turtles into small turtles (< 76 cm CCL) and large turtles (> 77 cm CCL), because the smallest turtle (in this study) with defining male characteristics was 77 cm CCL (Chaloupka and Limpus, 2005; Vander Zanden et al., 2012). In hawksbill turtles, I classified juveniles as < 70 cm CCL and adults as > 71 cm CCL (Bjorndal and Bolten, 2010; Limpus, 1992). I used one-way multivariate analyses of variance (MANOVA) or Kruskal Wallis Rank Sum Test (χ^2; when assumptions for parametric tests were not met) to test for differences in WB and EP stable $\delta^{13}C$ and $\delta^{15}N$ signatures separately. For each, I compared black morphotype green turtles between sites (Matapalito and Salinas), size, and season (dry: November – March, wet April – October), as well as to compare small turtles between species and season. For each statistically significant result, I conducted subsequent post-hoc ANOVAs to determine whether differences were within the $\delta^{15}N$ signature or the $\delta^{13}C$ signature. I applied a repeated measures MANOVA to compare the WB stable isotope signature to that of the EP for each turtle.

To test for diet items with similar signatures, I pooled all diet samples and used a multivariate analysis of variance (MANOVA; Zar, 2010) with post-hoc Tukey analysis and a K nearest-neighbor (KNN) randomization and then grouped diet items that did not differ significantly in bivariate space. I adjusted the isotopic signature of diet items using

discrimination factors established for green turtles with for both WB ($\Delta^{13}C = 0.55 \pm 0.58$ ‰, and $\Delta^{15}N = 3.23 \pm 0.38$ ‰; Vander Zanden et al., 2012) and EP ($\Delta^{13}C = 1.75 \pm 0.59$ ‰, and $\Delta^{15}N = 3.91 \pm 0.42$ ‰; Vander Zanden et al., 2012). Then I used the MixSIAR package in R statistical software to create mixing models for each species and estimate proportional input of each diet item within a Bayesian framework (Stock and Semmens, 2016). I ran individual models for each group of turtles (black, yellow and hawksbill) WB separately. I used 3 Markov Chain Monte Carlo (MCMC) chain runs until they reached convergence, defined as Rhat value < 1.01 and Geweke diagnostic with z-scores for 0 variables outside the range of ± 1.96 in each chain (Geweke, 1991; Brooks and Gelman, 1998). I employed kernel utilization density (KUD) methods to calculate the size of isotopic niche space and percent overlap of WB from turtles from three populations (black morphotype and yellow morphotype green turtles, and hawksbill turtles) for the 50 %, 75%, and 95% contours with the rKIN package in program R (Eckrich et al., *in review*; Eckrich et al., 2018). I did not conduct KUD on EP samples due to insufficient sample sizes (n < 10).

4.4 Results

Whole blood $\delta^{13}C$ values ranged from -17.9 – -15.57 ‰ in black morphotype green turtles (n = 39), -17.19 – -14.99 ‰ in yellow morphotype green turtles (n = 13), and -19.28 – -14.13 ‰ in hawksbill turtles (13), while $\delta^{15}N$ values ranged from 11.03 – 15.47 ‰ in black turtles, 11.66 – 13.36 ‰ in yellow turtles, and 12.15 – 13.18 ‰ in hawksbill turtles (Table 4.1). Linear regression revealed that $\delta^{13}C$ was related to body size in black morphotype green turtles for WB tissue ($R^2 = 0.359$, $F_{1,37} = 22.24$, $p < 0.001$) and EP tissue in hawksbill turtles ($R^2 = 0.575$, $F_{1,5} = 9.101$, $p = 0.03$; Fig. 4.2). I determined that within individual turtles, EP and WB samples varied in both $\delta^{13}C$ and $\delta^{15}N$ (‰) signatures ($F_{2,19} = 71.723$, Wilks' = 0.117, $p < 0.001$). Both $\delta^{13}C$ and $\delta^{15}N$ WB values were depleted compared to EP values ($\delta^{13}C$: $F_{1,20} = 62.640$, $p < 0.001$; $\delta^{15}N$: $F_{1,20} = 76.079$, $p < 0.001$).

For black morphotype green turtles, I determined statistical similarity between WB stable $\delta^{13}C$ and $\delta^{15}N$ signatures of turtles captured in Salinas and Matapalito ($\delta^{13}C$: $\chi_1^2 = 0.071$, $p = 0.79$; $\delta^{15}N$: $\chi_1^2 = 0.001$, $p = 0.973$), consequently, I did not include location in

further analyses. Within small black morphotype turtles, I observed depleted signatures in small turtles compared to large turtles in the $\delta^{13}C$ signature alone ($\chi_1^2 = 7.098$, $p = 0.008$) and no difference in $\delta^{15}N$ signatures ($\chi_1^2 = 0.824$, $p = 0.364$; Table 4.1). In large back morphotype turtles, $\delta^{13}C$ did not vary by season ($\chi_1^2 = 0.003$, $p = 0.955$), while turtles captured in the dry season had enriched $\delta^{15}N$ compared to turtles captured in the wet season ($\chi_1^2 = 11.538$, $p < 0.001$). In small black turtles, WB stable isotope signatures did not vary by season ($\delta^{13}C$: $\chi_1^2 = 0.32$, $p = 0.572$; $\delta^{15}N$: $\chi_1^2 = 1.28$, $p = 0.258$). In large black morphotype turtles, stable isotope signature varied by presumed sex in large turtles, in $\delta^{15}N$ signature alone ($\delta^{13}C$: $\chi_1^2 = 2.294$, $p = 0.130$; $\delta^{15}N$: $\chi_1^2 = 6.872$, $p = 0.009$). Because of the interaction between season and size class in black turtles, I did not statistically compare them to yellow and hawksbill turtles.

In yellow morphotype green turtles, I observed no size related variability ($\delta^{13}C$: $\chi_1^2 = 2.381$, $p = 0.123$; $\delta^{15}N$: $\chi_1^2 = 0.595$, $p = 0.440$) or seasonal variation ($\delta^{13}C$: $\chi_1^2 = 0.193$, $p = 0.661$; $\delta^{15}N$: $\chi_1^2 = 0.021$, $p = 0.8836$) in WB stable isotope signatures. Due to sample size, I was unable to determine differential WB stable isotope signatures between small and large hawksbill turtles. However, stable isotope signatures did not vary by season in small turtles ($F_{1,2} = 1.75$, $p = 0.228$, Wilks' = 0.720). Further, WB stable isotope signatures between small hawksbill turtles and all yellow morphotype green turtles were comparable ($F_{1,2} = 0.834$, $p = 0.4475$, Wilks' = 0.930).

The EP samples in this study ranged in $\delta^{13}C$ values from -16.89 – -14.05 ‰ in black morphotype green turtles (n = 15), -15.8 – -13.97 ‰ in yellow morphotype green turtles (n = 5), and -17.9 – -12.75 ‰ in hawksbill turtles (n = 7), while $\delta^{15}N$ values ranged from 14.04 – 16.06 ‰ in black morphotype green turtles, 12.92 – 15.07 ‰ in yellow morphotype green turtles, and 13.4 – 14.21 ‰ in hawksbill turtles (Table 4.1). Within black morphotype turtles, I recorded no variability in EP stable isotope signatures between Matapalito and Salinas ($F_{2,12} = 0.681$, $p = 0.525$, Wilks' = 0.898), between size classes ($F_{2,12} = 0.664$, $p = 0.533$, Wilks' = 0.9), or between season ($F_{2,12} = 0.177$, $p = 0.840$, Wilks' = 0.971). In yellow morphotype turtles, my results included five usable EP samples, all small individuals. Based on means (Table 4.1), I estimated that all stable isotope signatures were consistent across seasons. In hawksbill turtles, I only recorded EP results from one turtle captured in

the wet season (the sole large turtle). However, when reviewing the raw data, the $\delta^{13}C$ signature was enriched compared to the juvenile turtles, while the $\delta^{15}N$ was within the range of the remaining juvenile turtles (Table 4.1). Further, I identified morphotype specific stable isotope signatures ($F_{2,17} = 10.535$, $p = 0.001$, Wilks' = 0.447), in the $\delta^{15}N$ signature ($F_{1,18} = 22.269$, $p < 0.001$) but not the $\delta^{13}C$ ($F_{1,18} = 0.229$, $p = 0.553$). Similarly, black morphotype green turtles and hawksbill turtles had differential stable isotope signatures ($F_{2,19} = 30.014$, $p < 0.001$, Wilks' = 0.240), again a variability in the $\delta^{15}N$ signature ($F_{1,20} = 59.471$, $p < 0.001$) and not the $\delta^{13}C$ ($F_{1,20} = 1.722$, $p = 0.204$). Finally, yellow morphotype green turtles and hawksbills had statistically similar stable isotope signatures ($F_{2,9} = 0.150$, $p = 0.863$).

4.4.1 Diet Composition

Initially I collected stable isotope signatures from a range of green and red algae samples, sponges, tunicates, mobile invertebrates and sea grass. However, based on the results of my KNN and MANOVA analyses, I combined these diet items into five groups: green algae (GA), red algae (RA), mobile invertebrates (MI), sessile invertebrates (SI, which included sponges and tunicates), and sea grass (SG; Table 4.2). Due the stable isotope signatures of sea grass and the low likelihood that it contributed to the diet (positioned outside the mixing space of turtle signatures), I removed it from figures and models (Table 4.2; Fig. 4.3A, B). Initial assessment suggested that black turtles specialized in sponges and tunicates (sessile invertebrates), while yellow turtles and hawksbill turtles experienced a dietary shift from a combination diet (of sessile invertebrates and red algae) in EP tissue to a more specialized and recent diet (red algae) in WB tissue (Fig. 4.3). In both tissues, the single large hawksbill turtle consumed prey items with depleted $\delta^{13}C$ signatures compared to small turtles, and results from mixing model supported these observations. Specifically, black turtle diet specialized on sessile invertebrate, while yellow turtles and hawksbill turtles consumed a combination of red algae and sessile invertebrates (Table 4.3). Diet composition was similar across size classes in all populations.

4.4.2 Niche Space Modeling

Results from KUD of WB stable isotope signatures in small black turtles and all yellow turtles revealed that the 95% contour was four times larger than the 50% contour, while, in small hawksbill turtles, the 95% contour was three times larger than the 50% contour (Table 4.4). Of the three populations, all yellow turtles demonstrated significant overlap with small hawksbill turtle niche space, whereas small black turtles comprised distinct niche space (Fig. 4.4A). At the largest contour (95%), I measured 5 – 7% overlap in black and hawksbill turtle niche space, and 3 – 13% overlap between black and yellow morphotype green turtle niche space (Table 4.5). The core contour level (50%) revealed 0% overlap in both cases. Hawksbill and yellow turtles exhibited significant overlap in niche space, with core contour (50%) overlap from 44% up to 76% overlap at the 95% contour (Table 4.5). In large black turtles, niche space decreased in area at all contours suggesting a more uniform diet compared to small black turtles (Fig. 4.4B). Further, overlap between large black turtles and other populations increased at the 95% contour (hawksbill: 10 – 12% overlap; yellow: 14% overlap), while core contour overlap (50%) did not increase (Table 4.6).

4.5 Discussion

Trophic diversity appears to occur among spatially co-occurring sea turtle populations in recently discovered foraging grounds in North Pacific Costa Rica. Black morphotype green turtles consumed a distinct diet at a higher trophic level compared to yellow morphotype green turtles and hawksbills. Further, yellow morphotype green turtles' isotopic niche overlapped with hawksbill turtles' isotopic trophic niche, although the composition of the diets differed. Through the combination of comparative stable isotope assessment using multiple tissues, I documented a depletion in both carbon and nitrogen in EP tissue compared to WB tissue across all populations. This suggests a latitudinal habitat shift and dietary shift from gelatinous oceanic prey to a combination of sessile invertebrates and red algae (depending on the population) once residency was established along the coast. My results support prior research that green and hawksbill turtles segregate potential foraging resources when they overlap. My results also confirm studies suggesting that

hawksbill and yellow morph turtles are dietary specialists (Bjorndal and Bolten, 2010; Rincon-Diaz et al., 2011), while black morph turtles are generalist omnivores (López-Mendilaharsu et al., 2008; Sampson et al., 2018). Although stable isotope analysis measures assimilation as opposed to ingestion in gut analysis, my results support conclusions drawn from these studies.

Age-related ontogenetic shifts in diet predict that with increasing CCL, green turtle tissue should display an increase in $\delta^{13}C$ values (shifting from oceanic to coastal signatures; Cherel and Hobson, 2007) and a decrease in $\delta^{15}N$ signature (shifting from omnivory/carnivory to herbivory; Carman et al., 2014; Howell et al., 2016; Burgett et al., 2018). While my results confirm this trend in black morphotype turtle WB (positive relation between $\delta^{13}C$ and CCL), EP tissue displayed no $\delta^{13}C$ or $\delta^{15}N$ variability with body size, similar to WB $\delta^{15}N$ signature. Further, while no significant relationship was present between stable isotope signatures and CCL in yellow morphotype turtles, EP $\delta^{15}N$ displayed a negative relationship with CCL (supporting dietary shift towards herbivory). In hawksbill turtles, I expected to observe a similar enrichment in $\delta^{13}C$ values and depletion in $\delta^{15}N$ values over time (Ferreira et al., 2018). My results revealed no relationship between CCL and stable isotope signatures in WB; however, both $\delta^{13}C$ and $\delta^{15}N$ signatures were negatively related to body size (although only change in $\delta^{13}C$ was significant). Therefore, my results corroborate slight dietary shifts towards coastal adult diets (Cherel and Hobson, 2007), and I provide support for diet consistency over time in turtles included in this study.

Direct comparison of EP tissue to WB tissue within individual turtles revealed depletion in both stable isotope signatures. Because I captured turtles in coastal habitats, I assumed turtles initiated coastal foraging. While turtles could instead be using these coastal habitats for resting between foraging bouts to oceanic foraging habitats ($\delta^{13}C$ signature), this is unlikely because of their $\delta^{15}N$ signature. Carbon signatures vary across latitudes and the depletion recorded here could indicate a habitat shift from more tropical oceanic foraging sites to higher latitude coastal foraging sites (Cherel and Hobson, 2007). The ontogenetic shift between oceanic gelatinous planktivory to coastal adult diets is a slow process, often including years of intermediate diets and niche size (Cardona et al., 2012; Carman et al., 2014; Howell et al., 2016; Ferreira et al., 2018). Therefore, my results could

be quantifying varying degrees of this shift within the turtles sampled at the two sites and may not be indicative of sexually mature adult diets.

Diet composition suggested that foraging pattern s in my study sites might be an example of diet selection when sea turtles are able to freely select dietary sources (i.e., not confined by limited resources). Generalist dietary foraging strategies are common throughout black turtles foraging in the Eastern Pacific, however turtles often consume algae and supplement with animal matter, or prefer mobile invertebrates (Seminoff et al., 2002; López-Mendilaharsu et al., 2005; Lemons et al., 2011; Sampson et al., 2018). Therefore, it is unique to find black turtles consuming a diet composed primarily of sponges and tunicates. I observed slight variability in WB $\delta^{15}N$ signature across seasons suggesting a preference for higher tropic level prey during upwelling compared to non-upwelling (wet) seasons (López-Mendilaharsu et al., 2008). Diet variability generally is caused by availability of prey (Gama et al., 2016). When upwelling increases, secondary consumers recruit to coastal habitats to exploit the increase in productivity, potentially suggesting importance of other potential dietary sources (not measured here). Alternatively, shifts in nitrogen throughout the year could indicate shifts in environmental nutrient cycling (Dawes, 1986; Yamamuro et al., 2011; Stuhldreier et al., 2015). Lack of seasonal variability in yellow morphotype sea turtles, therefore, is consistent with an herbivorous diet which remains consistent throughout the year. Specialization in yellow morphotype green turtles (Hatase et al., 2006; Vander Zanden et al., 2013; Burgett et al., 2018; Thomson et al., 2018) and generalization in black turtle diets are common throughout their range (Amorocho and Reina, 2007; Russell et al., 2011; Sampson et al., 2018). My results supported these findings and suggested that because population diets are consistent throughout time (Conrad et al., 2018), morphological difference between sea turtle populations (morphotypes) could be a result of foraging niche segregation. While hawksbill turtles are generally spongivorous (Blumenthal et al., 2009; Berube et al., 2012; Wood et al., 2017), algivory is not unique to turtles in this study (Rincon-Diaz et al., 2011; Bell, 2013; von Brandis et al., 2014). However, foraging on algae is not commonly reported in East Pacific hawksbill turtles. Although many hawksbill nesting sites throughout Central America are undiscovered (Gaos et al., 2018), foraging locations exist throughout the region (Llamas et al., 2017). My results suggested that turtles within Matapalito, although

sharing the same spatial distribution, segregate nutritional resources promoting coexistence among ecologically similar species. Further, my data revealed that species divisions and foraging site were not sufficient indicators in predicting diet in green turtles. I supported prior conclusions that sea turtles are opportunistic feeders and that stable isotopes are a powerful tool to understanding inter- and intra-specific niche partitioning among populations of turtles within a single foraging ground.

Current diet (WB) KUD corroborated diet models and revealed distinct niche space between black morphotype turtles and both yellow morphotype turtles and hawksbill turtles, and overlapping niche space between the latter two populations (Bearhop et al., 2004). Further core niche space (50% contour) revealed increasing niche space from black turtles to hawksbill turtles to yellow turtles. Increasing trophic niche indicates an increase in dietary specialization in individuals among a generalist population (Flaherty and Ben-David, 2010; Cummings et al., 2012; Eckrich et al., 2018). Therefore, black turtles (consuming sessile invertebrates) were all foraging on the same range of dietary items, while in yellow and hawksbill turtles, individual specialization on either red algae, sessile invertebrates, or green algae lead to specialized diets. However, it is also plausible that black turtles were consuming alternative prey items not measured here, such as gelatinous organisms (Carman et al., 2014). Because the largest turtles in my study were still likely not sexually mature, it is possible that diets will continue to shift over time.

4.5.1 Ecological Implications

Consistency in WB stable nitrogen signatures across sizes suggests turtles forage in Matapalito and Salinas Bays during their neritic juvenile stage, sub-adult, and adult stages. Depletions in WB stable isotope signatures compared to EP stable isotope signatures indicated a shift in diet in recent decades. Matapalito and Salinas Bays are foraging habitats for East Pacific sea turtles supporting unique diet composition and rocky reefs that provide protected areas for turtles to rest thereby supporting sea turtles through multiple factors (MacDonald et al., 2012; Proietti et al., 2012). Moreover, due to the biodiversity within Matapalito, other resources such as cleaning by fish, could exist (Stampar et al., 2007). Further, low levels of anthropogenic waste within these areas decrease likelihood that turtles will ingest plastics, a common problem throughout the

world due to foraging strategies in sea turtles (Clukey et al., 2017). I argue these bays are not stopover or overwintering sites (Fukuoka et al., 2019), but are permanent foraging habitats and warrant vigilant protection.

The decline of sea turtles also negatively impacts environments because of the ecosystem services these species provide. Specifically, green turtles managing algae growth and increasing nutrient cycling in sea grass pastures (Thayer et al., 1982; Bjorndal and Bolten, 2003; Moran and Bjorndal, 2005) while the spongivorous hawksbill turtle promote reef biodiversity (Hill, 1998; Obura et al., 2010). Understanding resource use, diet, and niche overlap across species is critical for conservation and habitat management. In my study sites, diet and niche partitioning suggested sea turtles in Matapalito and Salinas were providing a wide range of ecosystems services central to the resilience and persistence of the small coral communities that exist within these bays (Wabnitz et al., 2010; Goatley et al., 2012). Therefore, sea turtle conservation in Costa Rica is central of environmental conservation and sustained biodiversity caused by unique upwelling patterns.

The continued understanding of diet, trophic niche, and niche overlap between spatially co-occurring species, and how these parameters transform temporally, requires comparative studies that vary in time and space. I recommend that future diet studies combine assessment techniques (i.e. stable isotope analysis, underwater observation) with spatial analysis (comparative studies from distinct habitats, satellite telemetry) to assess the importance of specific dietary items and foraging habitats within Central America.

4.6 Acknowledgments

I would like to thank K. Mora, R. Mora, M. Mora, A. Lara, M. Giry and all the volunteers with Equipo Tora Carey for their assistance and support in Costa Rica, Drs. P. Ruhl and J. Berl for their assistance with data analysis, and Drs. J. Spotila and R. Goforth for reviewing this manuscript. I would also like to thank the Stable Isotope Facility at the University of Wyoming for their assistance with sample analysis. This project was financially supported by The Leatherback Trust and the USDA National Institute of Food and Agriculture, Hatch Project 1004115 (to EAF). This research was conducted under approval by the Guanacaste Conservation Areas (ACG) of the Ministry of Environment of Costa Rica (ACG-PI-PC-019, R-ACG-057-2016), USFWS (CITES permit

17US06369C/9) and the Purdue Animal Care and Use Committee (protocol #1510001309).

4.7 Literature Cited

Amorocho, D.F., Reina, R.D., 2007. Feeding ecology of the East Pacific green sea turtle *Chelonia mydas agassizii* at Gorgona National Park, Colombia. Endang. Species Res. 3, 43–51.

Arrington, D.A., Winemiller, K.O., 2002. Preservation effects on stable isotope analysis of fish muscle. Trans. Am. Fish. Soc. 131(2), 337–342.

Bearhop, S., Adams, C.E., Waldron, S., Fuller, R.A., MacLeod, H., 2004. Determining trophic niche width: a novel approach using stable isotope analysis. J. Anim. Ecol. 73(5), 1007–1012.

Bell, I., 2013. Algivory in hawksbill turtles: *Eretmochelys imbricata* food selection within a foraging area on the Northern Great Barrier Reef. Mar. Ecol. 34(1), 43–55.

Bell, I., Jensen, M.P., 2018. Multinational genetic connectivity identified in western Pacific hawksbill turtles, *Eretmochelys imbricata*. Wildl. Res. 45(4), 307–315.

Berube, M.D., Dunbar, S.G., Rützler, K., Hayes, W.K., 2012. Home range and foraging ecology of juvenile hawksbill sea turtles (*Eretmochelys imbricata*) on inshore reefs of Honduras. Chelonian Conserv. Biol. 11(1), 33–43.

Bjorndal, K.A., Bolten, A.B., 2003. From ghosts to key species: restoring sea turtle populations to fulfill their ecological roles. Mar. Turtle Newsl. 100(100), 16–21.

Bjorndal, K.A., Bolten, A.B., 2010. Hawksbill sea turtles in seagrass pastures: success in a peripheral habitat. Mar. Biol. 157(1), 135–145.

Blumenthal, J.M., Austin, T.J., Bell, C.D.L., Bothwell, J.B., Broderick, A.C., Ebanks-Petrie, G., Gibb, J.A., Luke, K.E., Olynik, J.R., Orr, M.F., Solomon, J.L., 2009. Ecology of hawksbill turtles, *Eretmochelys imbricata*, on a western Caribbean foraging ground. Chelonian Conserv. Biol. 8(1), 1–10.

Bolten, A.B., 2003. Variation in sea turtle life history patterns: neritic versus oceanic developmental stages. In: Lutz PL, Musick JA, Wyneken J (eds) The biology of sea turtles. CRC Press, Boca Ratón, pp 243–257.

Bowen, B.W., Meylan, A.B., Ross, J.P., Limpus, C.J., Balazs, G.H., Avise, J.C., 1992. Global population structure and natural history of the green turtle (Chelonia mydas) in terms of matriarchal phylogeny. Evolution 46(4), 865–881.

Bowen, B.W., Nelson, W.S., Avise, J.C., 1993. A molecular phylogeny for marine turtles: trait mapping, rate assessment, and conservation relevance. Proc. Natl. Acad. Sci. 90(12), 5574– 5577.

Bradshaw, P.J., Broderick, A.C., Carreras, C., Inger, R., Fuller, W., Snape, R., Stokes, K.L., Godley, B.J., 2017. Satellite tracking and stable isotope analysis highlight differential recruitment among foraging areas in green turtles. Mar. Ecol. Prog. Ser. 582, 201–214.

Brooks, S.P., Gelman, A., 1998. General methods for monitoring convergence of iterative simulations. J. Comput. Graph. Stat. 7, 434–455.

Burgett, C.M., Burkholder, D.A., Coates, K.A., Fourqurean, V.L., Kenworthy, W.J., Manuel, S.A., Outerbridge, M.E., Fourqurean, J.W., 2018. Ontogenetic diet shifts of green sea turtles (*Chelonia mydas*) in a mid-ocean developmental habitat. Mar. Biol. 165(2), 33–44.

Burkholder, D.A., Heithaus, M.R., Thomson, J.A., Fourqurean, J.W., 2011. Diversity in trophic interactions of green sea turtles *Chelonia mydas* on a relatively pristine coastal foraging ground. Mar. Ecol. Prog. Ser. 439, 277–293.

Cardona, L., Alvarez de Quevedo, I., Borrell, A., Aguilar, A., 2012. Massive consumption of gelatinous plankton by Mediterranean apex predators. PLoS ONE 7, e31329.

Carman, V.G., Botto, F., Gaitán, E., Albareda, D., Campagna, C., Mianzan, H., 2014. A jellyfish diet for the herbivorous green turtle *Chelonia mydas* in the temperate SW Atlantic. Mar. Biol. 161(2), 339–349.

Carr, A., Stancyk, S., 1975. Observations on the ecology and survival outlook of the hawksbill turtle. Biol. Cons. 8(3), 161–172.

Carrión-Cortez, J., Canales-Cerro, C., Arauz, R., Riosmena-Rodríguez, R., 2013. Habitat use and diet of juvenile eastern Pacific hawksbill turtles (*Eretmochelys imbricata*) in the North Pacific coast of Costa Rica. Chelonian Conserv. Biol. 12(2), 235–245.

Chaloupka, M., Limpus, C., 2005. Estimates of sex-and age-class-specific survival probabilities for a southern Great Barrier Reef green sea turtle population. Mar. Biol. 146, 1251–1261.

Cherel, Y., Hobson, K.A., 2007. Geographical variation in carbon stable isotope signatures of marine predators: a tool to investigate their foraging areas in the Southern Ocean. Mar. Ecol. Prog. Ser. 329, 281–287.

Clukey, K.E., Lepczyk, C.A., Balazs, G.H., Work, T.M., Lynch, J.M., 2017. Investigation of plastic debris ingestion by four species of sea turtles collected as bycatch in pelagic Pacific longline fisheries. Mar. Pollut. Bull. 120(1-2), 117–125.

Conrad, C., Barceló, L.P., Seminoff, J.A., Tomaszewicz, C.T., Labonte, M., Kemp, B.M., Jones, E.L., Stoyka, M., Bruner, K., Pastron, A., 2018. Ancient DNA Analysis and Stable Isotope Ecology of Sea Turtles (*Cheloniidae*) from the Gold Rush-era (1850s) Eastern Pacific Ocean. Open Quaternary 4(3), 1–13.

Cummings, D.O., Buhl, J., Lee, R.W., Simpson, S.J., Holmes, S.P., 2012. Estimating niche width using stable isotopes in the face of habitat variability: a modelling case study in the marine environment. PLoS ONE 7(8), e40539.

Dawes, C.J., 1986. Seasonal proximate constituents and caloric values in seagrasses and algae on the west coast of Florida. J. Coastal Res. 2, 25–32.

Dodge, K.L., Logan, J.M., Lutcavage, M.E., 2011. Foraging ecology of leatherback sea turtles in the Western North Atlantic determined through multi-tissue stable isotope analyses. Mar. Biol. 158, 2813–2824.

Eckrich, C.A., Albeke, S.E., Flaherty, E.A., Bowyer, R.T., Ben-David, M., rKIN: Kernel-based method for estimating isotopic niche size and overlap. J. Anim. Ecol. *in review*

Eckrich, C.A., Flaherty, E.A., Ben-David, M., 2018. Functional and numerical responses of shrews to competition vary with mouse density. PLoS ONE 13(1), e0189471.

Ferreira, R.L., Ceia, F.R., Borges, T.C., Ramos, J.A., Bolten, A.B., 2018. Foraging niche segregation between juvenile and adult hawksbill turtles (*Eretmochelys imbricata*) at Príncipe Island, West Africa. J. Exp. Mar. Biol. Ecol. 498, 1–7.

Flaherty, E.A., Ben-David, M., 2010. Overlap and partitioning of the ecological and isotopic niches. Oikos 119(9), 1409–1416.

Fukuoka, T., Narazaki, T., Kinoshita, C., Sato, K., 2019. Diverse foraging habits of juvenile green turtles (*Chelonia mydas*) in a summer-restricted foraging habitat in the northwest Pacific Ocean. Mar. Biol. 166(3), 25–39.

Gama, L.R., Domit, C., Broadhurst, M.K., Fuentes, M.M., Millar, R.B., 2016. Green turtle *Chelonia mydas* foraging ecology at 25 S in the western Atlantic: evidence to support a feeding model driven by intrinsic and extrinsic variability. Mar. Ecol. Prog. Ser. 542, 209–219.

Gannes, L.Z., Del Rio, C.M., Koch, P., 1998. Natural abundance variations in stable isotopes and their potential uses in animal physiological ecology. Comp. Biochem. Physiol. 119A, 725–737.

Gaos, A.R., Lewison, R.L., Jensen, M.P., Liles, M.J., Henriquez, A., Chavarria, S., Pacheco, C.M., Valle, M., Melero, D., Gadea, V., Altamirano, E., 2017. Natal foraging philopatry in Eastern Pacific hawksbill turtles. R. Soc. Open Sci. 4(8), 170153.

Gaos, A.R., Lewison, R.L., Jensen, M.P., Liles, M.J., Henriquez, A., Chavarria, S., Pacheco, C.M., Valle, M., Melero, D., Gadea, V., Altamirano, E., 2018. Rookery contributions, movements and conservation needs of hawksbill turtles at foraging grounds in the eastern Pacific Ocean. Mar. Ecol. Prog. Ser. 586, 203–216.

Geweke, J., 1991. Evaluating the accuracy of sampling-based approaches to the calculation of posterior moments (Vol. 196). Minneapolis, MN, USA: Federal Reserve Bank of Minneapolis, Research Department.

Goatley, C.H., Hoey, A.S., Bellwood, D.R., 2012. The role of turtles as coral reef macroherbivores. PLoS ONE 7(6), e39979.

Hancock, J.M., Vieira, S., Jimenez, V., Rio, J.C., Rebelo, R., 2018. Stable isotopes reveal dietary differences and site fidelity in juvenile green turtles foraging around São Tomé Island, West Central Africa. Mar. Ecol. Prog. Ser. 600, 165–177.

Harrison, X.A., Blount, J.D., Inger, R., Norris, D.R., Bearhop, S., 2011. Carry-over effects as drivers of fitness differences in animals. J. Anim. Ecol. 80(1), 4–18.

Hatase, H., Sato, K., Yamaguchi, M., Takahashi, K., Tsukamoto, K., 2006. Individual variation in feeding habitat use by adult female green sea turtles (*Chelonia mydas*): are they obligately neritic herbivores? Oecologia 149(1), 52–64.

Heidemeyer, M., Arauz-Vargas, R., López-Agüero, E., 2014. New foraging grounds for hawksbill (*Eretmochelys imbricata*) and green turtles (*Chelonia mydas*) along the northern Pacific coast of Costa Rica, Central America. Rev. Biol. Trop. 62(4), 109–118.

Heidemeyer, M., Delgado-Trejo, C., Hart, C.E., Clyde-Brockway, C.E., Fonseca, L.G., Mora, R., Mora, M., Lara, A., Obando, R., 2018. Long-term in-water recaptures of adult black turtles (*Chelonia mydas*) provide implications for flipper tagging methods in the Eastern Pacific. Herpetol. Rev. 49(4), 653–657.

Hill, M.S., 1998. Spongivory on Caribbean reefs releases corals from competition with sponges. Oecologia 117(1-2), 143–150.

Howell, L.N., Reich, K.J., Shaver, D.J., Landry Jr., A.M., Gorga, C.C., 2016. Ontogenetic shifts in diet and habitat of juvenile green sea turtles in the northwestern Gulf of Mexico. Mar. Ecol. Prog. Ser. 559, 217–229.

IUCN, 2004. The international union for the conservation of nature, *Chelonia mydas*. https://www.iucnredlist.org/

IUCN, 2008. The international union for the conservation of nature, *Eretmochelys imbricata*. https://www.iucnredlist.org/

Kiljunen, M., Grey, J., Sinisalo, T., Harrod, C., Immonen, H., Jones, R.I., 2006. A revised model for lipid-normalizing δ13C values from aquatic organisms, with implications for isotope mixing models. J. Appl. Ecol. 43(6), 1213–1222.

Lemons, G., Lewison, R., Komoroske, L., Gaos, A., Lai, C.T., Dutton, P., Eguchi, T., LeRoux, R., Seminoff, J.A., 2011. Trophic ecology of green sea turtles in a highly urbanized bay: insights from stable isotopes and mixing models. J. Exp. Mar. Biol. Ecol. 405, 25–32.

Lemons, G.E., Eguchi, T., Lyon, B.N., LeRoux, R., Seminoff, J.A., 2012. Effects of blood anticoagulants on stable isotope values of sea turtle blood tissue. Aquat. Biol. 14(3), 201–206.

León, Y.M., Bjorndal, K.A., 2002. Selective feeding in the hawksbill turtle, an important predator in coral reef ecosystems. Mar. Ecol. Prog. Ser. 245, 249–258.

Limpus, C.J., 1992. The hawksbill turtle, *Eretmochelys imbricata*, in Queensland: population structure within a southern Great Barrier Reef feeding ground. Wildl. Res. 19(4), 489–505.

Llamas, I., Flores, E.E., Abrego, M.E., Seminoff, J.A., Hart, C.E., Donadi, R., Peña, B., Alvarez, G., Poveda, W., Amorocho, D.F., Gaos, A., 2017. Distribution, size range and growth rates of hawksbill turtles at a major foraging ground in the eastern Pacific Ocean. Lat. Am. J. Aquat. Res. 45(3), 585–596.

López-Mendilaharsu, M., Gardner, S.C., Seminoff, J.A., Riosmena-Rodriguez, R., 2005. Identifying critical foraging habitats of the green turtle (*Chelonia mydas*) along the Pacific coast of the Baja California peninsula, Mexico. Aquat. Conserv. Mar. Freshw. Ecosyst. 15(3), 259–269.

López-Mendilaharsu, M., Gardner, S.C., Riosmena-Rodriguez, R., Seminoff, J.A., 2008. Diet selection by immature green turtles (*Chelonia mydas*) at Bahía Magdalena foraging ground in the Pacific Coast of the Baja California Peninsula, México. J. Mar. Biol. Assoc. UK 88(3), 641–647.

MacDonald, B.D., Lewison, R.L., Madrak, S.V., Seminoff, J.A., Eguchi, T., 2012. Home ranges of East Pacific green turtles *Chelonia mydas* in a highly urbanized temperate foraging ground. Mar. Ecol. Prog. Ser. 461, 211–221.

Meylan, A., 1988. Spongivory in hawksbill turtles: a diet of glass. Science 239(4838), 393–395.

Moran, K.L., Bjorndal, K.A., 2005. Simulated green turtle grazing affects structure and productivity of seagrass pastures. Mar. Ecol. Prog. Ser. 305, 235–247.

Obura, D.O., Harvey, A., Young, T., Eltayeb, M.M., von Brandis, R., 2010. Hawksbill turtles as significant predators on hard coral. Coral Reefs 29(3), 759–759.

Owens, D.W., Ruiz, G.J., 1980. New Methods of Obtaining Blood and Cerebrospinal Fluid from Marine Turtles. Herpetologica 36, 17–20.

Parker, D.M., Dutton, P.H., Balazs, G.H., 2011. Oceanic diet and distribution of haplotypes for the green turtle, *Chelonia mydas*, in the Central North Pacific. Pac. Sci. 65(4), 419–432.

Parnell, A.C., Phillips, D.L., Berahop, S., Semmens, B.X., Ward, E.J., Moore, J.W., Jackson, A.J., Grey, J., Kelly, D.J., Inger, R., 2012. Bayesian stable isotope mixing models. Environmetrics 24, 387–399.

Pearson, R.M., van de Merwe, J.P., Limpus, C.J., Connolly, R.M., 2017. Realignment of sea turtle isotope studies needed to match conservation priorities. Mar. Ecol. Prog. Ser. 583, 259–271.

Post, D.M., 2002. Using stable isotopes to estimate trophic position: models, methods and assumptions. Ecology 83, 703–718.

Post, D.M., Layman, C.A., Arrington, D.A., Takimoto, G., Quattrochi, J., Montaña, C.G., 2007. Getting to the fat of the matter: models, methods and assumptions for dealing with lipids in stable isotope analyses. Oecologia 152, 179–189.

Pritchard, P.C., 1999. Status of the black turtle. Conser. Biol. 13(5), 1000–1003.

Proietti, M.C., Reisser, J.W., Secchi, E.R., 2012. Foraging by immature hawksbill sea turtles at Brazilian islands. Mar. Turtle Newsl. 135, 4–6.

Reich, K.J., Bjorndal, K.A., Bolten, A.B., 2007. The 'lost years' of green turtles: using stable isotopes to study cryptic life stages. Biol. Lett. 3, 712–714.

Rincon-Diaz, M.P., Diez, C.E., Van Dam, R.P., Sabat, A.M., 2011. Foraging selectivity of the hawksbill sea turtle (*Eretmochelys imbricata*) in the Culebra Archipelago, Puerto Rico. J. Herpetol. 45(3), 277–283.

Ross, J.P., 1984. Adult sex ratio in the green sea turtle. Copeia 1984 (3), 774–776.

Russell, D.J., Hargrove, S., Balazs, G.H., 2011. Marine sponges, other animal food, and nonfood items found in digestive tracts of the herbivorous marine turtle *Chelonia mydas* in Hawaii. Pac. Sci. 65, 375–381.

Sampson, L., Giraldo, A., Payán, L.F., Amorocho, D.F., Ramos, M.A., Seminoff, J.A., 2018. Trophic ecology of green turtle *Chelonia mydas* juveniles in the Colombian Pacific. J. Mar. Biol. Assoc. UK 98(7), 1817–1829.

Santos, R.G., Martins, A.S., Batista, M.B., Horta, P.A., 2015. Regional and local factors determining green turtle *Chelonia mydas* foraging relationships with the environment. Mar. Ecol. Prog. Ser. 529, 265–277.

Seminoff, J.A., Resendiz, A., Nichols, W.J., 2002. Diet of East Pacific green turtles (*Chelonia mydas*) in the central Gulf of California, Mexico. J. Herpetol. 36(3), 447–454.

Shimada, T., Limpus, C., Jones, R., Hazel, J., Groom, R., Hamann, M., 2016. Sea turtles return home after intentional displacement from coastal foraging areas. Mar. Biol. 163(1), 8–21.

Stampar, S.N., da Silva, P.F., Luiz Jr., O.J., 2007. Predation on the Zoanthid Palythoa caribaeorum (Anthozoa, Cnidaria) by a Hawksbill Turtle (*Eretmochelys imbricata*) in Southeastern Brazil. Mar. Turtle Newsl. 117, 3–5.

Stock, B.C., Semmens, B.X., 2016. MixSIAR GUI user manual, Version 3.1. https://github.com/brianstock/MixSIAR

Stringell, T.B., Clerveaux, W.V., Godley, B.J., Kent, F.E., Lewis, E.D., Marsh, J.E., Phillips, Q., Richardson, P.B., Sanghera, A., Broderick, A.C., 2016. Taxonomic distinctness in the diet of two sympatric marine turtle species. Mar. Ecol. 37(5), 1036–1049.

Stuhldreier, I., Sánchez-Noguera, C., Rixen, T., Cortés, J., Morales, A., Wild, C., 2015. Effects of seasonal upwelling on inorganic and organic matter dynamics in the water column of eastern Pacific coral reefs. PLoS ONE 10(11), e0142681.

Thayer, G.W., Engel, D.W., Bjorndal, K.A., 1982. Evidence for short-circuiting of the detritus cycle of seagrass beds by the green turtle, *Chelonia mydas* L. J. Exp. Mar. Biol. Ecol. 62(2), 173–183.

Thomson, J.A., Whitman, E.R., Garcia-Rojas, M.I., Bellgrove, A., Ekins, M., Hays, G.C., Heithaus, M.R., 2018. Individual specialization in a migratory grazer reflects long-term diet selectivity on a foraging ground: implications for isotope-based tracking. Oecologia 188(2), 429–439.

Tomaszewicz, C.N.T., Seminoff, J.A., Avens, L., Goshe, L.R., Rguez-Baron, J.M., Peckham, S.H., Kurle, C.M., 2018. Expanding the coastal forager paradigm: long-term pelagic habitat use by green turtles *Chelonia mydas* in the eastern Pacific Ocean. Mar. Ecol. Prog. Ser. 587, 217–234.

Vander Zanden, H.B., Bjorndal, K.A., Mustin, W., Ponciano, J.M., Bolten, A.B., 2012. Inherent variation in stable isotope values and discrimination factors in two life stages of green turtles. Physiol. Biochem. Zool. 85(5), 431–441.

Vander Zanden, H.B., Bjorndal, K.A., Bolten, A.B., 2013. Temporal consistency and individual specialization in resource use by green turtles in successive life stages. Oecologia 173(3), 767–777.

von Brandis, R.G., Mortimer, J.A., Reilly, B.K., van Soest, R.W.M., Branch, G.M., 2014. Taxonomic composition of the diet of hawksbill turtles (*Eretmochelys imbricata*) in the Republic of Seychelles. West Indian Ocean J. Mar. Sci. 13(1), 81–91.

Wabnitz, C.C., Balazs, G., Beavers, S., Bjorndal, K.A., Bolten, A.B., Christensen, V., Hargrove, S., Pauly, D., 2010. Ecosystem structure and processes at Kaloko Honokōhau, focusing on the role of herbivores, including the green sea turtle *Chelonia mydas*, in reef resilience. Mar. Ecol. Prog. Ser. 420, 27–44.

Wood, L.D., Milton, S.L., Maple, T.L., 2017. Foraging Behavior of Wild Hawksbill Turtles (*Eretmochelys imbricata*) in Palm Beach County, Florida, USA. Chelonian Conserv. Biol. 16(1), 70–75.

Yamamuro, M., Umezawa, Y., Koike, I., 2001. Seasonality in nutrient concentrations and stable isotope ratios of Halophila ovalis growing on the intertidal flat of SW Thailand. Limnology 2(3), 199–205.

Zar, J.H., 2010. Biostatistical Analysis (5th edition). Harlow, UK, Pearson Education Limited.

Table 4.1 Stable Isotope Results in Pacific Sea Turtles

Stable isotope signatures (‰), percent isotope composition (%), and $\delta^{13}C$ to $\delta^{15}N$ ratio (C:N) of whole blood (WB) and skin (EP) taken from black morphotype green turtles (EP), yellow morphotype green turtles (IP), and hawksbill turtles (EI) live-captured in-water in Costa Rica during 2017. I present data as mean ± SD (except where only one turtle is present). I classified large turtles (LG) as turtles with curved carapace length (CCL, in cm) > 77 cm and small turtles as those < 76 cm CCL. N = sample size.

	N	Size	Tissue	CCL (cm)	$\delta^{13}C$ (‰)	$\delta^{15}N$ (‰)	C (%)	N (%)	C:N
EP	25	LG	WB	85.5 ± 4	-16.32 ± 0.49	14.49 ± 0.60	46.79 ± 1.57	13.78 ± 0.63	3.4 ± 0.09
	10		EP		-15.1 ± 0.5	15.32 ± 0.58	46.56 ± 0.96	14.75 ± 0.4	3.16 ± 0.12
	14	SM	WB	72 ± 6.5	-16.95 ± 0.73	14.17 ± 1.0	46.11 ± 1.82	13.74 ± 0.61	3.36 ± 0.04
	5		EP		-15.62 ± 1.21	15.26 ± 0.23	45.82 ± 0.94	14.98 ± 0.51	3.06 ± 0.11
IP	4	LG	WB	81.5 ± 1.5	-16.23 ± 0.82	12.50 ± 0.52	48.15 ± 1.41	14.32 ± 0.40	3.36 ± 0.02
	9	SM	WB	67.5 ± 11	-15.53 ± 0.45	12.31 ± 0.58	44.70 ± 2.74	13.37 ± 0.86	3.34 ± 0.03
	5		EP		-15.03 ± 0.74	13.84 ± 0.89	46.88 ± 1.52	14.6 ± 0.67	3.22 ± 0.2
EI	1	LG	WB	83	-19.28	12.96	44.62	13.41	3.33
	1		EP		-17.9	13.81	49.87	14.92	3.34
	12	SM	WB	47.5 ± 6	-15.97 ± 1.02	12.61 ± 0.31	45.08 ± 2.75	13.51 ± 0.82	3.34 ± 0.03
	6		EP		-14.02 ± 1.03	13.74 ± 0.35	46.11 ± 1.64	14.70 ± 0.44	3.14 ± 0.21

Table 4.2 Stable Isotope Results of Diet Items

Stable isotope signatures (‰), percent isotope composition (%), and $\delta^{13}C$ to $\delta^{15}N$ ratio (C:N) of diet samples collected in Costa Rica in 2017. I present data as mean ± standard deviation. N = sample size.

Sample	N	$\delta^{13}C$	$\delta^{15}N$	%C	%N	C:N
Sessile Invertebrates	6	-16.73 ± 1.48	10.72 ± 0.33	33.95 ± 6.89	6.78 ± 2.23	5.63 ± 1.99
Mobile Invertebrates	8	-10.22 ± 4.25	9.19 ± 1	21.3 ± 8.3	2.75 ± 1.87	9.3 ± 3.26
Red Algae	9	-16.56 ± 2	8.73 ± 1	37.41 ± 2.27	3.6 ± 0.94	11.14 ± 3.78
Green Algae	7	-11.63 ± 8.07	7.73 ± 1.59	37.44 ± 3.69	3.16 ± 1.12	12.87 ± 3.47
Sea Grass	3	-6.73 ± 6.01	2.96 ± 1.25	38.57 ± 1.64	2.81 ± 0.90	15.05 ± 5.64

Table 4.3 Proportional Composition of Pacific Sea Turtle Diet

Proportional contribution of diet items to diet of turtles foraging in Matapalito and Salinas, Costa Rica, in 2017. LG = large (> 77 cm curved carapace length), SM = small (< 76 cm curved carapace length).

Group	Size	Green Algae	Mobile Invertebrate	Red Algae	Sessile Invertebrate
Black Turtles	LG	0.022 ± 0.02	0.039 ± 0.03	0.031 ± 0.03	0.907 ± 0.04
	SM	0.010 ± 0.01	0.013 ± 0.02	0.018 ± 0.03	0.959 ± 0.04
Yellow Turtle	LG	0.16 ± 0.15	0.079 ± 0.07	0.501 ± 0.22	0.260 ± 0.15
	SM	0.156 ± 17	0.074 ± 0.08	0.573 ± 0.25	0.194 ± 0.14
Hawksbill	All	0.149 ± 0.14	0.072 ± 0.07	0.442 ± 0.21	0.336 ± 0.14

Table 4.4 Trophic Niche of Pacific Sea Turtles

Isotopic niche space estimates generated using Kernel Utilization Density (KUD) methods for small and large black morphotype green turtle (Small < 76 cm CCL, Large > 77 cm CCL), all yellow morphotype green turtle, and small hawksbill (CCL < 70 cm) turtle whole blood (WB) at 50% 75% an 95% contour levels. I collected WB samples (< 1ml/kg) in 2017 from foraging individuals in Costa Rica (I combined Matapalito and Salinas due to statistical similarity). SM = small, LG = large, CCL = curved carapace length.

Group	Contour (%)	Area	Group	Contour (%)	Area
Black (SM)	50	1.58	Black (LG)	50	1.22
	75	3.71		75	2.54
	95	7.92		95	5.28
Yellow (all)	50	1.9	Yellow (all)	50	1.97
	75	3.87		75	3.87
	95	7.34		95	7.34
Hawksbill (SM)	50	1.78	Hawksbill (SM)	50	1.78
	75	3.34		75	3.33
	95	6.3		95	6.30

Table 4.5 Niche Overlap between Pacific Sea Turtles

Percent overlap estimates for small black morphotype green turtles (< 76 cm CCL), all yellow morphotype green turtles, and small hawksbill turtle (< 70 cm CCL) whole blood (WB) isotopic niche space generated using the Kernel Utilization Density (KUD) methods. I estimated KUD values at 50%, 75% and 95% contour levels. I collected WB samples (< 1ml/kg) during 2017 similarity in Costa Rica.

		Black			Yellow			Hawksbill		
		50%	75%	95%	50%	75%	95%	50%	75%	95%
Black	50%	-	-	-	0	0	0	0	0	0
	75%	0.426	-	-	0	0.021	0.063	0	0	0.005
	95%	0.2	0.468	-	0.024	0.063	0.13	0	0.009	0.058
Yellow	50%	0	0	0.096	-	-	-	0.446	0.627	0.852
	75%	0	0.021	0.129	0.51	-	-	0.347	0.547	0.769
	95%	0	0.032	0.141	0.269	0.528	-	0.243	0.427	0.655
Hawksbill	50%	0	0	0	0.493	0.754	-	-	-	-
	75%	0	0	0.022	0.371	0.635	0.939	0.534	-	-
	95%	0	0.003	0.072	0.267	0.473	0.764	0.283	0.53	-

Table 4.6 Niche Overlap between Pacific Sea Turtles

Percent overlap estimates for large black morphotype green turtles (> 77 cm CCL), all yellow morphotype green turtles, and small hawksbill turtle (< 70 cm CCL) whole blood (WB) isotopic niche space generated using the Kernel Utilization Density (KUD) methods. I estimated KUD values at 50%, 75% and 95% contour levels. I collected WB samples (< 1ml/kg) during 2017 in Costa Rica.

		Black			Yellow			Hawksbill		
		50%	75%	95%	50%	75%	95%	50%	75%	95%
Black	50%	-	-	-	0	0	0.08	0	0	0
	75%	0.482	-	-	0	0.021	0.106	0	0	0
	95%	0.232	0.481	-	0.049	0.141	0.204	0.066	0.085	0.116
Yellow	50%	0	0	0.13	-	-	-	0.446	0.626	0.852
	75%	0	0.014	0.192	0.51	-	-	0.348	0.547	0.769
	95%	0.013	0.037	0.147	0.269	0.528	-	0.243	0.426	0.655
Hawksbill	50%	0	0	0.194	0.493	0.754	-	-	-	-
	75%	0	0	0.135	0.372	0.636	0.94	0.536	-	-
	95%	0	0	0.098	0.267	0.473	0.764	0.283	0.529	-

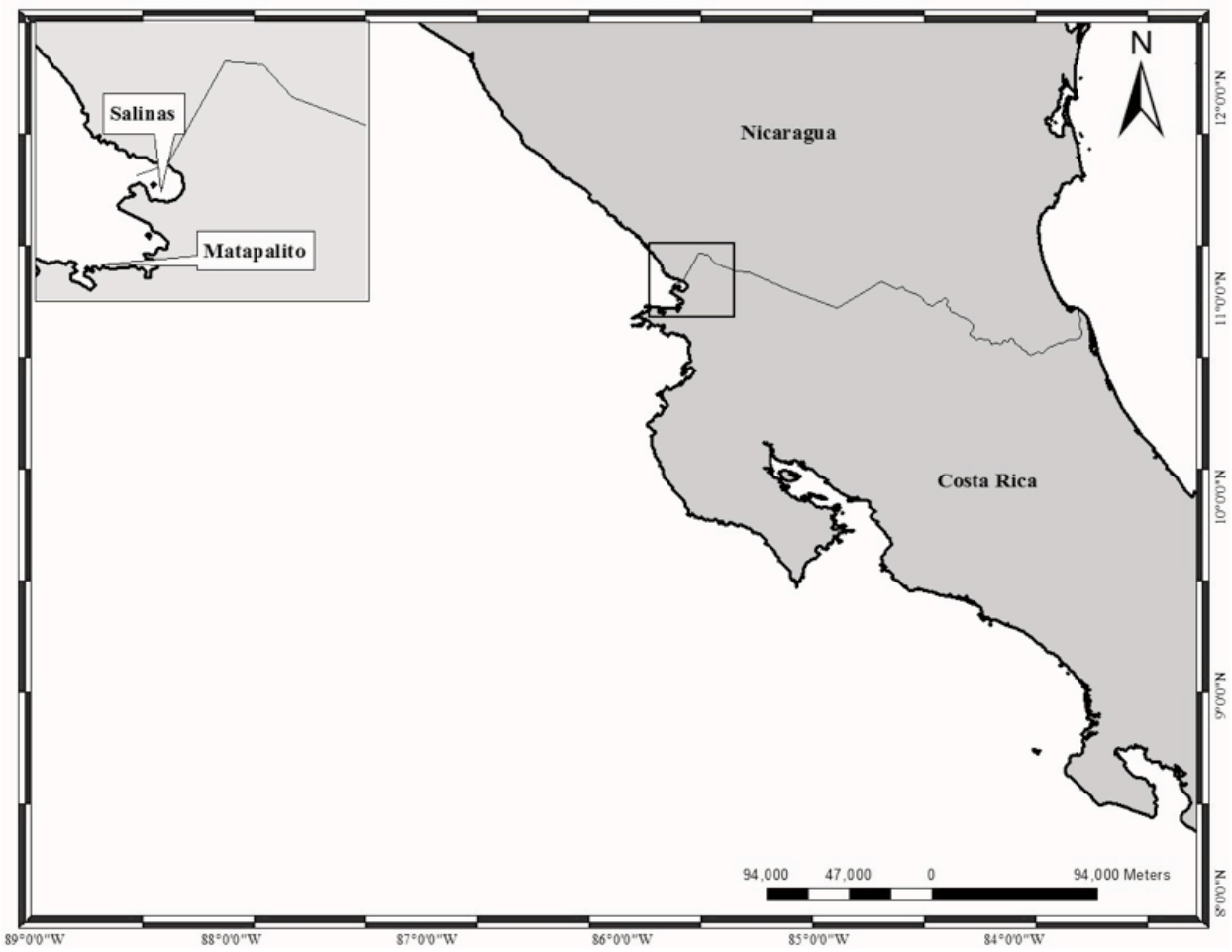

Figure 4.1 Study Sites, Costa Rica
Map of the study area showing both Salinas and Matapalito Bays, Costa Rica. I sampled at each location approximately once per month, weather permitting, during 2017. Salinas Bay is a foraging ground for adult and juvenile black morphotype green turtles; while Matapalito is a foraging ground for black turtles, yellow morphotype green turtles, and hawksbill turtles.

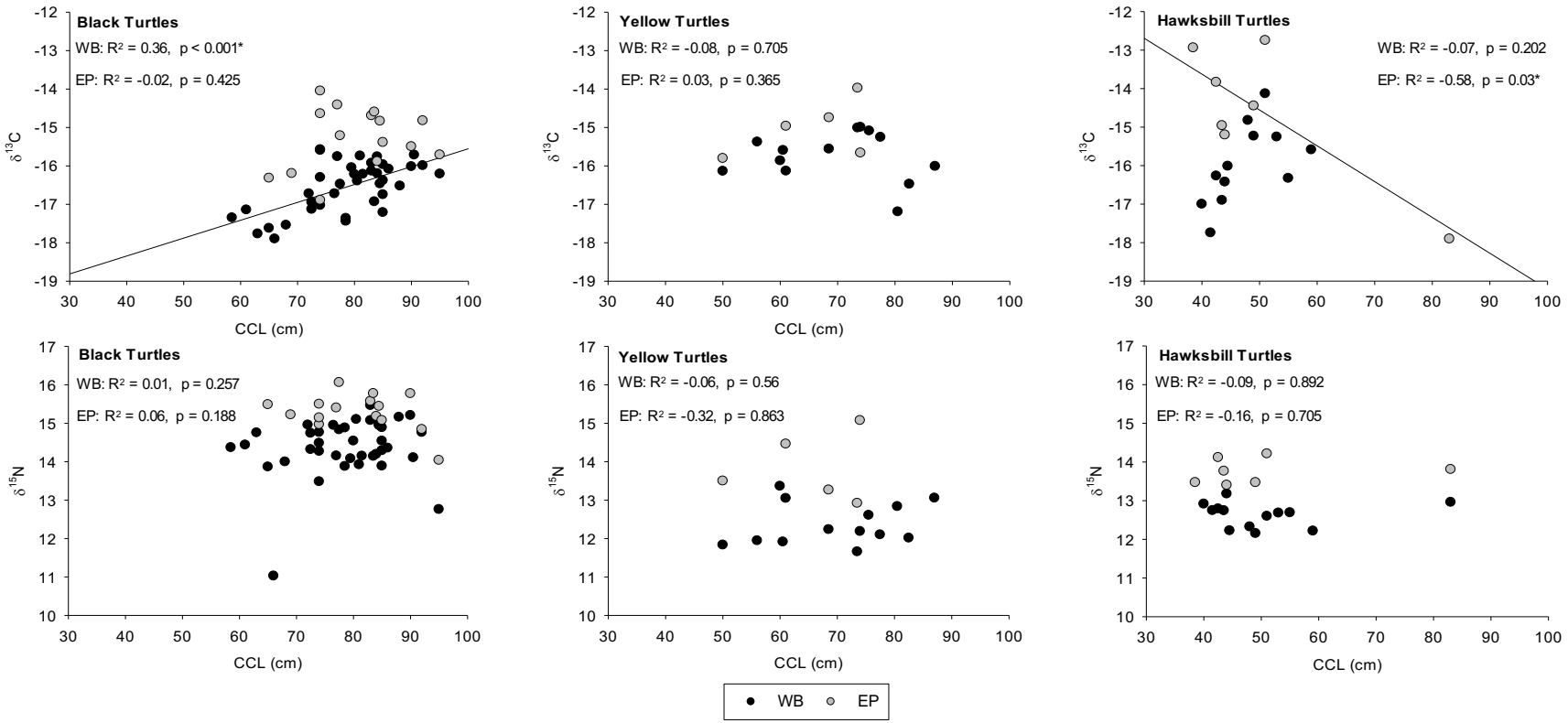

Figure 4.2 Stable Isotope Signatures and Body Length

Linear regressions of whole blood (WB, black circles) and epidermal (EP, gray circles) tissue $\delta^{13}C$ and $\delta^{15}N$ values (‰) relative to curved carapace length (CCL) for black and yellow morphotype green turtles and hawksbill turtles. (*) indicates significant relationship and is accompanied by a regression line.

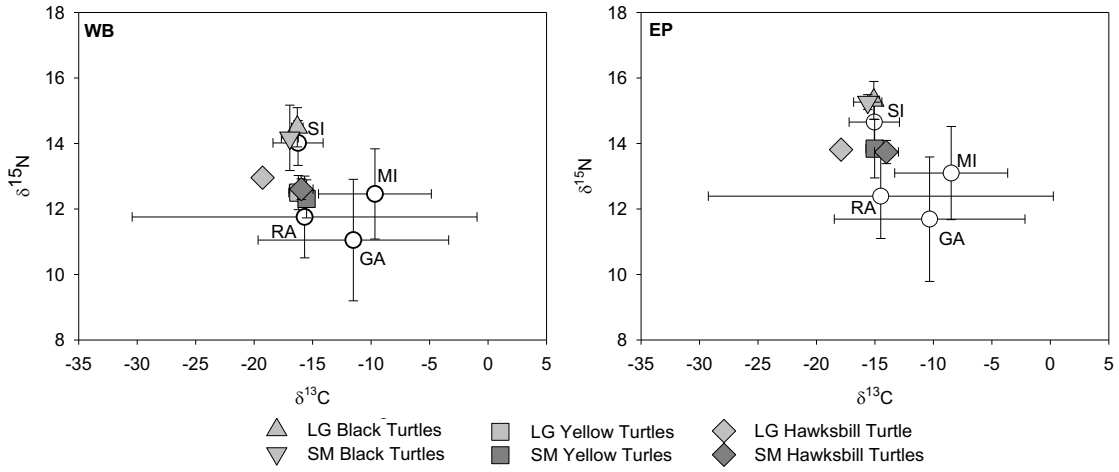

Figure 4.3 Stable Isotope Space Between Sea Turtles and Diet
Whole blood (WB) and epidermal (EP) isotopic means (± SD) for black morphotype green turtles (triangle), yellow morphotype green turtles (square), and hawksbill turtles (diamond) live-captured in Costa Rica in 2017. Potential diet sources included (mean ± SD) were adjusted for sea turtle discrimination factors (WB: $\Delta^{13}C = 0.55 \pm 0.58$ ‰, and $\Delta^{15}N = 3.23 \pm 0.38$ ‰; EP: $\Delta^{13}C = 1.75 \pm 0.59$ ‰, and $\Delta^{15}N = 3.91 \pm 0.42$ ‰; Vander Zanden et al. 2012). Isotopic mixing space is delineated by four potential diet sources, sessile invertebrates (SI, including sponges and tunicates), mobile invertebrates (MI), red algae (RA), and green algae (GA). Sample sizes listed in Table 1. There were no large yellow morphotype epidermal samples, and only 1 large hawksbill turtle. LG = large, SM = small.

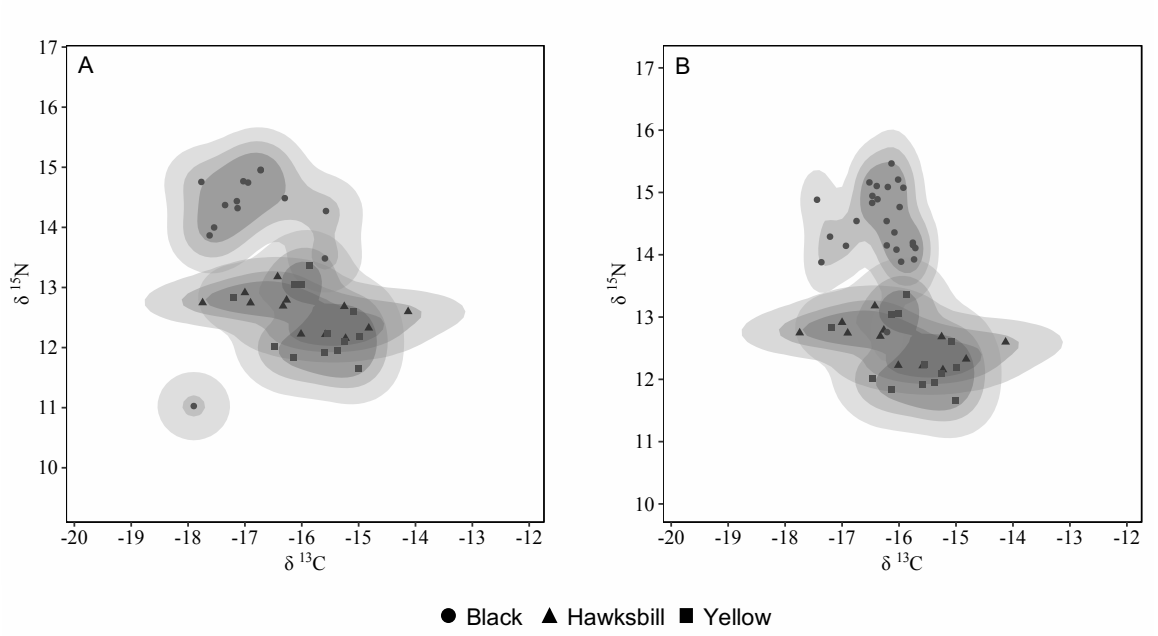

Figure 4.4 Trophic Niche in Pacific Sea Turtles
Isotopic niche estimates generated using kernel utilization density methods for whole blood samples from small black morphotype green turtles (A; < 76 cm CCL), or large black morphotype green turtles (B; > 77 cm CCL), all yellow morphotype green turtles, and small hawksbill turtles (< 70 cm CCL) at 50%, 75%, and 95% contour levels. Tissue samples were collected in Costa Rica in 2017.

CHAPTER 5. SUMMARY

5.1 Summary

Collectively, my dissertation investigates hypothermic stress, temperature adaption, and trophic niche overlap in green (*Chelonia mydas*) and hawksbill turtles (*Eretmochelys imbricata*). Because of their endangered status, maximizing ecological and physiological output with minimal handling is beneficial to future conservation. In order to survive, juvenile sea turtles need to congregate in safe habitats with foraging resources that foster growth and development, otherwise migration over long distances through dynamic ocean conditions to reproduce would be impossible. Because sea turtles are ectothermic, they rely on external heat to maintain functional metabolism. However, in many habitats, primary productivity is negatively correlated to water temperature as a result of oceanic upwelling. Therefore, as juveniles, sea turtles must use a combination of avoidance behavior and physiological adaptions to maintain body temperature while exploiting nutrient rich environments.

Turtles that fail to migrate when water currents shift, experience hypothermia resulting in an inability to swim or regulate buoyancy. My research documented the level of stress resulting from cold-stunning and subsequent transport to rehabilitation facilities. I discovered that although acutely stressful, more so than previous records of handling stress in green turtles, epidermal corticosterone suggested that the turtles were not exposed to ongoing chronic stress; results which I corroborated by comparisons to captive green turtles exposed to handling stress. Further, my dissertation suggested the presence of a more complex stress response than previously documented in sea turtle research. My results of low concentrations of stress hormone in epidermal tissue suggested low levels of chronic stress indicating that rehabilitation is important in this case. Although I provided estimates of stress hormones from samples collected once the turtles reached the rehabilitation facility, this failed to separate the compounding effect of cold-stunning and handling stress. Therefore, I provided a suggested framework for future investigations into the extended (> 24 hr) physiology of the stress response in sea turtles.

In ideal situations, sea turtles avoid cold water currents thereby avoiding hypothermic stunning. However, colder environments are linked to upwelling and increased primary productivity. In animals that are exposed to cold water throughout their lives, physiological adaptions exist. In mammals and reptiles alike, cold adaption results in shifts in the lipid composition of membranes to maintain fluidity in reduced temperatures. My dissertation identified shifts in proportional saturation of membrane lipids between complete lipid profiles and differential lipid profiles between seasons. However, compared to warm adapted herpetofauna, the turtles in this study appeared to be chronically cold adapted and have relevant lipids with longer chain lengths and higher levels of saturation. Therefore, my dissertation posed the question of how lipid profiles in the comparably cold Pacific Ocean relate to lipid profiles in turtles that inhabit warmer areas. In addition, I identified the presence of lipids associated with foraging physiology in turtles from both seasons. These data suggested that turtles in my study were foraging throughout the year, even though upwelling in North Pacific Costa Rica is seasonal. Therefore, I established support for the classification of Matapalito and Salinas as important habitats that support endangered sea turtle foraging year-round, as opposed to a stopover or resting site. Implementing conservation protection in Matapalito and Salinas is important both for the endangered sea turtles, and the ecosystem as a whole, because the combination of foraging green and hawksbill turtles provide a complex range of important ecosystem services. Further analyses should investigate the interwoven relationship between sea turtles and their environments, including specific lipid concentrations, and macromolecule composition of dietary items. These questions will improve our understanding of sea turtle foraging and its relationship to environmental quality.

Extensive research into diet composition has revealed that although sea turtles follow general diet trends, ultimately, they are opportunistic foragers. My dissertation revealed a preference for sponges and tunicates in black turtles, a combination diet in yellow turtles of red and brown algae, and that hawksbill turtles foraged on tunicates, sponges, red, and brown algae. Therefore, hawksbill turtles in Costa Rica are not as specialized as other foraging habitats around the world, where turtles consume sponges. Further, yellow turtles in this study, like conspecific populations in other ocean basins, were specialists, however, in my research, this specialization focused on algae as opposed

to sea grass. Trophic niche studies have identified site specific diet trends, and switching diets in response to changing environmental conditions especially when turtles of different populations and species inhabit the same foraging habitat. In my dissertation, foraging niche distinction in Matapalito did not align with species. Specifically, black morphotype green turtles had a distinct isotopic niche from yellow morphotype green turtles, while hawksbill turtles and yellow turtles fed at the same trophic level. These data further supported the importance of site-specific analyses and protecting sea turtles in order to maintain ecosystem services turtles provide through trophic niche segregation within Matapalito.

My dissertation provides baseline research on the expansion of the stress response in sea turtles, the field of lipidomics applied to reptile ecology, and investigation of trophic interactions between black and yellow morphotype green turtles when they overlap spatially with critically endangered hawksbill turtles. Additional studies quantifying the stress response in its entirety, expanding our understanding of lipid dynamics as indicators of ecology and disease, as well as fine-scale trophic interaction will further elucidate previously cloaked aspects of sea turtle physiology and its relationship to biotic and abiotic elements of turtle habitats.

APPENDIX

Methods Chapter 3

To investigate which lipids are present in sea turtle plasma, I created two reference samples, one for green turtles (CM), and one for hawksbill turtles (EI). I produced reference samples by combining 12.5 µL from 16 EI turtles and 16 CM (randomly selected) to generate two 200 µL reference samples. I agitated the reference samples to promote thorough mixing. Then I used the Bligh and Dyer (1959) method to extract lipids. Specifically, I added 450 µL chloroform ($CHCl_3$) and 250 µL of methanol (MeOH) and vortexed the samples for 10 sec. The solutions then rested at room temperature for 15 min. Next, I added 250 µL of ultrapure H_2O and 250 µL of $CHCl_3$, and centrifuged (Centrifuge model VSX, Taylor Scientific, St Louis, MO, USA) the sample for 10 min at 16,000 rpm. The resulting solution was biphasic with a top polar layer, and a bottom organic layer (lipids), separated by a paper-thin white layer (protein layer). I carefully transferred the bottom organic layer to a clean tube and evaporated the samples in a speedvac (Vacufuge 5301, Eppendorf North America, Hauppauge, NY, USA) for 1 hr at 37°C. I dried the samples and stored them at -80°C until analysis. For analysis, I resuspended dried samples in ACN+MeOH+300nM NH_4Ac 3:6.65:0.35 (v/v).

I compiled a set of methods by combining *m/z* for all molecular ions based on the LipidMAPS online database (http://www.lipidmaps.org/) with expected ions resulting from the Prec or NL scans (1,412 lipids). I combined all potential MRMs into 11 methods (no more than 200 MRM per method). For each method, I used a capillary pump connected to the autosampler (G1377A) then connected to an Agilent 6410 QQQ mass spectrometer (Agilent Technologies, Santa Clara, CA, USA). I flow-injected 8 µL of reference and blank samples into the capillary pump which had a flow rate of 20 µL/min and a pressure of 400 bar (voltage: 3.5 – 5 kV. Gas flow: 5.1L/min. Temp: 300°C). I processed the raw MRM mass spectrometry data using an in-house script and MRM transitions and exported the resulting ion intensity values to Microsoft Excel (v2016, Microsoft Corporation, Redmond, WA). I normalized the absolute ion intensity of lipids against the total ion current of the method for each turtle individually. I then selected any lipid that had a sample ion intensity

higher than the blank, resulting in 688 relevant lipids and metabolites from 10 lipid classes and one metabolite class and combined these 688 lipids and metabolites into four methods.

For individual turtle plasma samples, I used the same methods except I modified the extraction procedure to work with 20 μL of plasma (due to sensitivity of the technique), thereby dividing the above extraction procedure volumes by 10 (i.e. instead of adding 450 μL of chloroform I added 45 μL of chloroform). Again, after extraction, I store lipids at -80°C until analysis, resuspended the samples in the same manner, and analyzed them using a capillary pump connected to the autosampler (G1377A) then connected to an Agilent 6410 QQQ mass spectrometer (Agilent Technologies, Santa Clara, CA, USA). I processed raw mass spectrometry data using an in-house script, normalized by ion count and exported results using Microsoft Excel (v2016, Microsoft Corporation, Redmond, WA). I normalized the absolute ion intensity of lipids against the total ion current of the lipid class, instead of by method, for each turtle individually. The resulting relative ion intensity of lipids, therefore, represented the proportion of total lipid class ion current for each turtle. For the acyl-carnitine metabolite class, I only included the biologically significant lipid fragment (85.1).

Table A.5.1 Complete Lipid Profiles

Complete plasma lipid profiles from green and hawksbill turtles. Values presented are average (± SD) relative ion intensity. Because of the way relative ion intensity is calculated, lipid values can only be compared to those within the same class, not between classes. Bolded lipids were significantly different between species or seasons.

Lipid (**Differential**)	CM Wet	CM Dry	EI Wet	EI Dry
12:0 CE	0.004 ± 0.001	0.004 ± 0.002	0.003 ± 0.000	0.003 ± 0.000
14:1 CE	0.002 ± 0.000	0.003 ± 0.001	0.004 ± 0.001	0.004 ± 0.001
14:0 CE	0.008 ± 0.002	0.008 ± 0.002	0.008 ± 0.003	0.007 ± 0.001
15:0 CE	0.003 ± 0.000	0.004 ± 0.001	0.005 ± 0.002	0.004 ± 0.000
16:3 CE	0.003 ± 0.001	0.003 ± 0.001	0.003 ± 0.001	0.003 ± 0.000
16:2 CE, zymosteryl palmitoleate	0.003 ± 0.001	0.004 ± 0.001	0.004 ± 0.001	0.0045 ± 0.001
16:1 CE	0.026 ± 0.007	0.031 ± 0.009	0.040 ± 0.005	0.045 ± 0.008
15:1 CE_simulated	0.028 ± 0.007	0.033 ± 0.009	0.043 ± 0.005	0.048 ± 0.008
16:0 CE	0.014 ± 0.005	0.014 ± 0.007	0.015 ± 0.007	0.020 ± 0.007
15:0 CE_simulated	0.014 ± 0.004	0.014 ± 0.008	0.015 ± 0.006	0.020 ± 0.008
16:3 CE	0.002 ± 0.001	0.003 ± 0.001	0.003 ± 0.001	0.002 ± 0.000
16:2 CE	0.003 ± 0.001	0.004 ± 0.002	0.004 ± 0.001	0.003 ± 0.000
17:1 CE; 16:1 Campesteryl ester	0.014 ± 0.008	0.015 ± 0.005	0.023 ± 0.009	0.021 ± 0.004
17:0 CE	0.003 ± 0.001	0.003 ± 0.000	0.005 ± 0.003	0.004 ± 0.000
16:0 CE	0.003 ± 0.001	0.003 ± 0.001	0.005 ± 0.002	0.003 ± 0.001
16:3 Stigmasteryl ester	0.005 ± 0.003	0.008 ± 0.009	0.006 ± 0.005	0.010 ± 0.006
18:3 CE, 16:2 Stigmasteryl ester, 16:3 Sitosteryl ester	0.017 ± 0.008	0.022 ± 0.018	0.023 ± 0.015	0.037 ± 0.014
18:2 CE, zymosteryl oleate, 16:1 Stigmasteryl ester, 16:2 Sitosteryl ester	0.035 ± 0.010	0.036 ± 0.012	0.059 ± 0.021	0.078 ± 0.031
17:1 Campesteryl ester_simulated	0.175 ± 0.037	0.147 ± 0.028	0.163 ± 0.011	0.168 ± 0.019
18:1 CE, 16:0 Stigmasteryl ester, 16:1 Sitosteryl ester	0.174 ± 0.036	0.146 ± 0.030	0.164 ± 0.014	0.170 ± 0.019
17:0 Campesteryl ester_simulated	0.009 ± 0.002	0.009 ± 0.002	0.009 ± 0.001	0.009 ± 0.002
18:0 CE, 16:0 Sitosteryl ester	0.009 ± 0.002	0.009 ± 0.002	0.009 ± 0.001	0.009 ± 0.002
18:3 Campesteryl ester	0.003 ± 0.001	0.003 ± 0.001	0.003 ± 0.001	0.003 ± 0.001
lanosteryl palmitoleate, 18:2 Campesteryl ester	0.003 ± 0.002	0.003 ± 0.001	0.004 ± 0.002	0.005 ± 0.001
18:1 Campesteryl ester	0.006 ± 0.010	0.004 ± 0.002	0.005 ± 0.002	0.009 ± 0.007

Table A.5.1 continued

18:0 Campesteryl ester	0.003 ± 0.003	0.003 ± 0.001	0.003 ± 0.001	0.004 ± 0.002
19:0 CE_simulated, 17:0 sitosteryl ester_simulated	0.003 ± 0.003	0.003 ± 0.001	0.004 ± 0.001	0.005 ± 0.002
20:5 CE	0.114 ± 0.081	0.149 ± 0.061	0.049 ± 0.020	0.034 ± 0.013
20:4 CE, 18:3 Stigmasteryl ester	0.140 ± 0.054	0.133 ± 0.034	0.098 ± 0.023	0.058 ± 0.024
20:3 CE, 18:2 Stigmasteryl ester, 18:3 Sitosteryl ester	0.011 ± 0.004	0.012 ± 0.002	0.013 ± 0.004	0.014 ± 0.005
20:2 CE, 18:1 Stigmasteryl ester, 18:2 Sitosteryl ester	0.003 ± 0.002	0.004 ± 0.002	0.004 ± 0.001	0.006 ± 0.001
20:1 CE, 18:0 Stigmasteryl ester, 18:1 Sitosteryl ester	0.006 ± 0.006	0.005 ± 0.003	0.005 ± 0.003	0.011 ± 0.005
19:0 Campesteryl ester_simulated	0.005 ± 0.006	0.004 ± 0.002	0.004 ± 0.002	0.009 ± 0.007
20:0 CE, 18:0 Sitosteryl ester	0.005 ± 0.006	0.004 ± 0.002	0.005 ± 0.002	0.009 ± 0.007
20:3 Campesteryl ester	0.010 ± 0.008	0.012 ± 0.010	0.009 ± 0.006	0.007 ± 0.003
lanosteryl oleate, 20:2 Campesteryl ester	0.003 ± 0.001	0.003 ± 0.001	0.003 ± 0.001	0.003 ± 0.001
20:1 Campesteryl ester	0.003 ± 0.002	0.003 ± 0.001	0.003 ± 0.001	0.004 ± 0.001
Cholesteryl nitrolinoleate	0.003 ± 0.001	0.003 ± 0.001	0.004 ± 0.001	0.004 ± 0.001
20:0 Campesteryl ester	0.003 ± 0.002	0.003 ± 0.001	0.004 ± 0.001	0.005 ± 0.002
22:6 CE	0.050 ± 0.034	0.045 ± 0.025	0.091 ± 0.041	0.069 ± 0.037
22:5 CE	0.014 ± 0.005	0.017 ± 0.006	0.024 ± 0.016	0.010 ± 0.003
22:4 CE, 20:3 Stigmasteryl ester	0.005 ± 0.001	0.006 ± 0.001	0.009 ± 0.004	0.009 ± 0.003
ecdysone palmitate, 22:3 CE, 20:2 Stigmasteryl ester, 20:3 Sitosteryl ester	0.008 ± 0.009	0.009 ± 0.006	0.005 ± 0.001	0.006 ± 0.002
Cholesteryl 11-hydroperoxy-eicosatetraenoate, 22:2 CE, 20:1 Stigmasteryl ester, 20:2 Sitosteryl ester	0.007 ± 0.006	0.008 ± 0.007	0.005 ± 0.003	0.006 ± 0.002
22:1 CE, 20:0 Stigmasteryl ester, 20:1 Sitosteryl ester	0.003 ± 0.001	0.003 ± 0.001	0.003 ± 0.001	0.004 ± 0.001
22:0 CE, 20:0 Sitosteryl ester	0.002 ± 0.001	0.002 ± 0.001	0.002 ± 0.001	0.003 ± 0.000
22:3 Campesteryl ester	0.003 ± 0.003	0.003 ± 0.001	0.004 ± 0.002	0.003 ± 0.001

Table A.5.1 continued

22:2 Campesteryl ester	0.005 ± 0.006	0.005 ± 0.004	0.003 ± 0.001	0.004 ± 0.001
22:1 Campesteryl ester	0.005 ± 0.004	0.005 ± 0.003	0.003 ± 0.001	0.004 ± 0.001
22:0 Campesteryl ester	0.002 ± 0.001	0.003 ± 0.001	0.003 ± 0.000	0.003 ± 0.000
22:3 Stigmasteryl ester	0.004 ± 0.003	0.005 ± 0.003	0.006 ± 0.003	0.007 ± 0.002
22:2 Stigmasteryl ester, 22:3 Sitosteryl ester	0.002 ± 0.001	0.003 ± 0.001	0.003 ± 0.001	0.003 ± 0.001
22:1 Stigmasteryl ester, 22:2 Sitosteryl ester	0.002 ± 0.001	0.002 ± 0.001	0.003 ± 0.000	0.003 ± 0.001
24:1 CE, 22:0 Stigmasteryl ester, 22:1 Sitosteryl ester	0.004 ± 0.004	0.004 ± 0.002	0.003 ± 0.001	0.003 ± 0.001
22:0 Sitosteryl ester	0.003 ± 0.002	0.003 ± 0.002	0.003 ± 0.001	0.003 ± 0.001
Cer(d18:1/2:0)	0.030 ± 0.003	0.032 ± 0.002	0.031 ± 0.003	0.033 ± 0.002
Cer(d18:1/12:0)	0.037 ± 0.006	0.039 ± 0.010	0.033 ± 0.002	0.0334 ± 0.001
CerP(d18:1/8:0)	0.030 ± 0.003	0.031 ± 0.003	0.031 ± 0.003	0.032 ± 0.001
Cer(d14:2(4E,6E)/18:1(9Z)(2OH))	0.032 ± 0.003	0.033 ± 0.002	0.033 ± 0.004	0.033 ± 0.002
Cer(d14:2(4E,6E)/18:0(2OH))	0.030 ± 0.003	0.032 ± 0.002	0.032 ± 0.002	0.032 ± 0.001
Cer(d18:2/16:0)	0.030 ± 0.003	0.032 ± 0.002	0.031 ± 0.003	0.033 ± 0.001
Cer(d18:1/16:0)	0.049 ± 0.009	0.050 ± 0.010	0.059 ± 0.012	0.056 ± 0.009
CerP(d18:1/12:0)	0.030 ± 0.003	0.030 ± 0.002	0.031 ± 0.003	0.032 ± 0.001
Cer(d18:1/18:1(9Z))	0.032 ± 0.006	0.031 ± 0.002	0.031 ± 0.003	0.033 ± 0.001
Cer(d18:1/18:0)	0.035 ± 0.003	0.034 ± 0.001	0.037 ± 0.001	0.036 ± 0.003
Cer(d18:0/18:0)	0.030 ± 0.003	0.031 ± 0.003	0.032 ± 0.003	0.033 ± 0.001
Cer(d14:2(4E,6E)/22:1(13Z)(2OH))	0.030 ± 0.003	0.031 ± 0.002	0.031 ± 0.004	0.033 ± 0.002
Cer(d14:1(4E)/22:0(2OH))	0.030 ± 0.003	0.031 ± 0.002	0.031 ± 0.003	0.032 ± 0.001
CerP(d18:1/16:0)	0.030 ± 0.003	0.031 ± 0.002	0.032 ± 0.002	0.035 ± 0.005
Cer(d18:1/22:0)	0.046 ± 0.007	0.046 ± 0.009	0.045 ± 0.006	0.041 ± 0.004
Cer(d18:0/22:0(2OH))	0.030 ± 0.003	0.031 ± 0.001	0.031 ± 0.003	0.032 ± 0.001
CerP(d18:1/18:0)	0.032 ± 0.002	0.032 ± 0.002	0.033 ± 0.003	0.034 ± 0.002
Cer(d18:1/24:1(15Z))	0.116 ± 0.038	0.095 ± 0.017	0.093 ± 0.038	0.072 ± 0.011
Cer(d18:1/24:0)	0.066 ± 0.035	0.068 ± 0.014	0.060 ± 0.011	0.052 ± 0.004
Cer(d18:0/24:0)	0.031 ± 0.003	0.031 ± 0.002	0.031 ± 0.003	0.032 ± 0.001
Cer(t18:0/22:0(2OH))	0.044 ± 0.012	0.045 ± 0.013	0.047 ± 0.015	0.054 ± 0.018
Cer(d18:1/26:1(17Z))	0.034 ± 0.004	0.035 ± 0.003	0.032 ± 0.004	0.033 ± 0.002
Cer(t18:0/26:0(2OH))	0.030 ± 0.004	0.030 ± 0.002	0.031 ± 0.003	0.032 ± 0.001

Table A.5.1 continued

CerP(d18:1/24:1(15Z))	0.030 ± 0.003	0.030 ± 0.002	0.031 ± 0.002	0.034 ± 0.004
CerP(d18:1/24:0)	0.030 ± 0.003	0.030 ± 0.002	0.031 ± 0.002	0.032 ± 0.001
CerP(d18:1/26:1(17Z))	0.030 ± 0.003	0.030 ± 0.002	0.031 ± 0.003	0.032 ± 0.001
1-O-palmitoyl-Cer(d18:1/16:0)	0.030 ± 0.003	0.030 ± 0.002	0.030 ± 0.003	0.032 ± 0.001
C12:1	0.017 ± 0.003	0.019 ± 0.004	0.019 ± 0.003	0.016 ± 0.004
C12:0	0.025 ± 0.004	0.026 ± 0.006	0.023 ± 0.005	0.019 ± 0.004
C14:0	0.032 ± 0.005	0.033 ± 0.006	0.036 ± 0.005	0.037 ± 0.007
C15:0	0.035 ± 0.008	0.036 ± 0.009	0.036 ± 0.004	0.032 ± 0.007
C16:1	0.030 ± 0.022	0.026 ± 0.003	0.026 ± 0.004	0.025 ± 0.003
C16:0	0.14 ± 0.034	0.138 ± 0.025	0.139 ± 0.018	0.134 ± 0.021
C17:0	0.040 ± 0.008	0.039 ± 0.007	0.042 ± 0.005	0.040 ± 0.007
C18:4	0.019 ± 0.004	0.021 ± 0.005	0.021 ± 0.003	0.020 ± 0.004
C18:3	0.016 ± 0.002	0.018 ± 0.004	0.018 ± 0.003	0.018 ± 0.002
C18:2	0.022 ± 0.008	0.020 ± 0.004	0.020 ± 0.002	0.021 ± 0.005
C18:1	0.075 ± 0.052	0.063 ± 0.048	0.048 ± 0.022	0.055 ± 0.025
C18:0	0.199 ± 0.059	0.193 ± 0.053	0.209 ± 0.034	0.204 ± 0.035
C20:5	0.038 ± 0.018	0.045 ± 0.032	0.028 ± 0.005	0.031 ± 0.008
C20:4	0.045 ± 0.035	0.045 ± 0.031	0.035 ± 0.016	0.045 ± 0.015
C20:3	0.018 ± 0.004	0.020 ± 0.003	0.018 ± 0.002	0.019 ± 0.003
C22:6	0.033 ± 0.004	0.035 ± 0.007	0.036 ± 0.004	0.055 ± 0.025
C22:5	0.030 ± 0.008	0.034 ± 0.008	0.037 ± 0.018	0.033 ± 0.007
C22:4	0.023 ± 0.004	0.024 ± 0.003	0.029 ± 0.009	0.034 ± 0.011
C22:0	0.034 ± 0.007	0.035 ± 0.007	0.037 ± 0.003	0.033 ± 0.007
C24:6	0.021 ± 0.005	0.021 ± 0.004	0.022 ± 0.003	0.020 ± 0.003
C24:0	0.021 ± 0.004	0.021 ± 0.004	0.023 ± 0.005	0.022 ± 0.005
C26:0	0.019 ± 0.003	0.020 ± 0.004	0.021 ± 0.004	0.019 ± 0.003
C28:0	0.018 ± 0.004	0.019 ± 0.004	0.021 ± 0.003	0.018 ± 0.003
C30:0	0.018 ± 0.003	0.018 ± 0.004	0.019 ± 0.003	0.017 ± 0.003
C32:0	0.018 ± 0.004	0.019 ± 0.004	0.020 ± 0.003	0.019 ± 0.003
C34:0	0.013 ± 0.003	0.014 ± 0.003	0.016 ± 0.002	0.013 ± 0.003
PC (30:2)	0.002 ± 0.000	0.002 ± 0.000	0.002 ± 0.000	0.002 ± 0.000
PC (30:1)	0.034 ± 0.010	0.023 ± 0.008	0.031 ± 0.006	0.021 ± 0.008
PC (30:0)	0.004 ± 0.001	0.003 ± 0.001	0.003 ± 0.001	0.003 ± 0.001
PCo(32:3)	0.001 ± 0.000	0.001 ± 0.000	0.001 ± 0.000	0.001 ± 0.000
PCo(32:2)	0.002 ± 0.001	0.002 ± 0.001	0.002 ± 0.001	0.001 ± 0.000
PCo(32:1)	0.005 ± 0.002	0.004 ± 0.001	0.004 ± 0.001	0.004 ± 0.001
PCo(32:0)	0.002 ± 0.001	0.002 ± 0.001	0.002 ± 0.000	0.002 ± 0.000

Table A.5.1 continued

PC (32:4)	0.001 ± 0.000	0.001 ± 0.000	0.001 ± 0.000	0.001 ± 0.000
PC (32:3)	0.001 ± 0.000	0.001 ± 0.000	0.001 ± 0.000	0.001 ± 0.000
PC (32:2)	0.002 ± 0.001	0.002 ± 0.000	0.002 ± 0.001	0.002 ± 0.000
PC (32:1)	0.011 ± 0.002	0.010 ± 0.002	0.011 ± 0.001	0.011 ± 0.001
PC (32:0)	0.004 ± 0.001	0.003 ± 0.001	0.003 ± 0.000	0.003 ± 0.001
PCp(32:4)	0.001 ± 0.000	0.001 ± 0.000	0.001 ± 0.000	0.001 ± 0.000
PCo(34:4)	0.001 ± 0.000	0.001 ± 0.000	0.001 ± 0.000	0.001 ± 0.000
PCo(34:3)	0.002 ± 0.001	0.002 ± 0.001	0.002 ± 0.001	0.002 ± 0.000
PCo(34:2)	0.010 ± 0.005	0.007 ± 0.004	0.009 ± 0.003	0.008 ± 0.003
PCo(34:1)	0.023 ± 0.006	0.017 ± 0.006	0.028 ± 0.024	0.055 ± 0.036
PCo(34:0)	0.003 ± 0.001	0.003 ± 0.001	0.004 ± 0.002	0.006 ± 0.003
PC (34:6)	0.002 ± 0.002	0.002 ± 0.001	0.002 ± 0.00	0.001 ± 0.000
PC (34:5)	0.001 ± 0.000	0.001 ± 0.000	0.001 ± 0.000	0.001 ± 0.000
PC (34:4)	0.002 ± 0.000	0.002 ± 0.001	0.002 ± 0.000	0.002 ± 0.000
PC (34:3)	0.002 ± 0.001	0.004 ± 0.004	0.003 ± 0.002	0.006 ± 0.002
PC (34:2)	0.012 ± 0.003	0.015 ± 0.007	0.020 ± 0.008	0.028 ± 0.005
PC (34:1)	0.155 ± 0.024	0.132 ± 0.019	0.132 ± 0.031	0.156 ± 0.017
PC (34:0)	0.014 ± 0.002	0.012 ± 0.002	0.012 ± 0.002	0.014 ± 0.001
PCp(36:5)	0.002 ± 0.000	0.002 ± 0.000	0.002 ± 0.000	0.002 ± 0.000
PCo(36:5)	0.010 ± 0.004	0.014 ± 0.006	0.008 ± 0.005	0.007 ± 0.002
PCo(36:4)	0.022 ± 0.009	0.026 ± 0.006	0.014 ± 0.002	0.018 ± 0.003
PCo(36:3)	0.005 ± 0.001	0.006 ± 0.001	0.005 ± 0.001	0.006 ± 0.001
PCo(36:2)	0.009 ± 0.003	0.008 ± 0.003	0.008 ± 0.002	0.007 ± 0.001
PC (36:8)	0.008 ± 0.003	0.006 ± 0.002	0.009 ± 0.003	0.008 ± 0.002
PCo(36:1)	0.009 ± 0.004	0.007 ± 0.003	0.011 ± 0.003	0.009 ± 0.002
PC (36:7)	0.002 ± 0.001	0.002 ± 0.001	0.002 ± 0.001	0.002 ± 0.000
PCo(36:0)	0.003 ± 0.002	0.002 ± 0.001	0.003 ± 0.001	0.002 ± 0.001
PC (36:6)	0.002 ± 0.000	0.002 ± 0.000	0.002 ± 0.001	0.002 ± 0.000
PC (36:5)	0.017 ± 0.013	0.034 ± 0.015	0.012 ± 0.003	0.016 ± 0.005
PC (36:4)	0.047 ± 0.016	0.059 ± 0.013	0.049 ± 0.012	0.055 ± 0.010
PC (36:3)	0.012 ± 0.003	0.015 ± 0.004	0.013 ± 0.004	0.021 ± 0.004
PC (36:2)	0.037 ± 0.014	0.030 ± 0.005	0.021 ± 0.002	0.021 ± 0.004
PC (36:1)	0.046 ± 0.011	0.043 ± 0.012	0.036 ± 0.005	0.027 ± 0.003
PC (36:0); PCp(38:6)	0.013 ± 0.002	0.014 ± 0.002	0.012 ± 0.002	0.011 ± 0.001
PCo(38:6)	0.017 ± 0.007	0.016 ± 0.005	0.020 ± 0.008	0.026 ± 0.006
PCo(38:5)	0.027 ± 0.012	0.030 ± 0.007	0.020 ± 0.008	0.015 ± 0.005
PCo(38:4)	0.015 ± 0.004	0.018 ± 0.004	0.015 ± 0.003	0.015 ± 0.002
PCo(38:3)	0.005 ± 0.002	0.005 ± 0.002	0.005 ± 0.001	0.005 ± 0.002
PC (38:9)	0.005 ± 0.002	0.004 ± 0.001	0.005 ± 0.001	0.004 ± 0.001

Table A.5.1 continued

PCo(38:2)	0.006 ± 0.003	0.005 ± 0.001	0.006 ± 0.001	0.005 ± 0.001
PC (38:8)	0.004 ± 0.001	0.003 ± 0.001	0.006 ± 0.001	0.004 ± 0.001
PCo(38:1)	0.005 ± 0.002	0.004 ± 0.001	0.008 ± 0.002	0.005 ± 0.001
PC (38:7)	0.002 ± 0.001	0.002 ± 0.001	0.003 ± 0.001	0.004 ± 0.002
PCo(38:0)	0.002 ± 0.001	0.002 ± 0.001	0.003 ± 0.001	0.005 ± 0.002
PC (38:6)	0.023 ± 0.012	0.024 ± 0.008	0.039 ± 0.015	0.057 ± 0.012
PC (38:5)	0.045 ± 0.024	0.065 ± 0.023	0.044 ± 0.018	0.034 ± 0.008
PC (38:4)	0.095 ± 0.027	0.088 ± 0.022	0.096 ± 0.018	0.072 ± 0.017
PC (38:3)	0.017 ± 0.003	0.016 ± 0.003	0.018 ± 0.004	0.015 ± 0.002
PC (38:2)	0.034 ± 0.009	0.027 ± 0.008	0.036 ± 0.011	0.026 ± 0.005
PC (38:1)	0.007 ± 0.001	0.006 ± 0.001	0.007 ± 0.001	0.006 ± 0.001
PCp(40:6)	0.008 ± 0.004	0.006 ± 0.002	0.008 ± 0.003	0.007 ± 0.002
PC (38:0)	0.009 ± 0.005	0.007 ± 0.002	0.009 ± 0.004	0.007 ± 0.003
PCo(40:6)	0.008 ± 0.003	0.009 ± 0.002	0.013 ± 0.004	0.010 ± 0.002
PCo(40:5)	0.007 ± 0.002	0.008 ± 0.002	0.010 ± 0.004	0.008 ± 0.002
PCo(40:4)	0.005 ± 0.002	0.006 ± 0.002	0.007 ± 0.003	0.005 ± 0.001
PC (40:10)	0.004 ± 0.002	0.004 ± 0.002	0.004 ± 0.002	0.004 ± 0.002
PCo(40:3)	0.004 ± 0.003	0.005 ± 0.003	0.005 ± 0.002	0.005 ± 0.003
PC (40:9)	0.0034 ± 0.001	0.004 ± 0.001	0.004 ± 0.001	0.004 ± 0.001
PCo(40:2)	0.004 ± 0.001	0.004 ± 0.001	0.005 ± 0.001	0.004 ± 0.001
PC (40:8)	0.002 ± 0.000	0.002 ± 0.001	0.002 ± 0.001	0.002 ± 0.000
PCo(40:1)	0.002 ± 0.000	0.002 ± 0.001	0.002 ± 0.001	0.002 ± 0.001
PC (40:7)	0.003 ± 0.001	0.004 ± 0.001	0.004 ± 0.001	0.004 ± 0.001
PCo(40:0)	0.004 ± 0.001	0.005 ± 0.001	0.004 ± 0.001	0.005 ± 0.001
PC (40:6)	0.015 ± 0.007	0.016 ± 0.005	0.023 ± 0.011	0.019 ± 0.004
PC (40:5)	0.013 ± 0.006	0.017 ± 0.006	0.016 ± 0.009	0.009 ± 0.003
PC (40:4)	0.007 ± 0.002	0.010 ± 0.003	0.010 ± 0.004	0.008 ± 0.001
PC (40:3)	0.004 ± 0.001	0.004 ± 0.001	0.003 ± 0.001	0.003 ± 0.000
PC (40:2)	0.003 ± 0.001	0.003 ± 0.001	0.003 ± 0.000	0.003 ± 0.001
PC (40:1)	0.001 ± 0.000	0.001 ± 0.000	0.001 ± 0.000	0.001 ± 0.000
PCp(42:6)	0.001 ± 0.000	0.002 ± 0.001	0.002 ± 0.000	0.001 ± 0.000
PC (40:0)	0.002 ± 0.000	0.002 ± 0.001	0.002 ± 0.001	0.001 ± 0.000
PCo(42:6)	0.002 ± 0.001	0.002 ± 0.001	0.002 ± 0.001	0.002 ± 0.000
PCp(42:4)	0.002 ± 0.001	0.002 ± 0.001	0.003 ± 0.001	0.002 ± 0.001
PC (42:11)	0.001 ± 0.001	0.002 ± 0.001	0.002 ± 0.001	0.002 ± 0.001
PCo(42:4)	0.002 ± 0.001	0.002 ± 0.001	0.002 ± 0.001	0.002 ± 0.001
PC (42:10)	0.002 ± 0.001	0.002 ± 0.001	0.002 ± 0.000	0.002 ± 0.001
PCo(42:3)	0.002 ± 0.000	0.002 ± 0.001	0.002 ± 0.000	0.002 ± 0.001
PC (42:9)	0.002 ± 0.001	0.002 ± 0.001	0.002 ± 0.000	0.002 ± 0.000

Table A.5.1 continued

PCo(42:2)	0.002 ± 0.001	0.002 ± 0.001	0.002 ± 0.001	0.002 ± 0.000
PC (42:8)	0.001 ± 0.001	0.001 ± 0.000	0.001 ± 0.000	0.002 ± 0.000
PCo(42:1)	0.002 ± 0.001	0.001 ± 0.000	0.002 ± 0.000	0.002 ± 0.000
PC (42:7)	0.001 ± 0.000	0.001 ± 0.000	0.001 ± 0.000	0.001 ± 0.000
PCo(42:0)	0.001 ± 0.000	0.001 ± 0.000	0.001 ± 0.000	0.001 ± 0.000
PC (42:6)	0.001 ± 0.000	0.002 ± 0.000	0.001 ± 0.001	0.001 ± 0.000
PC (42:5)	0.001 ± 0.000	0.001 ± 0.000	0.001 ± 0.000	0.001 ± 0.000
PC (42:4)	0.001 ± 0.000	0.001 ± 0.000	0.001 ± 0.000	0.001 ± 0.000
PC (42:3)	0.001 ± 0.000	0.001 ± 0.000	0.001 ± 0.000	0.001 ± 0.000
PC (42:2)	0.001 ± 0.000	0.001 ± 0.000	0.001 ± 0.000	0.001 ± 0.000
PC (42:1)	0.001 ± 0.000	0.001 ± 0.000	0.001 ± 0.000	0.001 ± 0.000
PC (42:0)	0.001 ± 0.000	0.001 ± 0.000	0.001 ± 0.000	0.001 ± 0.000
PC (44:12)	0.001 ± 0.000	0.001 ± 0.000	0.001 ± 0.000	0.001 ± 0.000
PCo(44:5)	0.001 ± 0.000	0.001 ± 0.000	0.001 ± 0.000	0.001 ± 0.000
PCo(44:4)	0.001 ± 0.000	0.001 ± 0.000	0.001 ± 0.000	0.001 ± 0.000
PC (44:10)	0.001 ± 0.000	0.001 ± 0.000	0.001 ± 0.000	0.001 ± 0.000
PCo(44:3)	0.001 ± 0.000	0.001 ± 0.000	0.001 ± 0.000	0.001 ± 0.000
PC (44:8)	0.001 ± 0.000	0.001 ± 0.000	0.001 ± 0.000	0.001 ± 0.000
PC (44:7)	0.001 ± 0.000	0.001 ± 0.000	0.001 ± 0.000	0.001 ± 0.000
PC (44:6)	0.001 ± 0.000	0.001 ± 0.000	0.001 ± 0.000	0.001 ± 0.000
PC (44:5)	0.001 ± 0.000	0.001 ± 0.000	0.001 ± 0.001	0.001 ± 0.000
PC (44:4)	0.001 ± 0.000	0.001 ± 0.000	0.001 ± 0.000	0.001 ± 0.000
PC (44:3)	0.001 ± 0.000	0.001 ± 0.000	0.001 ± 0.000	0.001 ± 0.000
PC (44:2)	0.001 ± 0.000	0.001 ± 0.000	0.001 ± 0.000	0.001 ± 0.000
PC (44:1)	0.001 ± 0.000	0.001 ± 0.000	0.001 ± 0.000	0.001 ± 0.000
PC (44:0)	0.001 ± 0.000	0.001 ± 0.000	0.001 ± 0.000	0.001 ± 0.000
PC (46:0)	0.001 ± 0.000	0.001 ± 0.000	0.001 ± 0.000	0.001 ± 0.000
PC (48:0)	0.001 ± 0.000	0.001 ± 0.000	0.001 ± 0.000	0.001 ± 0.000
PE (12:0)	0.011 ± 0.004	0.011 ± 0.002	0.011 ± 0.003	0.013 ± 0.003
PE (14:1)	0.011 ± 0.003	0.011 ± 0.002	0.011 ± 0.003	0.013 ± 0.003
PEp (16:0)	0.016 ± 0.005	0.017 ± 0.004	0.016 ± 0.004	0.019 ± 0.005
PE (18:0)	0.011 ± 0.003	0.012 ± 0.003	0.012 ± 0.003	0.014 ± 0.003
PEo (20:0)	0.013 ± 0.003	0.013 ± 0.003	0.012 ± 0.003	0.014 ± 0.003
PE (20:5)	0.011 ± 0.003	0.012 ± 0.002	0.012 ± 0.003	0.014 ± 0.003
PE (20:4)	0.011 ± 0.003	0.012 ± 0.003	0.012 ± 0.003	0.014 ± 0.003
PE (20:3)	0.011 ± 0.003	0.011 ± 0.002	0.011 ± 0.002	0.013 ± 0.003
PE (22:4)	0.011 ± 0.003	0.012 ± 0.002	0.011 ± 0.003	0.014 ± 0.003
PE (24:0)	0.011 ± 0.003	0.011 ± 0.002	0.011 ± 0.003	0.013 ± 0.003
PE (32:3)	0.021 ± 0.002	0.021 ± 0.004	0.019 ± 0.004	0.023 ± 0.002

Table A.5.1 continued

PE (32:0)	0.012 ± 0.003	0.013 ± 0.002	0.013 ± 0.003	0.015 ± 0.002
PEo (34:3)	0.011 ± 0.003	0.012 ± 0.002	0.011 ± 0.003	0.013 ± 0.002
PEo (34:1)	0.014 ± 0.002	0.014 ± 0.001	0.015 ± 0.002	0.018 ± 0.004
PE (34:3)	0.024 ± 0.006	0.024 ± 0.004	0.021 ± 0.003	0.022 ± 0.005
PE (34:2)	0.014 ± 0.003	0.017 ± 0.005	0.015 ± 0.002	0.018 ± 0.002
PE (34:1)	0.020 ± 0.003	0.024 ± 0.004	0.021 ± 0.003	0.024 ± 0.006
PEp (36:5)	0.023 ± 0.004	0.024 ± 0.003	0.022 ± 0.002	0.020 ± 0.002
PEo (36:5)	0.106 ± 0.039	0.104 ± 0.027	0.102 ± 0.033	0.063 ± 0.028
PEo (36:2)	0.053 ± 0.030	0.065 ± 0.022	0.041 ± 0.015	0.031 ± 0.006
PE (36:4)	0.028 ± 0.010	0.023 ± 0.002	0.027 ± 0.008	0.030 ± 0.011
PE (36:3)	0.012 ± 0.003	0.012 ± 0.002	0.012 ± 0.003	0.015 ± 0.002
PE (36:1)	0.011 ± 0.003	0.012 ± 0.002	0.012 ± 0.002	0.014 ± 0.002
PEp (36:6)	0.012 ± 0.003	0.013 ± 0.002	0.013 ± 0.003	0.014 ± 0.002
PE (36:0)	0.019 ± 0.003	0.017 ± 0.003	0.017 ± 0.004	0.016 ± 0.001
PEo (38:6)	0.016 ± 0.003	0.016 ± 0.003	0.013 ± 0.002	0.015 ± 0.001
PEo (38:5)	0.016 ± 0.003	0.017 ± 0.001	0.017 ± 0.004	0.019 ± 0.005
PEo (38:4)	0.025 ± 0.001	0.019 ± 0.003	0.024 ± 0.007	0.021 ± 0.004
PEo (38:3)	0.031 ± 0.012	0.026 ± 0.004	0.031 ± 0.014	0.028 ± 0.010
PEo (38:1)	0.017 ± 0.005	0.016 ± 0.001	0.016 ± 0.003	0.017 ± 0.001
PE (38:7)	0.011 ± 0.003	0.012 ± 0.002	0.011 ± 0.003	0.014 ± 0.003
PE (38:6)	0.011 ± 0.003	0.012 ± 0.002	0.012 ± 0.003	0.014 ± 0.003
PE (38:5)	0.013 ± 0.003	0.015 ± 0.002	0.015 ± 0.002	0.015 ± 0.001
PE (38:4)	0.011 ± 0.003	0.011 ± 0.002	0.011 ± 0.003	0.013 ± 0.003
PE (38:3)	0.018 ± 0.006	0.017 ± 0.003	0.015 ± 0.003	0.019 ± 0.005
PE (40:2)	0.011 ± 0.003	0.011 ± 0.002	0.011 ± 0.003	0.013 ± 0.002
PE0 (40:7)	0.013 ± 0.003	0.015 ± 0.001	0.013 ± 0.003	0.015 ± 0.003
PEo (40:6)	0.012 ± 0.002	0.013 ± 0.002	0.012 ± 0.003	0.014 ± 0.003
PEo (40:5)	0.011 ± 0.003	0.012 ± 0.002	0.012 ± 0.003	0.013 ± 0.003
PEo (40:4)	0.012 ± 0.003	0.013 ± 0.002	0.013 ± 0.003	0.014 ± 0.002
PE (40:10)	0.019 ± 0.003	0.021 ± 0.004	0.020 ± 0.004	0.020 ± 0.004
PEo (40:3)	0.035 ± 0.024	0.033 ± 0.015	0.034 ± 0.014	0.026 ± 0.006
PEo (40:1)	0.042 ± 0.020	0.024 ± 0.003	0.041 ± 0.017	0.041 ± 0.011
PE (40:7)	0.018 ± 0.005	0.017 ± 0.003	0.016 ± 0.002	0.017 ± 0.001
PEo (40:0)	0.011 ± 0.003	0.012 ± 0.002	0.012 ± 0.002	0.014 ± 0.003
PE (40:6)	0.012 ± 0.003	0.013 ± 0.001	0.013 ± 0.002	0.014 ± 0.002
PE (40:4)	0.016 ± 0.002	0.016 ± 0.002	0.019 ± 0.004	0.017 ± 0.002
PE (40:3)	0.021 ± 0.005	0.022 ± 0.004	0.027 ± 0.013	0.019 ± 0.002
PE (40:0)	0.026 ± 0.007	0.024 ± 0.005	0.034 ± 0.010	0.025 ± 0.006
PEp (42:2)	0.011 ± 0.003	0.011 ± 0.002	0.011 ± 0.002	0.013 ± 0.002

Table A.5.1 continued

PE (42:9)	0.014 ± 0.002	0.015 ± 0.002	0.014 ± 0.002	0.016 ± 0.002
PEo (42:2)	0.011 ± 0.003	0.011 ± 0.002	0.011 ± 0.003	0.013 ± 0.003
PEo (42:0)	0.011 ± 0.003	0.011 ± 0.002	0.011 ± 0.002	0.013 ± 0.002
PE (42:3)	0.014 ± 0.002	0.014 ± 0.001	0.014 ± 0.002	0.018 ± 0.003
PE (42:2); PE (42:2)	0.013 ± 0.002	0.014 ± 0.002	0.013 ± 0.003	0.014 ± 0.002
PG (12:0)	0.026 ± 0.003	0.026 ± 0.002	0.028 ± 0.001	0.027 ± 0.001
PGp (18:0)	0.026 ± 0.003	0.025 ± 0.002	0.028 ± 0.001	0.028 ± 0.002
PG (16:0)	0.047 ± 0.011	0.041 ± 0.004	0.048 ± 0.008	0.051 ± 0.015
PG (18:4)	0.025 ± 0.002	0.025 ± 0.002	0.027 ± 0.001	0.027 ± 0.002
PG (18:2)	0.026 ± 0.003	0.026 ± 0.002	0.028 ± 0.001	0.027 ± 0.002
PG (18:1)	0.027 ± 0.002	0.026 ± 0.002	0.028 ± 0.002	0.028 ± 0.002
PG (18:0)	0.027 ± 0.002	0.027 ± 0.003	0.029 ± 0.001	0.028 ± 0.002
PGo (20:0)	0.059 ± 0.017	0.052 ± 0.007	0.061 ± 0.015	0.064 ± 0.019
PG (20:1)	0.026 ± 0.003	0.025 ± 0.002	0.028 ± 0.001	0.028 ± 0.002
LPG (20:0)	0.038 ± 0.013	0.034 ± 0.005	0.033 ± 0.003	0.037 ± 0.006
PG (20:0)	0.037 ± 0.008	0.033 ± 0.003	0.039 ± 0.002	0.040 ± 0.007
PG (22:2)	0.026 ± 0.003	0.025 ± 0.002	0.027 ± 0.001	0.027 ± 0.001
PG (24:0)	0.030 ± 0.005	0.031 ± 0.012	0.029 ± 0.003	0.029 ± 0.003
PG (24:1)	0.025 ± 0.002	0.025 ± 0.002	0.027 ± 0.002	0.026 ± 0.002
PG (30:1)	0.034 ± 0.012	0.033 ± 0.005	0.026 ± 0.001	0.027 ± 0.002
PG (32:0)	0.060 ± 0.018	0.054 ± 0.022	0.046 ± 0.025	0.041 ± 0.012
PGo (34:3)	0.024 ± 0.002	0.024 ± 0.002	0.026 ± 0.001	0.026 ± 0.002
PG (34:2)	0.029 ± 0.006	0.032 ± 0.006	0.027 ± 0.002	0.029 ± 0.002
PG (34:1)	0.041 ± 0.020	0.047 ± 0.015	0.032 ± 0.006	0.033 ± 0.003
PGo (36:5)	0.024 ± 0.002	0.024 ± 0.002	0.026 ± 0.001	0.026 ± 0.002
PG (36:8)	0.025 ± 0.002	0.026 ± 0.001	0.027 ± 0.001	0.027 ± 0.002
PGo (36:1)	0.026 ± 0.002	0.027 ± 0.002	0.027 ± 0.000	0.027 ± 0.001
PG (36:6)	0.024 ± 0.002	0.024 ± 0.002	0.026 ± 0.001	0.026 ± 0.001
PG (36:4)	0.025 ± 0.002	0.026 ± 0.002	0.027 ± 0.001	0.027 ± 0.002
PG (36:3)	0.026 ± 0.001	0.028 ± 0.005	0.027 ± 0.001	0.027 ± 0.002
PG (36:2)	0.038 ± 0.024	0.053 ± 0.017	0.030 ± 0.005	0.028 ± 0.002
PGo (38:3)	0.025 ± 0.002	0.024 ± 0.001	0.026 ± 0.001	0.026 ± 0.002
PG (38:5)	0.025 ± 0.002	0.028 ± 0.003	0.027 ± 0.001	0.027 ± 0.002
PG (38:1)	0.026 ± 0.002	0.027 ± 0.002	0.028 ± 0.001	0.027 ± 0.002
PGo (40:9)	0.026 ± 0.003	0.025 ± 0.002	0.028 ± 0.001	0.027 ± 0.002
PGo (40:2)	0.026 ± 0.003	0.025 ± 0.002	0.028 ± 0.002	0.027 ± 0.001
PG (42:11)	0.025 ± 0.002	0.025 ± 0.002	0.028 ± 0.001	0.027 ± 0.002
PG (44:10)	0.025 ± 0.003	0.025 ± 0.002	0.028 ± 0.001	0.027 ± 0.002
PI (12:0)	0.011 ± 0.003	0.012 ± 0.002	0.012 ± 0.002	0.012 ± 0.002

Table A.5.1 continued

PI (14:0)	0.011 ± 0.003	0.011 ± 0.002	0.012 ± 0.002	0.013 ± 0.002
PI (16:0)	0.011 ± 0.003	0.011 ± 0.002	0.012 ± 0.002	0.012 ± 0.001
PI (18:3)	0.011 ± 0.003	0.010 ± 0.002	0.012 ± 0.002	0.012 ± 0.001
PI (18:2)	0.011 ± 0.003	0.010 ± 0.002	0.012 ± 0.002	0.012 ± 0.001
PI (18:1)	0.011 ± 0.003	0.011 ± 0.002	0.012 ± 0.003	0.012 ± 0.002
PIo (20:5)	0.016 ± 0.007	0.015 ± 0.005	0.017 ± 0.005	0.014 ± 0.003
PI (20:4)	0.011 ± 0.003	0.010 ± 0.002	0.012 ± 0.002	0.012 ± 0.002
PI (20:3)	0.011 ± 0.002	0.010 ± 0.002	0.012 ± 0.002	0.012 ± 0.001
PI (20:0)	0.013 ± 0.004	0.013 ± 0.003	0.013 ± 0.003	0.014 ± 0.003
PI (22:6)	0.011 ± 0.003	0.011 ± 0.002	0.012 ± 0.003	0.012 ± 0.001
PI (22:4)	0.011 ± 0.002	0.010 ± 0.002	0.011 ± 0.002	0.012 ± 0.001
PI (22:1)	0.011 ± 0.003	0.010 ± 0.002	0.011 ± 0.002	0.012 ± 0.001
PI (28:1)	0.011 ± 0.002	0.010 ± 0.002	0.011 ± 0.002	0.011 ± 0.001
PIp (32:1)	0.011 ± 0.003	0.010 ± 0.002	0.011 ± 0.002	0.011 ± 0.001
PIo (32:0)	0.011 ± 0.002	0.010 ± 0.002	0.011 ± 0.002	0.011 ± 0.001
PI (32:1)	0.012 ± 0.002	0.011 ± 0.002	0.012 ± 0.002	0.013 ± 0.002
PIo (34:1), PIp (34:0)	0.011 ± 0.003	0.011 ± 0.002	0.013 ± 0.002	0.013 ± 0.001
PI (34:3)	0.011 ± 0.002	0.011 ± 0.002	0.012 ± 0.002	0.013 ± 0.001
PI (34:2)	0.013 ± 0.002	0.014 ± 0.002	0.015 ± 0.002	0.017 ± 0.002
PI (34:1)	0.017 ± 0.003	0.017 ± 0.002	0.019 ± 0.003	0.022 ± 0.004
PI (34:0)	0.012 ± 0.002	0.011 ± 0.002	0.012 ± 0.002	0.013 ± 0.002
PI (36:8)	0.012 ± 0.002	0.011 ± 0.002	0.014 ± 0.002	0.013 ± 0.002
PI (36:5)	0.013 ± 0.002	0.014 ± 0.003	0.013 ± 0.002	0.014 ± 0.001
PI (36:4)	0.021 ± 0.003	0.026 ± 0.006	0.025 ± 0.005	0.033 ± 0.007
PI (36:3)	0.018 ± 0.002	0.019 ± 0.005	0.019 ± 0.004	0.024 ± 0.003
PI (36:2)	0.032 ± 0.007	0.031 ± 0.004	0.029 ± 0.005	0.037 ± 0.011
PI (36:1)	0.033 ± 0.013	0.033 ± 0.005	0.026 ± 0.006	0.027 ± 0.007
PIp (38:6)	0.013 ± 0.002	0.012 ± 0.002	0.013 ± 0.002	0.013 ± 0.002
PI (36:0)	0.013 ± 0.002	0.012 ± 0.002	0.013 ± 0.003	0.013 ± 0.001
PIo (38:5), PIp (38:4)	0.013 ± 0.003	0.013 ± 0.002	0.013 ± 0.002	0.013 ± 0.001
PIo (38:4), PIp (38:3)	0.017 ± 0.004	0.017 ± 0.004	0.019 ± 0.004	0.017 ± 0.002
PS (44:7)	0.011 ± 0.002	0.010 ± 0.002	0.012 ± 0.002	0.012 ± 0.001
PIo (38:3), PIp (38:2)	0.012 ± 0.002	0.012 ± 0.002	0.013 ± 0.002	0.013 ± 0.001
PI (38:6)	0.014 ± 0.002	0.015 ± 0.003	0.014 ± 0.002	0.018 ± 0.002
PI (38:5)	0.062 ± 0.029	0.087 ± 0.028	0.040 ± 0.011	0.045 ± 0.011
PI (38:4)	0.256 ± 0.065	0.246 ± 0.055	0.236 ± 0.065	0.196 ± 0.034
PI (38:3)	0.043 ± 0.008	0.041 ± 0.007	0.042 ± 0.006	0.044 ± 0.007
PI (38:2)	0.013 ± 0.002	0.012 ± 0.002	0.014 ± 0.001	0.014 ± 0.001
PIo (40:4), PIp (40:3)	0.013 ± 0.003	0.013 ± 0.002	0.016 ± 0.002	0.015 ± 0.002

Table A.5.1 continued

PI (40:10)	0.011 ± 0.002	0.011 ± 0.002	0.012 ± 0.002	0.013 ± 0.001
PIo (40:3), PIp (40:2)	0.012 ± 0.003	0.011 ± 0.002	0.012 ± 0.002	0.013 ± 0.001
PIo (40:7)	0.012 ± 0.003	0.012 ± 0.002	0.012 ± 0.002	0.013 ± 0.001
PI (40:6)	0.016 ± 0.003	0.016 ± 0.002	0.019 ± 0.004	0.021 ± 0.002
PI (40:5)	0.020 ± 0.005	0.020 ± 0.004	0.023 ± 0.006	0.019 ± 0.002
PI (40:4)	0.015 ± 0.002	0.015 ± 0.002	0.019 ± 0.004	0.022 ± 0.004
PI (40:3)	0.012 ± 0.002	0.011 ± 0.002	0.012 ± 0.002	0.013 ± 0.001
PI (40:1)	0.011 ± 0.003	0.011 ± 0.002	0.012 ± 0.002	0.012 ± 0.001
PIp (42:6)	0.013 ± 0.004	0.013 ± 0.003	0.014 ± 0.002	0.015 ± 0.002
PI (42:4)	0.011 ± 0.002	0.010 ± 0.002	0.011 ± 0.002	0.011 ± 0.001
PS (14:1)	0.093 ± 0.030	0.074 ± 0.021	0.087 ± 0.041	0.125 ± 0.043
PS (14:0)	0.035 ± 0.003	0.035 ± 0.003	0.036 ± 0.005	0.035 ± 0.001
PSp (16:0)	0.058 ± 0.028	0.064 ± 0.022	0.068 ± 0.032	0.043 ± 0.004
PS (18:4)	0.033 ± 0.002	0.034 ± 0.002	0.032 ± 0.002	0.032 ± 0.002
PS (18:2)	0.034 ± 0.002	0.035 ± 0.002	0.033 ± 0.002	0.033 ± 0.003
PS (18:1)	0.033 ± 0.002	0.034 ± 0.002	0.033 ± 0.003	0.033 ± 0.002
PSo (20:0)	0.044 ± 0.011	0.050 ± 0.018	0.055 ± 0.022	0.037 ± 0.004
PS (20:5)	0.034 ± 0.002	0.034 ± 0.002	0.033 ± 0.002	0.033 ± 0.002
PS (20:0)	0.058 ± 0.028	0.054 ± 0.024	0.046 ± 0.013	0.045 ± 0.007
PS (22:4)	0.033 ± 0.002	0.033 ± 0.002	0.033 ± 0.003	0.033 ± 0.002
PS (22:2)	0.033 ± 0.002	0.033 ± 0.002	0.033 ± 0.003	0.033 ± 0.003
PS (22:0)	0.033 ± 0.002	0.033 ± 0.002	0.032 ± 0.002	0.033 ± 0.002
PS (26:1)	0.033 ± 0.002	0.033 ± 0.002	0.032 ± 0.003	0.032 ± 0.002
PS (28:0)	0.097 ± 0.012	0.103 ± 0.007	0.101 ± 0.009	0.101 ± 0.011
PS (32:2)	0.039 ± 0.003	0.038 ± 0.003	0.042 ± 0.004	0.043 ± 0.005
PS (34:3)	0.032 ± 0.002	0.033 ± 0.002	0.032 ± 0.002	0.032 ± 0.002
PS (36:8)	0.037 ± 0.003	0.037 ± 0.003	0.037 ± 0.005	0.039 ± 0.003
PS (36:1)	0.036 ± 0.003	0.036 ± 0.002	0.036 ± 0.004	0.036 ± 0.002
PS (36:5)	0.032 ± 0.002	0.033 ± 0.001	0.032 ± 0.002	0.032 ± 0.002
PS (38:0)	0.035 ± 0.002	0.036 ± 0.002	0.036 ± 0.003	0.035 ± 0.002
PSo (40:5)	0.034 ± 0.002	0.034 ± 0.002	0.034 ± 0.002	0.033 ± 0.002
PSo (42:2)	0.035 ± 0.003	0.036 ± 0.002	0.033 ± 0.003	0.035 ± 0.003
PS (42:1)	0.034 ± 0.002	0.034 ± 0.002	0.033 ± 0.002	0.033 ± 0.002
PS (44:7)	0.034 ± 0.002	0.034 ± 0.002	0.033 ± 0.002	0.033 ± 0.002
SM (d18:1/12:0)	0.099 ± 0.017	0.100 ± 0.017	0.017 ± 0.003	0.019 ± 0.004
SM (d18:0/12:0)	0.009 ± 0.001	0.010 ± 0.002	0.003 ± 0.001	0.003 ± 0.000
SM (d18:2/14:0)	0.005 ± 0.001	0.008 ± 0.003	0.005 ± 0.001	0.007 ± 0.002
SM (d18:1/14:0)	0.239 ± 0.018	0.251 ± 0.027	0.236 ± 0.021	0.225 ± 0.016
SM (d18:0/14:0)	0.023 ± 0.002	0.024 ± 0.003	0.024 ± 0.003	0.023 ± 0.002

Table A.5.1 continued

SM (d16:1/18:1)	0.004 ± 0.001	0.008 ± 0.004	0.004 ± 0.001	0.005 ± 0.001
SM (d18:1/16:0)	0.134 ± 0.025	0.110 ± 0.026	0.158 ± 0.017	0.125 ± 0.032
SM (d18:0/16:0)	0.016 ± 0.003	0.013 ± 0.003	0.019 ± 0.003	0.017 ± 0.002
SM (d18:2/18:1)	0.001 ± 0.000	0.002 ± 0.001	0.001 ± 0.000	0.002 ± 0.000
SM (d18:1/18:1)9Z))	0.002 ± 0.000	0.002 ± 0.000	0.002 ± 0.001	0.002 ± 0.000
SM (d18:1/18:0)	0.014 ± 0.004	0.012 ± 0.004	0.016 ± 0.003	0.013 ± 0.004
SM (d18:0/18:0)	0.006 ± 0.001	0.006 ± 0.001	0.008 ± 0.001	0.009 ± 0.002
SM (d18:2/20:1)	0.002 ± 0.000	0.002 ± 0.001	0.002 ± 0.001	0.003 ± 0.001
SM (d16:1/22:1)	0.004 ± 0.001	0.005 ± 0.003	0.003 ± 0.002	0.007 ± 0.002
SM (d18:1/20:0)	0.014 ± 0.004	0.016 ± 0.006	0.019 ± 0.007	0.028 ± 0.005
SM (d18:0/20:0)	0.084 ± 0.019	0.086 ± 0.016	0.087 ± 0.026	0.127 ± 0.021
SM (d18:2/22:1)	0.029 ± 0.011	0.042 ± 0.013	0.036 ± 0.010	0.048 ± 0.008
SM (d16:1/24:1)	0.047 ± 0.031	0.029 ± 0.011	0.020 ± 0.003	0.028 ± 0.006
SM (d16:1/24:0)	0.037 ± 0.012	0.039 ± 0.008	0.041 ± 0.002	0.041 ± 0.006
SM (d18:0/22:0)	0.028 ± 0.007	0.030 ± 0.006	0.026 ± 0.005	0.025 ± 0.003
SM (d18:2/24:1)	0.068 ± 0.020	0.073 ± 0.012	0.088 ± 0.020	0.080 ± 0.013
SM (d18:1/24:1)15Z))	0.102 ± 0.019	0.097 ± 0.017	0.142 ± 0.021	0.122 ± 0.007
SM (d18:1/24:0)	0.021 ± 0.006	0.022 ± 0.004	0.031 ± 0.004	0.027 ± 0.002
SM (d18:0/24:0)	0.004 ± 0.001	0.005 ± 0.001	0.005 ± 0.001	0.005 ± 0.001
SM (d18:1/26:1)17Z))	0.004 ± 0.001	0.004 ± 0.001	0.004 ± 0.001	0.004 ± 0.001
SM (d18:1/26:0)	0.002 ± 0.001	0.002 ± 0.001	0.003 ± 0.001	0.003 ± 0.001
SM (d18:0/26:0)	0.001 ± 0.000	0.002 ± 0.001	0.002 ± 0.001	0.002 ± 0.000
TAG(48:0)_FA 16:0	0.010 ± 0.003	0.011 ± 0.002	0.012 ± 0.002	0.013 ± 0.003
TAG(48:0)_FA 18:0	0.008 ± 0.001	0.009 ± 0.002	0.006 ± 0.001	0.006 ± 0.001
TAG(48:1)_FA 16:0	0.029 ± 0.009	0.027 ± 0.006	0.045 ± 0.017	0.041 ± 0.012
TAG(48:1)_FA 16:1	0.005 ± 0.001	0.006 ± 0.001	0.008 ± 0.000	0.010 ± 0.002
TAG(48:1)_FA 18:1	0.034 ± 0.013	0.039 ± 0.014	0.023 ± 0.009	0.016 ± 0.007
TAG(48:1)_FA 18:0	0.025 ± 0.013	0.036 ± 0.016	0.005 ± 0.002	0.005 ± 0.001
TAG(48:2)_F A18:0	0.005 ± 0.001	0.005 ± 0.002	0.003 ± 0.001	0.003 ± 0.001
TAG(48:2)_FA 16:0	0.006 ± 0.001	0.006 ± 0.001	0.012 ± 0.003	0.010 ± 0.003
TAG(48:2)_FA 16:1	0.007 ± 0.002	0.008 ± 0.002	0.009 ± 0.003	0.011 ± 0.003
TAG(48:2)_FA 18:1	0.082 ± 0.041	0.094 ± 0.044	0.011 ± 0.004	0.008 ± 0.002
TAG(48:2)_FA 18:2	0.006 ± 0.001	0.006 ± 0.002	0.007 ± 0.002	0.005 ± 0.001
TAG(48:3)_FA 16:0	0.004 ± 0.001	0.003 ± 0.001	0.004 ± 0.001	0.004 ± 0.001
TAG(48:3)_FA 16:1	0.003 ± 0.001	0.003 ± 0.001	0.004 ± 0.001	0.004 ± 0.001
TAG(48:3)_FA 18:0	0.003 ± 0.001	0.003 ± 0.001	0.003 ± 0.001	0.003 ± 0.001
TAG(48:3)_FA 18:1	0.008 ± 0.003	0.008 ± 0.002	0.004 ± 0.001	0.003 ± 0.001
TAG(48:3)_FA 18:2	0.008 ± 0.003	0.007 ± 0.002	0.004 ± 0.001	0.003 ± 0.001

Table A.5.1 continued

TAG(49:7)_FA 18:1	0.004 ± 0.000	0.004 ± 0.001	0.004 ± 0.001	0.004 ± 0.001
TAG(50:0)_FA 16:0	0.008 ± 0.002	0.007 ± 0.002	0.010 ± 0.002	0.011 ± 0.002
TAG(50:1)_FA 18:0	0.008 ± 0.002	0.007 ± 0.001	0.008 ± 0.002	0.008 ± 0.001
TAG(50:1)_FA 18:1	0.004 ± 0.001	0.004 ± 0.001	0.005 ± 0.001	0.004 ± 0.001
TAG(50:2)_FA 16:0	0.036 ± 0.014	0.029 ± 0.008	0.072 ± 0.024	0.076 ± 0.026
TAG(50:2)_FA 16:1	0.004 ± 0.001	0.004 ± 0.001	0.005 ± 0.000	0.007 ± 0.001
TAG(50:2)_FA 18:0	0.011 ± 0.004	0.015 ± 0.006	0.010 ± 0.005	0.010 ± 0.006
TAG(50:2)_FA 18:1	0.021 ± 0.005	0.022 ± 0.005	0.027 ± 0.007	0.027 ± 0.006
TAG(50:2)_FA 18:2	0.003 ± 0.001	0.003 ± 0.001	0.004 ± 0.001	0.003 ± 0.001
TAG(50:3)_FA 16:0	0.014 ± 0.005	0.013 ± 0.006	0.032 ± 0.015	0.030 ± 0.011
TAG(50:3)_FA 16:1	0.009 ± 0.002	0.007 ± 0.002	0.014 ± 0.003	0.016 ± 0.005
TAG(50:3)_FA 18:0	0.004 ± 0.001	0.004 ± 0.001	0.004 ± 0.001	0.004 ± 0.001
TAG(50:3)_FA 18:1	0.034 ± 0.015	0.038 ± 0.012	0.028 ± 0.013	0.020 ± 0.006
TAG(50:3)_FA 18:2	0.005 ± 0.001	0.006 ± 0.003	0.010 ± 0.005	0.009 ± 0.003
TAG(50:4)_FA 16:0	0.004 ± 0.001	0.007 ± 0.007	0.007 ± 0.002	0.008 ± 0.002
TAG(50:4)_FA 16:1	0.005 ± 0.001	0.004 ± 0.001	0.007 ± 0.002	0.008 ± 0.002
TAG(50:4)_FA 18:0	0.003 ± 0.001	0.003 ± 0.001	0.003 ± 0.001	0.003 ± 0.001
TAG(50:4)_FA 18:1	0.006 ± 0.001	0.006 ± 0.001	0.006 ± 0.002	0.005 ± 0.001
TAG(50:4)_FA 18:2	0.005 ± 0.001	0.005 ± 0.001	0.006 ± 0.001	0.005 ± 0.001
TAG(52:0)_FA 16:0	0.006 ± 0.002	0.006 ± 0.002	0.006 ± 0.001	0.006 ± 0.001
TAG(52:0)_FA 18:0	0.009 ± 0.003	0.007 ± 0.002	0.009 ± 0.002	0.009 ± 0.002
TAG(52:0)_FA 18:1	0.003 ± 0.001	0.003 ± 0.001	0.003 ± 0.001	0.003 ± 0.001
TAG(52:0)_FA 20:0	0.004 ± 0.002	0.004 ± 0.002	0.003 ± 0.001	0.003 ± 0.001
TAG(52:1)_FA 16:0	0.010 ± 0.002	0.011 ± 0.002	0.012 ± 0.003	0.013 ± 0.003
TAG(52:1)_FA 16:1	0.003 ± 0.001	0.003 ± 0.001	0.003 ± 0.001	0.004 ± 0.001
TAG(52:1)_FA 18:0	0.009 ± 0.001	0.009 ± 0.001	0.010 ± 0.002	0.011 ± 0.003
TAG(52:1)_FA 18:1	0.009 ± 0.001	0.009 ± 0.002	0.009 ± 0.002	0.010 ± 0.002
TAG(52:1)_FA20:0	0.004 ± 0.001	0.004 ± 0.001	0.003 ± 0.001	0.003 ± 0.001
TAG(52:2)_FA 16:0	0.020 ± 0.006	0.016 ± 0.004	0.019 ± 0.006	0.017 ± 0.003
TAG(52:2)_FA 16:1	0.005 ± 0.001	0.005 ± 0.001	0.005 ± 0.001	0.006 ± 0.001
TAG(52:2)_FA 18:0	0.005 ± 0.001	0.005 ± 0.001	0.006 ± 0.001	0.006 ± 0.001
TAG(52:2)_FA 18:1	0.030 ± 0.012	0.026 ± 0.006	0.028 ± 0.010	0.023 ± 0.004
TAG(52:3)_FA 16:0	0.006 ± 0.001	0.007 ± 0.002	0.007 ± 0.002	0.008 ± 0.002
TAG(52:3)_FA 16:1	0.007 ± 0.002	0.006 ± 0.002	0.006 ± 0.002	0.006 ± 0.001
TAG(52:3)_FA 18:0	0.003 ± 0.001	0.003 ± 0.001	0.003 ± 0.001	0.003 ± 0.000
TAG(52:3)_FA 18:1	0.011 ± 0.005	0.011 ± 0.004	0.012 ± 0.004	0.010 ± 0.001
TAG(52:3)_FA 18:2	0.005 ± 0.001	0.005 ± 0.002	0.006 ± 0.001	0.006 ± 0.001
TAG(52:3)_FA 20:4	0.003 ± 0.001	0.003 ± 0.001	0.003 ± 0.001	0.003 ± 0.001
TAG(52:4)_FA 16:0	0.005 ± 0.001	0.007 ± 0.003	0.005 ± 0.001	0.006 ± 0.002

Table A.5.1 continued

TAG(52:4)_FA 16:1	0.003 ± 0.001	0.003 ± 0.001	0.004 ± 0.001	0.004 ± 0.001
TAG(52:4)_FA 18:1	0.004 ± 0.001	0.004 ± 0.002	0.004 ± 0.000	0.004 ± 0.001
TAG(52:4)_FA 20:4	0.006 ± 0.003	0.007 ± 0.003	0.005 ± 0.001	0.006 ± 0.002
TAG(52:5)_FA 16:0	0.005 ± 0.003	0.007 ± 0.003	0.004 ± 0.000	0.005 ± 0.001
TAG(52:5)_FA 16:1	0.003 ± 0.001	0.003 ± 0.001	0.003 ± 0.001	0.004 ± 0.001
TAG(52:5)_FA 18:1	0.004 ± 0.001	0.004 ± 0.001	0.003 ± 0.001	0.003 ± 0.001
TAG(52:5)_FA 20:4	0.006 ± 0.002	0.007 ± 0.002	0.006 ± 0.002	0.006 ± 0.001
TAG(52:6)_FA 16:0	0.003 ± 0.001	0.004 ± 0.003	0.003 ± 0.001	0.004 ± 0.000
TAG(52:6)_FA 16:1	0.003 ± 0.001	0.003 ± 0.001	0.003 ± 0.001	0.003 ± 0.001
TAG(52:6)_FA 18:0	0.003 ± 0.001	0.002 ± 0.001	0.003 ± 0.001	0.003 ± 0.001
TAG(52:6)_FA 18:1	0.004 ± 0.001	0.005 ± 0.002	0.003 ± 0.001	0.003 ± 0.001
TAG(52:6)_FA 18:2	0.003 ± 0.001	0.003 ± 0.001	0.003 ± 0.001	0.003 ± 0.001
TAG(52:6)_FA 20:4	0.004 ± 0.001	0.003 ± 0.001	0.004 ± 0.001	0.004 ± 0.001
TAG(54:0)_FA 16:0	0.003 ± 0.001	0.003 ± 0.001	0.003 ± 0.001	0.003 ± 0.001
TAG(54:0)_FA 18:0	0.006 ± 0.002	0.005 ± 0.002	0.006 ± 0.002	0.006 ± 0.001
TAG(54:1)_FA 16:0	0.004 ± 0.001	0.004 ± 0.001	0.003 ± 0.001	0.004 ± 0.001
TAG(54:1)_FA 16:1	0.003 ± 0.001	0.002 ± 0.001	0.003 ± 0.001	0.003 ± 0.001
TAG(54:1)_FA 18:0	0.004 ± 0.001	0.004 ± 0.001	0.004 ± 0.001	0.005 ± 0.001
TAG(54:1)_FA 18:1	0.004 ± 0.001	0.004 ± 0.001	0.004 ± 0.001	0.004 ± 0.001
TAG(54:1)_FA 20:0	0.004 ± 0.001	0.004 ± 0.001	0.003 ± 0.001	0.003 ± 0.001
TAG(54:2)_FA 16:0	0.003 ± 0.001	0.003 ± 0.001	0.004 ± 0.001	0.004 ± 0.000
TAG(54:2)_FA 18:0	0.006 ± 0.001	0.005 ± 0.002	0.005 ± 0.001	0.005 ± 0.001
TAG(54:2)_FA 18:1	0.008 ± 0.002	0.009 ± 0.004	0.008 ± 0.002	0.007 ± 0.002
TAG(54:2)_FA 18:2	0.003 ± 0.001	0.003 ± 0.001	0.003 ± 0.001	0.003 ± 0.001
TAG(54:3)_FA 16:0	0.003 ± 0.001	0.003 ± 0.001	0.004 ± 0.001	0.004 ± 0.000
TAG(54:3)_FA 16:1	0.003 ± 0.001	0.003 ± 0.001	0.003 ± 0.001	0.003 ± 0.000
TAG(54:3)_FA 18:0	0.003 ± 0.001	0.003 ± 0.001	0.004 ± 0.001	0.004 ± 0.001
TAG(54:3)_FA 18:1	0.013 ± 0.005	0.015 ± 0.009	0.010 ± 0.004	0.009 ± 0.002
TAG(54:3)_FA 18:2	0.003 ± 0.001	0.003 ± 0.001	0.004 ± 0.001	0.004 ± 0.001
TAG(54:3)_FA 20:0	0.003 ± 0.001	0.003 ± 0.001	0.003 ± 0.001	0.003 ± 0.001
TAG(54:4)_FA 16:0	0.004 ± 0.001	0.004 ± 0.001	0.005 ± 0.001	0.006 ± 0.002
TAG(54:4)_FA 16:1	0.003 ± 0.001	0.002 ± 0.001	0.003 ± 0.001	0.003 ± 0.001
TAG(54:4)_FA 18:0	0.003 ± 0.001	0.003 ± 0.001	0.004 ± 0.001	0.004 ± 0.001
TAG(54:4)_FA 18:1	0.005 ± 0.001	0.005 ± 0.001	0.005 ± 0.001	0.005 ± 0.001
TAG(54:4)_FA 20:0	0.003 ± 0.001	0.002 ± 0.001	0.003 ± 0.001	0.003 ± 0.001
TAG(54:4)_FA 20:4	0.005 ± 0.001	0.004 ± 0.001	0.005 ± 0.001	0.006 ± 0.001
TAG(54:5)_FA 16:0	0.005 ± 0.001	0.005 ± 0.001	0.006 ± 0.001	0.006 ± 0.002
TAG(54:5)_FA 16:1	0.003 ± 0.001	0.003 ± 0.001	0.004 ± 0.001	0.004 ± 0.001
TAG(54:5)_FA 18:0	0.003 ± 0.001	0.003 ± 0.001	0.003 ± 0.001	0.003 ± 0.001

Table A.5.1 continued

TAG(54:5)_FA 18:1	0.005 ± 0.001	0.005 ± 0.001	0.005 ± 0.001	0.005 ± 0.001
TAG(54:5)_FA 20:4	0.007 ± 0.002	0.008 ± 0.003	0.008 ± 0.003	0.008 ± 0.003
TAG(54:6)_FA 16:0	0.005 ± 0.001	0.005 ± 0.001	0.005 ± 0.001	0.006 ± 0.003
TAG(54:6)_FA 16:1	0.003 ± 0.001	0.003 ± 0.001	0.004 ± 0.001	0.004 ± 0.001
TAG(54:6)_FA 18:0	0.003 ± 0.001	0.003 ± 0.001	0.003 ± 0.001	0.003 ± 0.001
TAG(54:6)_FA 18:1	0.004 ± 0.001	0.004 ± 0.001	0.004 ± 0.001	0.004 ± 0.000
TAG(54:6)_FA 20:4	0.004 ± 0.001	0.004 ± 0.001	0.005 ± 0.001	0.005 ± 0.001
TAG(54:7)_FA 16:0	0.004 ± 0.001	0.003 ± 0.001	0.004 ± 0.001	0.004 ± 0.001
TAG(54:7)_FA 16:1	0.003 ± 0.001	0.003 ± 0.001	0.003 ± 0.001	0.004 ± 0.001
TAG(54:7)_FA 18:0	0.003 ± 0.001	0.003 ± 0.001	0.004 ± 0.001	0.003 ± 0.001
TAG(54:7)_FA 18:2	0.003 ± 0.001	0.003 ± 0.001	0.003 ± 0.001	0.003 ± 0.001
TAG(54:7)_FA 20:4	0.003 ± 0.001	0.003 ± 0.001	0.003 ± 0.001	0.003 ± 0.001
TAG(54:8)_FA 16:0	0.003 ± 0.001	0.003 ± 0.001	0.003 ± 0.001	0.003 ± 0.001
TAG(54:8)_FA 18:0	0.003 ± 0.001	0.003 ± 0.001	0.003 ± 0.001	0.004 ± 0.001
TAG(54:8)_FA 18:1	0.003 ± 0.001	0.003 ± 0.001	0.003 ± 0.001	0.004 ± 0.001
TAG(54:8)_FA 20:4	0.003 ± 0.001	0.003 ± 0.000	0.003 ± 0.001	0.003 ± 0.001
TAG(56:1)_FA 16:0	0.003 ± 0.001	0.002 ± 0.001	0.003 ± 0.001	0.003 ± 0.001
TAG(56:1)_FA 16:1	0.003 ± 0.001	0.003 ± 0.001	0.003 ± 0.001	0.003 ± 0.001
TAG(56:1)_FA 18:2	0.003 ± 0.001	0.002 ± 0.001	0.003 ± 0.001	0.003 ± 0.001
TAG(56:1)_FA 20:0	0.003 ± 0.001	0.002 ± 0.001	0.003 ± 0.001	0.003 ± 0.001
TAG(56:2)_FA 16:0	0.003 ± 0.001	0.002 ± 0.001	0.003 ± 0.001	0.003 ± 0.001
TAG(56:2)_FA 18:1	0.003 ± 0.001	0.003 ± 0.001	0.003 ± 0.001	0.003 ± 0.001
TAG(56:2)_FA 18:2	0.003 ± 0.001	0.002 ± 0.001	0.003 ± 0.001	0.003 ± 0.001
TAG(56:3)_FA 16:0	0.003 ± 0.001	0.003 ± 0.001	0.003 ± 0.001	0.003 ± 0.001
TAG(56:3)_FA 18:1	0.003 ± 0.001	0.003 ± 0.001	0.003 ± 0.001	0.003 ± 0.001
TAG(56:3)_FA 18:2	0.003 ± 0.001	0.002 ± 0.001	0.003 ± 0.001	0.003 ± 0.001
TAG(56:3)_FA 20:0	0.003 ± 0.001	0.003 ± 0.001	0.003 ± 0.001	0.003 ± 0.001
TAG(56:4)_FA 16:0	0.003 ± 0.001	0.003 ± 0.001	0.003 ± 0.001	0.004 ± 0.001
TAG(56:4)_FA 18:0	0.003 ± 0.001	0.003 ± 0.001	0.003 ± 0.001	0.004 ± 0.001
TAG(56:4)_FA 18:1	0.003 ± 0.001	0.003 ± 0.001	0.003 ± 0.001	0.003 ± 0.001
TAG(56:4)_FA 20:4	0.004 ± 0.002	0.003 ± 0.001	0.003 ± 0.001	0.003 ± 0.001
TAG(56:5)_FA 16:0	0.003 ± 0.001	0.003 ± 0.001	0.004 ± 0.001	0.004 ± 0.001
TAG(56:5)_FA 18:0	0.003 ± 0.001	0.003 ± 0.001	0.003 ± 0.001	0.004 ± 0.001
TAG(56:5)_FA 18:1	0.003 ± 0.001	0.003 ± 0.001	0.004 ± 0.001	0.004 ± 0.001
TAG(56:5)_FA 18:2	0.003 ± 0.001	0.002 ± 0.001	0.003 ± 0.001	0.003 ± 0.001
TAG(56:5)_FA 20:0	0.003 ± 0.001	0.003 ± 0.001	0.003 ± 0.001	0.003 ± 0.001
TAG(56:5)_FA 20:4	0.004 ± 0.001	0.004 ± 0.001	0.004 ± 0.001	0.004 ± 0.001
TAG(56:6)_FA 16:0	0.003 ± 0.001	0.003 ± 0.001	0.004 ± 0.001	0.005 ± 0.001
TAG(56:6)_FA 16:1	0.003 ± 0.001	0.003 ± 0.001	0.003 ± 0.001	0.003 ± 0.001

Table A.5.1 continued

TAG(56:6)_FA 18:0	0.003 ± 0.001	0.003 ± 0.001	0.003 ± 0.001	0.004 ± 0.001
TAG(56:6)_FA 18:1	0.004 ± 0.001	0.004 ± 0.001	0.004 ± 0.001	0.004 ± 0.001
TAG(56:6)_FA 18:2	0.003 ± 0.001	0.003 ± 0.001	0.003 ± 0.001	0.003 ± 0.001
TAG(56:6)_FA 20:4	0.004 ± 0.001	0.004 ± 0.002	0.004 ± 0.001	0.004 ± 0.001
TAG(56:7)_FA 16:0	0.003 ± 0.001	0.003 ± 0.001	0.004 ± 0.001	0.005 ± 0.001
TAG(56:7)_FA 16:1	0.003 ± 0.001	0.003 ± 0.001	0.003 ± 0.001	0.003 ± 0.001
TAG(56:7)_FA 18:1	0.004 ± 0.001	0.004 ± 0.001	0.004 ± 0.001	0.004 ± 0.001
TAG(56:7)_FA 20:4	0.004 ± 0.001	0.003 ± 0.001	0.003 ± 0.001	0.003 ± 0.001
TAG(56:8)_FA 16:1	0.003 ± 0.001	0.003 ± 0.001	0.004 ± 0.001	0.003 ± 0.001
TAG(56:8)_FA 18:1	0.003 ± 0.001	0.003 ± 0.001	0.003 ± 0.001	0.003 ± 0.001
TAG(56:8)_FA 20:4	0.004 ± 0.002	0.005 ± 0.001	0.004 ± 0.001	0.004 ± 0.001
TAG(58:0)_FA 18:0	0.003 ± 0.001	0.003 ± 0.001	0.003 ± 0.001	0.003 ± 0.001
TAG(58:1)_FA 18:2	0.003 ± 0.001	0.002 ± 0.001	0.003 ± 0.001	0.003 ± 0.001
TAG(58:10)_FA 16:0	0.003 ± 0.001	0.002 ± 0.001	0.003 ± 0.001	0.003 ± 0.001
TAG(58:10)_FA 18:1	0.003 ± 0.001	0.003 ± 0.001	0.003 ± 0.001	0.003 ± 0.001
TAG(58:10)_FA 20:4	0.004 ± 0.001	0.004 ± 0.001	0.003 ± 0.001	0.004 ± 0.001
TAG(58:2)_FA 16:0	0.003 ± 0.001	0.002 ± 0.001	0.003 ± 0.001	0.003 ± 0.001
TAG(58:2)_FA 20:0	0.003 ± 0.001	0.002 ± 0.001	0.003 ± 0.001	0.003 ± 0.001
TAG(58:3)_FA 20:4	0.003 ± 0.001	0.002 ± 0.001	0.003 ± 0.001	0.003 ± 0.001
TAG(58:4)_FA 18:1	0.003 ± 0.001	0.002 ± 0.001	0.003 ± 0.001	0.003 ± 0.001
TAG(58:5)_FA 18:1	0.003 ± 0.001	0.002 ± 0.001	0.003 ± 0.001	0.003 ± 0.001
TAG(58:5)_FA 20:0	0.003 ± 0.001	0.002 ± 0.001	0.003 ± 0.001	0.003 ± 0.001
TAG(58:5)_FA 20:4	0.003 ± 0.001	0.003 ± 0.001	0.003 ± 0.001	0.003 ± 0.001
TAG(58:6)_FA 16:0	0.003 ± 0.001	0.002 ± 0.001	0.003 ± 0.001	0.003 ± 0.001
TAG(58:6)_FA 18:1	0.003 ± 0.001	0.003 ± 0.001	0.003 ± 0.001	0.004 ± 0.001
TAG(58:7)_FA 18:1	0.003 ± 0.001	0.003 ± 0.001	0.003 ± 0.001	0.003 ± 0.001
TAG(58:8)_FA 18:1	0.003 ± 0.001	0.003 ± 0.001	0.003 ± 0.001	0.003 ± 0.001
TAG(58:8)_FA 20:4	0.003 ± 0.001	0.003 ± 0.001	0.004 ± 0.001	0.004 ± 0.001
TAG(58:9)_FA 18:1	0.003 ± 0.001	0.003 ± 0.001	0.003 ± 0.001	0.003 ± 0.001
TAG(58:9)_FA 20:4	0.004 ± 0.001	0.004 ± 0.001	0.004 ± 0.000	0.004 ± 0.001
TAG(60:1)_FA 18:0	0.003 ± 0.001	0.002 ± 0.001	0.003 ± 0.001	0.003 ± 0.001
TAG(60:10)_FA 18:0	0.003 ± 0.001	0.002 ± 0.001	0.003 ± 0.001	0.003 ± 0.001
TAG(60:10)_FA 20:4	0.003 ± 0.001	0.003 ± 0.001	0.003 ± 0.001	0.003 ± 0.001
TAG(60:11)_FA 20:4	0.003 ± 0.001	0.003 ± 0.001	0.003 ± 0.001	0.003 ± 0.001
TAG(60:4)_FA 20:4	0.003 ± 0.001	0.003 ± 0.001	0.003 ± 0.001	0.003 ± 0.001
TAG(60:5)_FA 18:0	0.003 ± 0.001	0.002 ± 0.001	0.003 ± 0.001	0.003 ± 0.001
TAG(60:6)_FA 18:0	0.003 ± 0.001	0.002 ± 0.001	0.003 ± 0.001	0.003 ± 0.001
TAG(60:8)_FA 18:1	0.003 ± 0.001	0.002 ± 0.001	0.003 ± 0.001	0.003 ± 0.001

Table A.5.2 Complete Metabolite Profile

Complete plasma acyl-carnitine (metabolite) profile from green and hawksbill turtles. Values presented are average (± SD) relative ion intensity. Bolded metabolites were significantly different between species or seasons.

Metabolite **(Differential)**	CM Wet	CM Dry	EI Wet	EI Dry
Propenoylcarnitine	0.011 ± 0.0	0.012 ± 0.0	0.011 ± 0.001	0.011 ± 0.0
Propionylcarnitine	0.012 ± 0.001	0.012 ± 0.0	0.011 ± 0.001	0.012 ± 0.001
Butyrylcarnitine, Isobutyryl-L-carnitine	0.012 ± 0.001	0.012 ± 0.001	0.012 ± 0.001	0.012 ± 0.0
Hydroxypropionylcarnitine	0.012 ± 0.001	0.012 ± 0.001	0.012 ± 0.001	0.012 ± 0.001
Valerylcarnitine, Isovalerylcarnitine	0.016 ±0.001	0.017 ± 0.001	0.017 ± 0.001	0.016 ± 0.001
O-malonylcarnitine, Hydroxybutyrylcarnitine	0.018 ± 0.001	0.018 ± 0.002	0.018 ± 0.002	0.017 ± 0.001
2-Hexenoylcarnitine	0.016 ± 0.001	0.016 ± 0.001	0.016 ± 0.001	0.016 ± 0.001
Fumarycarnitine, Hexanoylcarnitine	0.015 ± 0.001	0.015 ± 0.001	0.015 ± 0.001	0.015 ± 0.001
O-glutarylcarnitine, Hydroxyhexanoycarnitine, Glutarylcarnitine	0.02 ± 0.002	0.021 ± 0.001	0.020 ± 0.001	0.02 ± 0.001
(2E)-octenoylcarnitine, 2-octenoyl-L-carnitine	0.017 ± 0.001	0.016 ± 0.001	0.017 ± 0.002	0.017 ± 0.001
(2E)-hexenedioylcarnitine, O-octanoylcarnitine	0.03 ± 0.004	0.029 ± 0.003	0.029 ± 0.002	0.03 ± 0.003
O-adipoylcarnitine	0.0243 ± 0.002	0.026 ± 0.002	0.025 ± 0.001	0.025 ± 0.002
3-hydroxy-cis-5-octenoylcarnitine; 2,6 dimethylheptanoyl carnitine, Nonanoylcarnitine	0.021 ± 0.002	0.021 ± 0.001	0.022 ± 0.001	0.021 ± 0.002
(2E,5Z,7E)-decatrienoylcarnitine	0.02 ± 0.001	0.02 ± 0.001	0.021 ± 0.001	0.021 ± 0.002
(2E,4Z)-decadienoylcarnitine	0.016 ± 0.001	0.016 ± 0.001	0.017 ± 0.001	0.018 ± 0.002
(4Z)-decenoylcarnitine, 9-Decenoylcarnitine, CIS-4-DECENOYL CARNITINE	0.018 ± 0.002	0.018 ± 0.003	0.018 ± 0.001	0.018 ± 0.002
4,8 dimethylnonanoyl carnitine, Undecanoylcarnitine, 6-Keto-decanoylcarnitine	0.025 ± 0.002	0.026 ± 0.002	0.024 ± 0.001	0.024 ± 0.002
Dodecanoylcarnitine, O-dodecanoylcarnitine	0.022 ± 0.002	0.022 ± 0.001	0.022 ± 0.001	0.022 ± 0.001
O-sebacoylcarnitine	0.026 ± 0.002	0.027 ± 0.002	0.026 ± 0.001	0.027 ± 0.002

Table A.5.2 continued

(9Z)-3-hydroxydodecenoylcarnitine	0.022 ± 0.001	0.022 ± 0.002	0.021 ± 0.002	0.021 ± 0.002
cis-5-Tetradecenoylcarnitine	0.021 ± 0.003	0.021 ± 0.003	0.021 ± 0.001	0.02 ± 0.001
, TetradecanoylcarnitineO-tetradecanoylcarnitine	0.022 ± 0.003	0.02 ± 0.002	0.02 ± 0.001	0.02 ± 0.002
O-(11-carboxyundecanoyl)carnitine	0.033 ± 0.002	0.033 ± 0.002	0.032 ± 0.002	0.033 ± 0.002
(5Z,8Z)-3-hydroxytetradecadienoylcarnitine	0.017 ± 0.002	0.018 ± 0.001	0.017 ± 0.001	0.017 ± 0.002
2-Hydroxymyristoylcarnitine, 3-hydroxytetradecanoylcarnitine	0.023 ± 0.002	0.023 ± 0.001	0.024 ± 0.001	0.023 ± 0.002
O-palmitoleoylcarnitine, trans-Hexadec-2-enoyl carnitine	0.019 ± 0.001	0.018 ± 0.001	0.018 ± 0.001	0.018 ± 0.002
O-(13-carboxytridecanoyl)carnitine	0.024 ± 0.002	0.023 ± 0.002	0.023 ± 0.001	0.023 ± 0.001
(9Z,12Z)-3-hydroxyhexadecadienoyl carnitine	0.018 ± 0.001	0.017 ± 0.001	0.017 ± 0.001	0.018 ± 0.001
3-hydroxypalmitoleoylcarnitine, Heptadecanoyl carnitine	0.019 ± 0.002	0.019 ± 0.001	0.019 ± 0.001	0.02 ± 0.002
Stearidonyl carnitine	0.034 ± 0.003	0.035 ± 0.002	0.037 ± 0.002	0.034 ± 0.002
Linoelaidyl carnitine, O-linoleoylcarnitine, 9,12-Hexadecadienylcarnitine	0.022 ± 0.002	0.022 ± 0.002	0.021 ± 0.001	0.023 ± 0.002
O-oleoylcarnitine, Elaidic carnitine	0.02 ± 0.002	0.019 ± 0.001	0.019 ± 0.003	0.019 ± 0.001
Stearoylcarnitine, hexadecanedioic acid mono-L-carnitine ester	0.02 ± 0.005	0.017 ± 0.001	0.018 ± 0.002	0.018 ± 0.002
(9Z,12Z,15Z)-3-hydroxyoctadecatrienoylcarnitine	0.023 ± 0.002	0.023 ± 0.001	0.024 ± 0.002	0.023 ± 0.002
3-hydroxylinoleoylcarnitine,	0.019 ± 0.001	0.019 ± 0.002	0.019 ± 0.001	0.019 ± 0.001

Table A.5.2 continued

(9Z)-3-hydroxyoctadecenoylcarnitine	0.017 ± 0.001	0.017 ± 0.001	0.016 ± 0.001	0.017 ± 0.002
O-arachidonoylcarnitine	0.029 ± 0.002	0.03 ± 0.002	0.029 ± 0.002	0.03 ± 0.002
(11Z,14Z)-eicosadienoylcarnitine	0.034 ± 0.003	0.035 ± 0.003	0.035 ± 0.003	0.036 ± 0.004
(11Z)-eicoseneoylcarnitine	0.021 ± 0.002	0.022 ± 0.001	0.021 ± 0.001	0.022 ± 0.002
Arachidyl carnitine, O-[(9Z)-17-carboxyheptadec-9-enoyl]carnitine	0.017 ± 0.001	0.016 ± 0.001	0.016 ± 0.001	0.016 ± 0.001
O-(17-carboxyheptadecanoyl)carnitine	0.016 ± 0.001	0.016 0.002	0.017 ± 0.001	0.017 ± 0.001
3-hydroxyarachidonoylcarnitine	0.025 ± 0.001	0.025 ± 0.002	0.026 ± 0.002	0.025 ± 0.001
3-hydroxyeicosanoylcarnitine, Cervonyl carnitine	0.017 ± 0.001	0.017 ± 0.001	0.017 ± 0.001	0.018 ± 0.001
Docosa-4,7,10,13,16-pentaenoyl carnitine, Clupanodonyl carnitine	0.031 ± 0.003	0.031 ± 0.003	0.033 ± 0.002	0.03 ± 0.002
(7Z,10Z,13Z,16Z)-docosatetraenoylcarnitine	0.027 ± 0.002	0.026 ± 0.002	0.028 ± 0.002	0.027 ± 0.002
(13Z,16Z)-docosadienoylcarnitine	0.022 ± 0.002	0.021 ± 0.002	0.022 ± 0.002	0.022 ± 0.001
O-behenoylcarnitine	0.0178 ± 0.001	0.018 ± 0.002	0.018 ± 0.001	0.019 ± 0.001
Hexacosanoyl carnitine	0.018 ± 0.001	0.018 ± 0.001	0.017 ± 0.001	0.019 ± 0.002

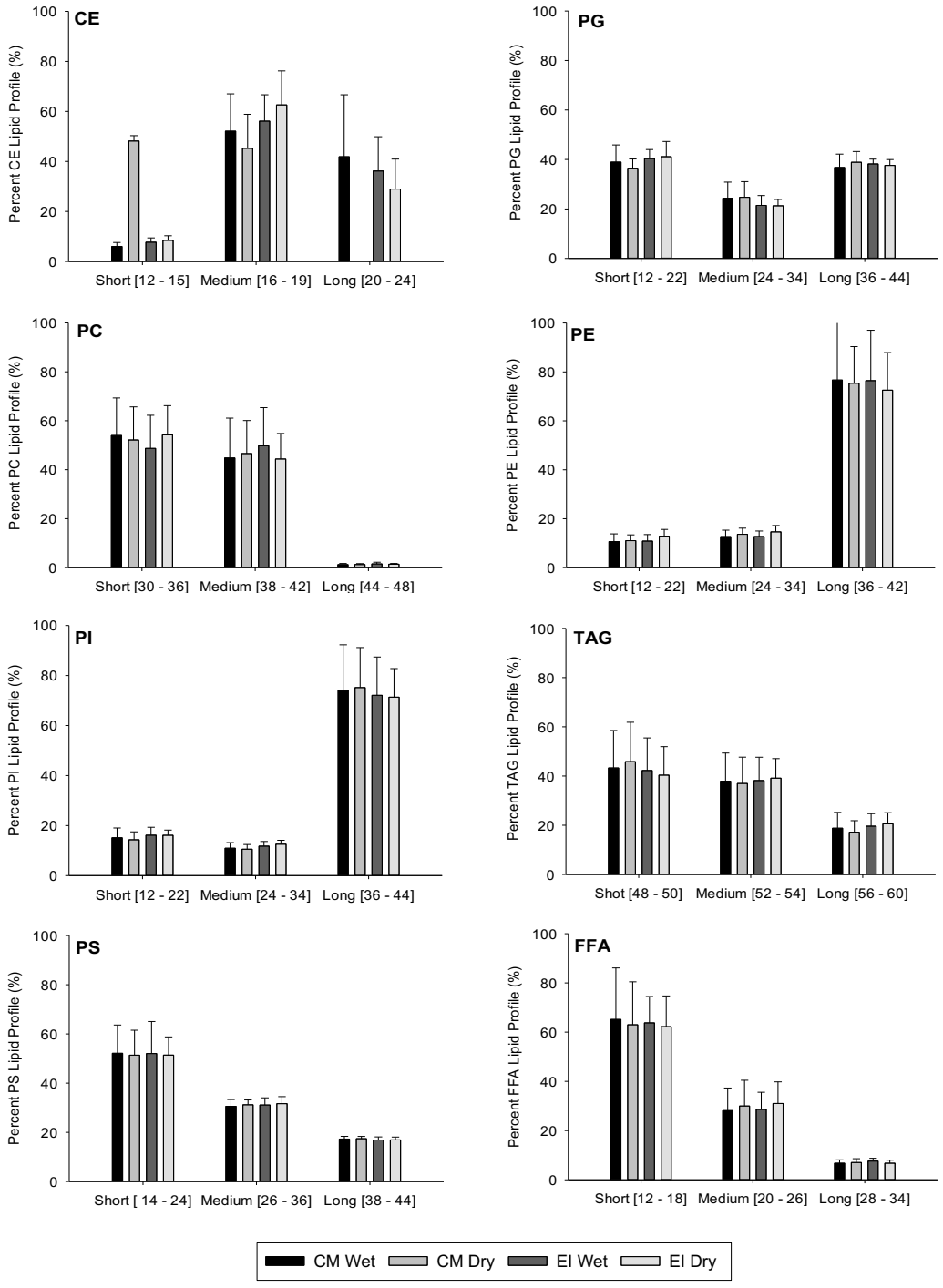

Figure A.5.1 Percent Chain Length
Percent composition of short, medium, and long chain lipids within each lipid class profile from turtles in this study, divided by season (mean ± SD). The classification of length varied by lipid class and was divided differently in each class to match the data (as listed on the x-axis).

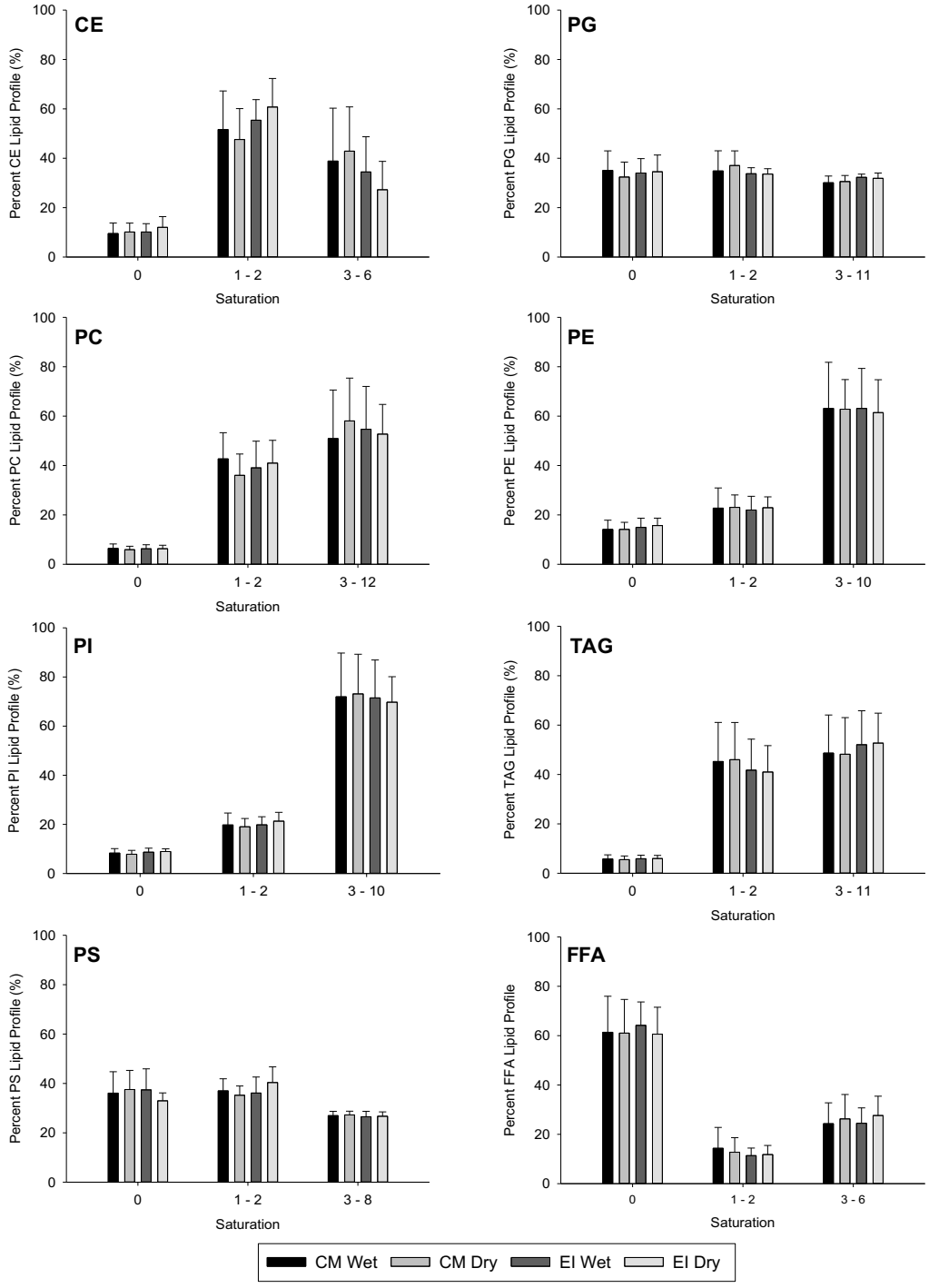

Figure A.5.2 Percent Saturation
Percent saturation of lipids within each lipid class profile from sea turtles divided by season (wet and dry) and by species (green turtle = CM, hawksbill = EI). The x-axis represents saturation level where 0 = unsaturation, 1 – 2 = mono and di unsaturated, and 3+ = polyunsaturated lipids. Bars and error bars represent mean ± standard deviation.

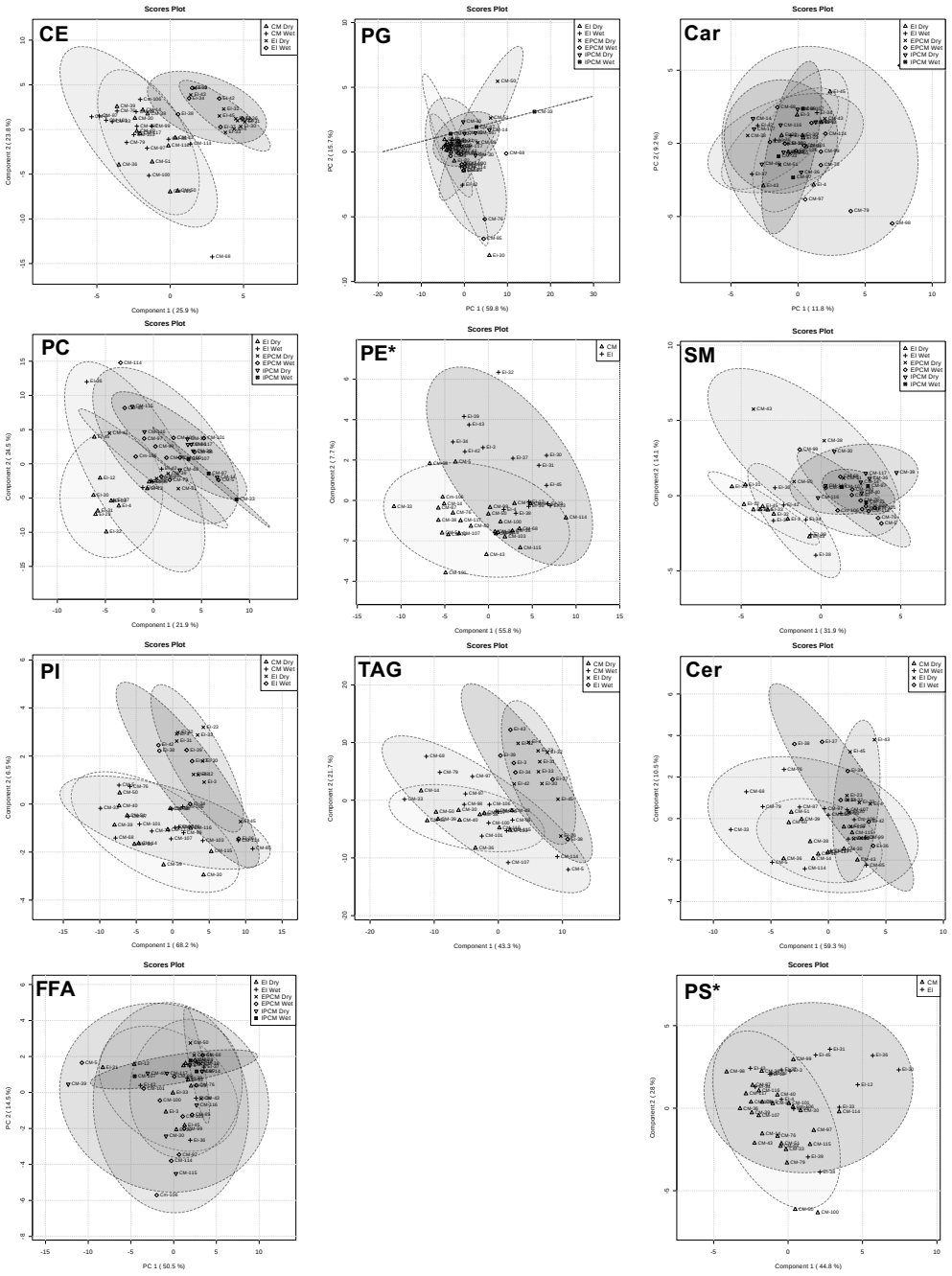

Figure A.5.3 Principle Component Analyses
Principal component analysis (PCA; Car, FFA, PG) 2D score plots and partial least-squares discriminant analysis (PLS-DA; CE, Cer, PC, PE, PI, PS, SM, TAG) 2D score plots generated using principle component 1 (x-axis) and principle component 2 (y-axis) demonstrating species and seasonal clusters as a result of lipids and metabolites (Car) in green turtles (CM) and hawksbill turtles (EI) between seasons (wet and dry). We captured all turtles in North Pacific Costa Rica in 2017. *PE and PS lipid classes had no seasonal variability so plots are by species alone.

VITA

CHELSEA E. CLYDE-BROCKWAY
Graduate Research Assistant
Department of Forestry and Natural Resources
Purdue University

EDUCATION
Purdue University, Wildlife Science, Ph.D., 2019
Purdue University, Fort Wayne, Biology, M.S., 2014
Sonoma State University, Marine Biology, B.S., 2011

APPOINTMENTS

2015-2019	PhD graduate research assistant, Purdue University
2017	Biologist for Eqipo Tora Carey
2012-2019	Biologist for The Leatherback Trust
2012-2014	Graduate Research Assistant; Purdue University, Fort Wayne (masters)
2012-2013	Biologist/Guide for Earthwatch.org
2011	Marine Ecology Lab Manager at Sonoma State University
2010-2011	Endocrinology/Physiology Lab Tech, Sonoma State University
2010	BS research assistant. Dr. Daniel Crocker. Sonoma State University.

HONORS/AWARDS

2018	Second place poster presentation, Forestry and Natural Resources Research Symposium, Purdue University, West Lafayette, IN
2014	First place poster presentation, Sigma Xi Honor Society. Purdue University, Fort Wayne, IN
2014	Master of Science, Purdue University, Fort Wayne. Summa Cum Laude
2011	Bachelor's of Science, Sonoma State University. Magnum Cum Laude

PUBLICATIONS (* = mentored student)

*Mettler, E., **Clyde-Brockway, C.,** Honavar, S., and Paladino, F.V. Newly discovered migratory corridor and foraging grounds for Altantic green turtles, *Chelonia mydas,* nesting on Bioko Island, Equatorial Guinea. PLoS ONE. *In review*.

Clyde-Brockway, C.E., Robinson, N.J., Blanco, G.S., Santidrian Tomillo, P., Spotila, J.R., Morreale, S.J., Paladino, F.V. Comparing the behavior of East Pacific green turtles from two nearby beaches on the Pacific Coast of Costa Rica. Chelonian Conservation and Biology. *In review.*

Heidemeyer, M., Delgado-Trejo, C., Hart, C.E., **Clyde-Brockway, C.,** Fonseca, L.G., Mora, R., Mora, M., Lara, A., and Obando, R. 2018. Long-term in-water recaptures of adult Black Turtles *(Chelonia mydas)* provide implications for flipper tagging methods in the Eastern Pacific. Herpetological Review 49(4): 652–656.

Clyde-Brockway, C.E. 2017. The Leatherback Turtle: Conservation and Biology, Book Review. Copeia 2017 (105): 164-178

PRESENTATIONS (* = mentored student)

Clyde-Brockway, C.E., Ferreira, C.R., Flaherty, F.A., and Paladino, F.V. 2019. Lipidomics suggest species specificity and cold acclimation in Pacific green and hawksbill turtles. Forestry and Natural Resources Research Symposium, Purdue University. West Lafayette, IN. Poster Presentation.

Clyde-Brockway, C.E., Heidemeyer, M., Flaherty, E.A., and Paladino, F.V. 2019. Stable isotope analysis reveals foraging niche segregation and resource use of green and hawksbill turtles in Pacific Costa Rica. International Sea Turtle Symposium, the 39th annual meeting of the International Sea Turtle Society, Charleston, SC. Poster Presentation. Abstract Published.

Clyde-Brockway, C.E., Flaherty, E.A., and Paladino, F.V. 2019. High circulating corticosterone in cold-stunned juvenile green turtles suggests transient stress in otherwise healthy turtles. International Sea Turtle Symposium, the 39th annual meeting of the International Sea Turtle Society, Charleston, SC. Poster Presentation. Abstract Published.

*Mettler, E., **Clyde-Brockway, C.E.,** Honarvar, S., Paladino, F.V. 2019. Satellite telemetry analysis of green sea turtle movements in the Gulf of Guinea. International Sea Turtle Symposium, the 39th annual meeting of the International Sea Turtle Society, Charleston, SC. Poster Presentation. Abstract Published.

Clyde-Brockway, C.E., Paladino, F.V., Flaherty, E.A. 2018. Sea Turtles Species Composition at a North Pacific Costa Rican Foraging Ground. Forestry and Natural Resources Research Symposium, Purdue University. West Lafayette, IN. Poster Presentation.

Clyde-Brockway, C.E., Paladino, F.V., Flaherty, E.A. 2018 Trophic Niche and Diet Assessment in Costa Rican Sea Turtles. The Wildlife Society annual conference, Cleveland, OH, USA. Abstract Published.

*Mettler, E., **Clyde-Brockway, C.E.,** Honarvar, S., and Paladino, F.V. 2018. Satellite telemetry analysis of green sea turtle movements in the Gulf of Guinea. The Wildlife Society annual conference, Cleveland, OH, USA. Abstract Published.

*Truelock, Z.T., **Clyde-Brockway, C.E.,** and Flaherty, E.A. 2018. Ecological responses of Midwestern snakes to prescribed fire. Forestry and Natural Resources Research Symposium, Purdue University. West Lafayette, IN. Poster Presentation.

*Truelock, Z.T., **Clyde-Brockway, C.E.,** and Flaherty, E.A. 2017. Ecological responses of Midwestern snakes to prescribed fire. Annual Meeting of the Midwest Partners in Amphibian and Reptile Conservation, Bradford Woods, Indiana.

Clyde-Brockway, C.E., Robinson, N.J., Blanco, G.S., Santidrian Tomillo, P., Spotila, J.R., Morreale, S.J., and Paladino, F.V. 2016. Comparing the behavior of East Pacific green turtles from two nearby beaches on the Pacific Coast of Costa Rica. Joint Meeting of Ichthyologists and Herpetologists, New Orleans, LA. Abstract published.

Clyde-Brockway, C.E., Santidrian Tomillo, P., and Paladino, F.V. 2014. Interactions of oceanographic factors with inter-nesting habitat selection and behavior of East Pacific green turtles (*Chelonia mydas agassizii*) from Playa Cabuyal, Guanacaste, Costa Rica. International Sea Turtle Symposium, the 34th annual meeting of the International Sea Turtle Society, New Orleans, LA. Abstract Published.

Clyde-Brockway, C.E., Santidrian Tomillo, P., Paladino, F.V. 2014. Inter-nesting and post-nesting movements of East Pacific green turtles (*Chelonia mydas agassizii*) from Playa Cabuyal, Guanacaste, Costa Rica. Sigma Xi honors society poster presentation, Purdue University, Fort Wayne, IN. Poster Published.

Clyde-Brockway, C.E., Santidrian Tomillo, P., Morreale, S.J., and Paladino, F.V. 2013. Preliminary satellite telemetry of East Pacific green turtles nesting on Playa Cabuyal, Costa Rica. Sigma Xi honors society poster presentation, Purdue University, Fort Wayne, IN. Poster Published.

SCHOLARSHIPS/GRANTS

2017	D. Woods Thomas Memorial Fund Award: $1000
2014	PhD Fellowship. The Leatherback Trust: $24,000 stipend/year
2013	Graduate Research Fellowship, Community Foundation, Sonoma County: $40,000

SERVICE

2018	Graduate Student Reviewer for Ecography Journal
2018-current	Nominations Committee; Herpetologists League
2018-current	Member of the Diversity and Inclusion Committee; Herpetologists League
2017	Reviewer for The Journal of the Utah Academy of Science, Arts, and Letters
2015-current	Graduate Chair to the Herpetologists League
2016-current	Assist in maintaining the Herpetologists' League Facebook and Twitter profiles, and service on the board of trustees.

TEACHING

2018	Marine Biology, Purdue University, West Lafayette, IN. Lecture TA
2018	Marine Vascular Plants, Marine Biology, Purdue University, West Lafayette, IN. Single Lecture
2017	Case Study: Decline of the Western Arctic Caribou Herd in Alaska. Wildlife Habitat Management, Purdue University, West Lafayette, IN. Single Lecture
2015	Spatial Ecology and GIS. Purdue University, West Lafayette, IN. Solo Lab TA
2014	Mammal Physiology. Purdue University, Fort Wayne, IN. Solo Lab TA
2014	Pre-Med Anatomy. Purdue University, Fort Wayne, IN. Solo Lab TA
2014	Muscle Physiology, Mammal Physiology, Purdue University, Fort Wayne, IN. Single Lecture
2013	Pre-Nursing Anatomy/Physiology, first and second semester. Purdue University, Fort Wayne, IN. Solo Lab TA
2013	General Animal Biology. Purdue University, Fort Wayne, IN. TA
2007	Afternoon teacher at a charter school for minority and low-income children in California. Santa Rosa, CA. Assistant Teacher

GUEST LECTURES

2018 Stable Isotope Analysis Reveals Foraging Niche Segregation and Resource Use of Green and Hawksbill turtles in Pacific Costa Rica. Marine Biology, Purdue University, IN. Guest Lecture

2017 From Beaches to Tangle Nets. Marine Biology, Purdue University, West Lafayette, IN. Guest Lecture

2016 Coastal Management Flipped Classroom Lecture, Wildlife Habitat Management, Purdue University, West Lafayette, IN. Guest Lecture

2015 Coastal Management and Development, Wildlife Habitat Management, Purdue University, West Lafayette, IN. Guest Lecture

EXTENSION/OUTREACH

2018 In Wildlife Program. Purdue University. Speaker

2018 Mock Interview Workshop for undergraduate students, Purdue University. Speaker

2018 Herpetologists' League Student Workshop Organizer. "Public Image in Herpetology: Communication, Engagement and Transparency." Joint Meeting of Ichthyologists and Herpetologists, Rochester, NY.

2017 Environmental Education Program. "Diet Assessment Techniques in Sea Turtles." El Jobo Grade School, Costa Rica. Speaker

2017 Herpetologists' League Student Workshop Organizer. "Peer Review: Tips and tricks to publishing and reviewing articles." Joint Meeting of Ichthyologists and Herpetologists, Austin, TX.

2016 Live trapping demonstration for high school students at the Familiar Faces Project, West Lafayette, IN. Speaker

2016 Herpetologists' League Student Workshop Organizer. "What do you do with your degree?" Joint Meeting of Ichthyologists and Herpetologists, New Orleans, LA.

2015 Herpetologists' League Student Workshop. "Research Resources: Field Stations, Museums, and Managed Lands." Joint Meeting of Ichthyologists and Herpetologists, Reno, NV